Establishing a homogeneous and stable sand pack to study parameters during spontaneous imbibition

PETROLEUM TECHNOLOGY

A Master Thesis in Reservoir Physics

Author: Anders Sundgot Saunes

June 3, 2018

Abstract

Spontaneous imbibition is an important process for oil production during water flooding in porous media and has been widely studied for decades to understand the physics of the process for different boundary conditions. This thesis study spontaneous imbibition in unconsolidated sands, where experimental protocols have been improved to mitigate challenges associated with displacement processes in such systems. An initial focus was to establish uniform and stable sand packs that enable tests to be repeated without changes in permeability and porosity due to poor packing or loss of sand. Homogeneous sand packs allowed for reproducible tests to compare the influence of initial water saturation on spontaneous imbibition. Sand packs were also used in spontaneous imbibition tests with different wetting fluid viscosity, where brine viscosity was increased by adding glycerol or an HPAM polymer powder. This enabled a systematic investigation of wettability alteration by polymer solutions in unconsolidated sands.

A new sand packing method in glass tubes was developed where the sand was compressed by pressure to achieve a narrow pore size distribution. End pieces that enabled flow in and out of the sand packs were redesigned to eliminate the need for threaded glass tubes, leading to less leakage and glass tube shattering.

The presence of an initial water saturation reduced recovery efficiency and production rate during spontaneous imbibition conducted in sand packs: average recovery factor without initial water (RF=79%OOIP) was 40% higher than with initial water (RF=56%OOIP).

Spontaneous imbibition with HPAM polymer added to the brine yielded 3% higher recovery than spontaneous imbibition with a glycerol solution. This contradicts earlier findings where a 5% higher recovery was observed with glycerol compared to HPAM polymer. Unlike earlier studies, the polymer solution used in this thesis was filtered to remove microgels and other multimolecular structures. By filtering the solution, retention in the filter was prevented, and the polymer solution could imbibe freely. In addition, measurements of the Amott-Harvey wettability index (I_{AH}) indicated that the HPAM polymer altered the wettability of the sand. Average I_{AH} for sand packs where HPAM polymer had been present was 0.92, whereas, for sand packs where it had not been present, the value was 0.97.

Acknowledgements

I would like to thank my supervisors Professor Martin Fernø and Dr. Bergit Brattekås at the Department of Physics and Technology here at the University of Bergen. Your knowledge and guidance has helped me a lot through this year. In addition, I would like to thank Professor Arne Graue and Associate Professor Geir Ersland for their contributions to the reservoir physics group.

I would also like to thank Roald Langøen and Charles Sebastiampillai for always welcoming me at the mechanical shop, and for their help making all my designs come to life.

Thanks to all my fellow students during these five years at the University of Bergen. Thank you, Eldri, for taking me on small walks to the water cooler. Thank you, Simon, for useful discussions and company at the lab. And thank you, Stine, for always being a sunshine when it's needed.

Thank you to my parents, who haven't lost faith in me (yet).

Last but not least, thank you Marte. You are my biggest achievement and inspiration. Thank you for supporting me during these last years, and for being my guiding light. Without you, I would have never been where I am today.

Bergen, June 2018

Anders Sundgot Saunes.

Contents

Part I

Theory and introduction

1 Introduction

Spontaneous imbibition is an important process occurring in various types of porous media, including: paper towels, the human skin, and petroleum reservoir. It occurs as a response to capillary forces arising between two immiscible fluids, causing the wetting fluid to spontaneously displace the non-wetting fluid out of the porous medium. The process has been widely studied for decades, and experiments related to spontaneous imbibition in petroleum reservoirs are of special interest. Experiments studies factors affecting spontaneous imbibition, such as fluid viscosities (Haugen et al. 2015, Meng et al. 2016), boundary conditions (Standnes 2004), and porous structure (Meng et al. 2015, 2016). Traditionally, experiments have been carried out in consolidated porous media, but lately, studies in unconsolidated porous media have flourished (Meng et al. 2015, Vabø 2016, Haugland 2016, Føyen 2017).

Sand represents an affordable and efficient way of constructing the unconsolidated porous medium. However, previous experimental challenges have made it difficult to conduct experiments with reproducible results (Vabø 2016, Haugland 2016). Affecting the validity of findings, a reproducible framework is needed to investigate the complex nature of spontaneous imbibition in unconsolidated sands.

Experimental studies of spontaneous imbibition in sand and the effect of polymers on the spontaneous imbibition behavior is of special interest due to a planned polymer injection pilot on the Johan Sverdrup field, containing unconsolidated sand units. Moreover, an ongoing research project at The Departement of Physics and Technology, University of Bergen, aims to study the effect of polymers on spontaneous imbibition.

In this thesis, a methodological work has been conducted to develop a reproducible framework for spontaneous imbibition investigations in unconsolidated sands. In addition, experiments using synthetic polymer has been carried out as a continuation of Haugland (2016) experiments to study the effect on spontaneous imbibition, relevant for the planned Johan Sverdrup field pilot.

2 Fundamentals

2.1 Porosity and permeability

Porosity and permeability are two important properties of porous media. Porosity is the storage capacity of a porous medium, whereas permeability is its capacity to transport fluids within its voids. Porosity is often subdivided into two categories: *absolute* and *effective*. *Absolute* porosity is the ratio of the total volume of voids to the bulk volume of the medium, whereas *effective* porosity is the ratio of the volume of interconnected voids to the bulk volume. In this thesis, *effective* porosity was measured and will be described as porosity. The volume of the voids, V_p, has been calculated by the weight difference after and before saturation of the medium, divided by the density, ρ_i, of the saturating fluid.

$$\phi = \frac{V_p}{V_b} = \frac{m_{sat} - m_{dry}}{\rho_i} \frac{1}{V_b} \tag{2.1}$$

where ϕ is the *effective* porosity, V_b is the bulk volume of the medium, and m_{sat} and m_{dry} are the weight of the porous medium after and before it was saturated, respectively.

Permeability can be subdivided into *absolute*, *effective*, and *relative* permeability. *Absolute* permeability is constant for a porous medium, and is defined by Darcy's law:

$$q = -K \frac{A}{\mu} \frac{dp}{dx} \tag{2.2}$$

where A is the cross-sectional area of the porous medium, K is the *absolute* permeability, μ is the viscosity of the fluid, and $\frac{dp}{dx}$ is the differential change in pressure over a unit length of the porous medium in the direction of the fluid flow.

Effective permeability is defined as the permeability of a specific fluid when two or more immiscible fluids flow in the porous medium. It is defined by a generalization of Darcy's law. The *effective* permeability k_{je} of fluid i is defined as:

$$k_{ie} = q_i \frac{\mu_i}{A} \frac{\Delta x}{\Delta p_i} \tag{2.3}$$

where q_i is the volumetric flow of fluid i, and Δp_i is the pressure drop in fluid i.

In this thesis, *relative* permeability will be used instead of *effective* permeability. It is defined as the ratio between the *effective* and the *absolute* permeability:

$$k_{ri} = \frac{k_{ie}}{K} \tag{2.4}$$

The *relative* permeability of each fluid depends on rock properties, the wettability of the rock, and the saturation of the fluid Anderson (1987*b*). The saturation of a fluid i in a porous medium is defined as the fractional space of the total void volume of the medium. The relative permeabilities dependence on wettability and saturation is illustrated in figure 2.1. As the saturation of fluid i increases, its relative permeability increases. In general, the relative permeability of a fluid is lower if it is the wetting fluid. In a strongly water-wet porous medium, it is expected that the end-point relative permeability of the non-wetting fluid is larger than for the wetting fluid. The end-point relative permeability is the relative permeability of one fluid when the other is immobile. This is shown by the largest relative permeability values of each fluid in figure 2.1. Wettability is further elaborated in section 2.2.

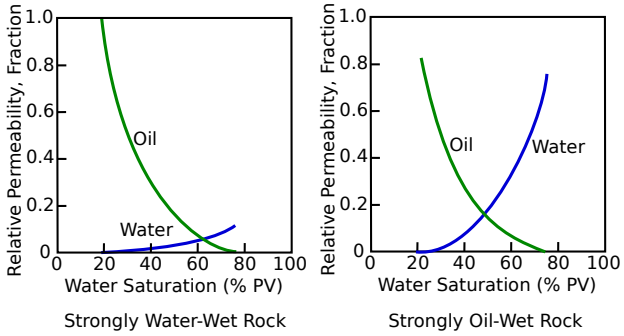

Figure 2.1: Relationship between the relative permeability of oil and water as a function of water saturation and its dependence on wettability.

There are generally two categories of porous media related to the aggregation of sand sediments; consolidated, and unconsolidated sands. In unconsolidated sands, grains are not cemented together, which, in general, gives them higher porosity and permeability compared to consolidated sand. This will be discussed in the next section.

2.1.1 Porosity and permeability in unconsolidated sands

In unconsolidated sands, because the grains are not cemented together, all voids are interconnected (Graton & Fraser 1935) and the *absolute* porosity and *effective* porosity are equal. Generally,

both permeability and porosity of unconsolidated media are higher than for consolidated media (Coskun et al. 1993), and both properties are affected by the mean grain size, grain size distribution, and the sorting of the grains (Fraser 1935, Krumbein & Monk 1943, Masch & Denny 1966, Morrow et al. 1969). The more poorly sorted a sand pack is, the lower its porosity will be because smaller grains will fill the voids between the larger grains (Rogers & Head 1961). For well-sorted sands, Rogers & Head (1961) found that porosity is independent of grain size, whereas, for poorly sorted sands, finer sands are more porous than coarser ones. Fraser (1935), Graton & Fraser (1935), and Morrow et al. (1969) showed that permeability increases as the size of the grains increase, and that poor sorting generally decreases the permeability of unconsolidated sands. In general, porosity and absolute permeability of unconsolidated sand decreases with higher compression (Domenico 1977, Gobran et al. 1987).

Because of these relationships between grain size and sorting, there is no strong relationship between porosity and permeability in unconsolidated sands (Coskun et al. 1993). For consolidated sands, however, there is a more evident relationship between porosity and permeability. These differences are thought to be because, in unconsolidated sand, a decrease in porosity does not eliminate flow channels, whereas, in consolidated sand, flow channels get blocked by cement.

2.2 Wettability

Wettability can be described as "the tendency of one fluid to spread on or adhere to a solid surface in the presence of other immiscible fluids" (Craig 1971). There are different kinds of wettability conditions, including water-wet, oil-wet, neutral-wet, mixed-wet, and fractionally-wet. In a uniformly strongly water-wet system, water will coat most surfaces, and it will fully saturate the smallest pores with radius up to a threshold size. And vice-versa for strongly oil-wet systems. A neutrally-wet system is neither water- nor oil-wet. In a mixed-wet system, the wettability of the pores depends on the pore size (Salathiel 1973). For example, in a mixed-wet large system, the larger pores are water-wet whereas the smaller are oil-wet. In a fractionally-wet system, the wettability is randomly distributed throughout the system, independent of pore size.

Wettability influences important flow properties such as capillary pressure and *relative* permeabilities, which in turn influences the distribution of fluids (Anderson 1986*a*), e.g. water breakthrough occurs faster in oil-wet systems during waterflooding compared to water-wet systems (Anderson 1987*c*), as illustrated in figure 2.2. It also affects spontaneous imbibition, which is the process where the wetting fluid spontaneously displaces the non-wetting fluid without applying any additional pressure. This process is important for the production of oil in fractured reservoirs because,

from the low permeable rock matrix, oil must be displaced to the high permeable fractures by spontaneous imbibition to be produced (Fernø et al. 2011). Spontaneous imbibition and capillary pressure will be defined in the following sections.

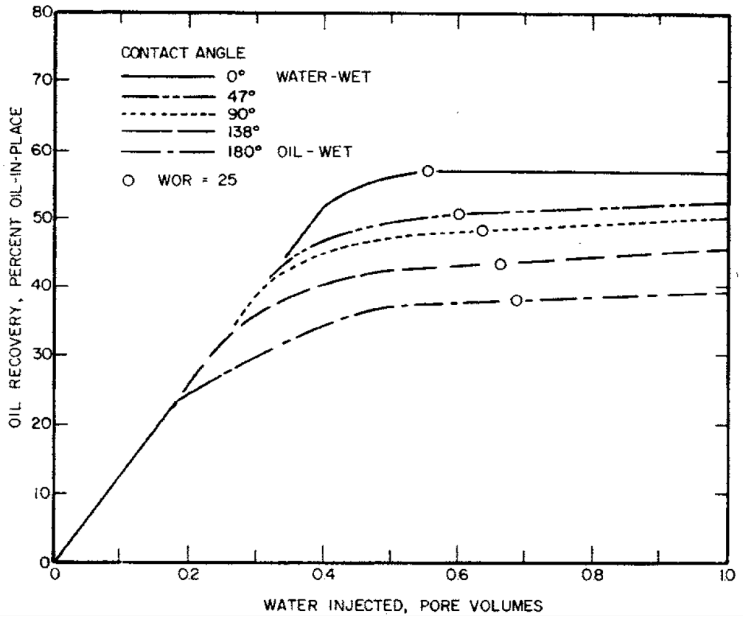

Figure 2.2: Oil recovery as a function of water injected during waterflooding. Note that water breakthrough occurs when the curve breaks of its linear path. (Anderson 1987*c*).

2.3 Spontaneous imbibition

The process of imbibition occurs when the wetting phase displaces the non-wetting phase and its saturation increases. Imbibition can occur under three different conditions: Dynamic spontaneous imbibition, pseudo-quasistatic spontaneous imbibition, and forced imbibition (Morrow & Mason 2001, Li et al. 2003). For this thesis, dynamic spontaneous imbibition and forced imbibition were conducted. For the imbibition processes, the recovery factor (R_f) was calculated as the fraction of oil volume produced (N_p) to the oil volume originally in place (OOIP, V_{oi}):

$$R_f = \frac{N_p}{V_{oi}} \tag{2.5}$$

Dynamic spontaneous imbibition Capillary forces drive dynamic spontaneous imbibition, and no additional pressure gradient is applied to displace the non-wetting fluid. Under these con-

ditions, gravity is neglected as a contributor to the flow of fluids (Li et al. 2003). Spontaneous imbibition is affected by the wettability of the porous medium, the viscosity of the fluids involved and the interfacial tension between them, the structure of the pores, and the initial and historical saturation of the medium (Torsaeter 1984). Spontaneous imbibition can occur both by counter-current and co-current spontaneous imbibition. During counter-current spontaneous imbibition the wetting and non-wetting phase flow in the opposite direction. During co-current spontaneous imbibition, wetting and non-wetting phase flow in the same direction (Li et al. 2003). Both of these were observed during experiments.

For spontaneous imbibition to occur, the porous medium needs to have a wetting preference and, theoretically, it will occur for all contact angles other than 90°. It has, however, been shown that for water displacing oil, there is no spontaneous imbibition when the contact angle is as low as 49° (Anderson 1987*a*). This is due to the effect of pore structures and pore roughness in porous media. The wetting preference of a porous medium can be quantified or qualitatively expressed by for example imbibition tests, as explained later in chapter 2.4.

Dynamic spontaneous imbibition tests were conducted during the experimental work associated with this thesis.

Pseudo-quasistatic spontaneous imbibition During pseudo-quasistatic spontaneous imbibition, the saturation of the wetting phase is increased in a controlled manner by reducing the capillary pressure in steps (Morrow & Mason 2001).

Forced imbibition During forced imbibition, a pressure gradient is applied either externally or by gravity to the imbibing fluid, forcing it to displace the non-wetting phase (Li et al. 2003). Forced imbibition has been conducted after spontaneous imbibition to calculate relative permeability of water, and to look at the ratio of oil produced spontaneously to oil produced by forced imbibition. This ratio can determine the wettability of the porous medium and will be explained in section 2.4.

2.3.1 Pressure acting during spontaneous imbibition

The main pressure acting during spontaneous imbibition is the capillary pressure at the saturation front, $P_{c,f}$. In front of the saturation front, the water saturation is such that it can no longer flow. Behind the saturation front, the oil saturation is such that it can no longer flow. This is illustrated

in figure 2.1 as the saturation where the water and oil relative permeability is zero, respectively. The capillary pressure is defined as the difference between the non-wetting phase pressure (P_{nw}) and the wetting phase pressure (P_w), and is given by Laplace's equation (Anderson 1987*a*):

$$P_c = P_{nw} - P_w = \sigma \left(\frac{1}{r_1} + \frac{1}{r_2} \right) \tag{2.6}$$

where r_1 and r_2 are the radii of the curvature of the interface between the two phases, and σ is the interfacial tension between the two phases.

For porous media, the equation of interfacial curvature is, in most cases, too complicated to be solved analytically and must be solved experimentally(Anderson 1987*a*). This gives a non-trivial relation between the capillary pressure and the contact angle between the phases involved. There is, however, one simple case where the relation between the contact angle and the capillary pressure is easily derived. For a capillary tube, P_c acts as a function of wettability, geometry, and interfacial tension.

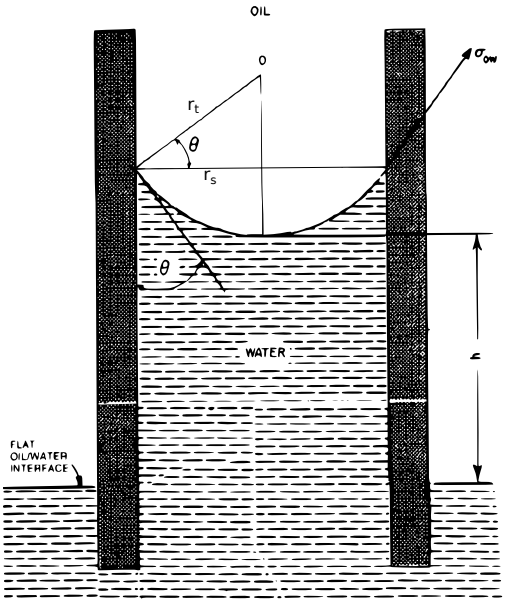

Figure 2.3: Illustration of oil/water interface in a capillary tube. Figure 1 in Anderson (1987*a*, p. 1284)

When two immiscible fluids are present in a capillary tube, an interface occurs between them as illustrated in figure 2.3. The interface between the two phases can be approximated by the portion of a sphere with both principal radii equal and denoted r_s. The relationship between the radius of

the capillary tube, r_t, and the radius of the sphere, r_s, is:

$$\frac{r_t}{r_s} = \cos\theta \tag{2.7}$$

where θ is the contact angle to the solid surface measured through the denser phase, in this case, water. Substituting r_t into equation 2.6 gives the capillary pressure in a capillary tube:

$$P_c = \frac{2\sigma\cos\theta}{r_t} \tag{2.8}$$

In addition to the capillary pressure at the saturation front, a pressure in the non-wetting fluid arises at the face open to the wetting fluid. This pressure is denoted capillary back pressure, $P_{c,o}$ (Meng et al. 2017), and arises as an opposing pressure to the production of non-wetting fluid at a face open to the wetting fluid (Li et al. 2003, Unsal et al. 2009). The process of producing the non-wetting fluid at the face open to the wetting fluid can be compared to a drainage process where the non-wetting fluid displaces the wetting fluid. Depending on the boundary conditions for the spontaneous imbibition, one or more faces are open to the wetting fluid.

Boundary conditions

Several boundary conditions have been used in earlier experimental work, including "All Faces Open" (AFO), "Two Ends Closed" (TEC), "One End Open" (OEO), "Two Ends Open" (TEO), and recently "Two Ends Open Free Spontaneous Imbibition" (TEOFSI). All boundary conditions are illustrated in figure 2.4 (AFO, TEC, OEO, TEO) and 2.5 (TEOFSI). For this thesis, only AFO and TEOFSI have been used.

Because experiments on sandstone cores were done as preliminary investigations to the sand pack investigations, a simple and quick experimental set-up was chosen. Therefore, AFO was used when conducting spontaneous imbibition experiments on sandstone cores. The boundary condition demands little preparation, and it is the most common boundary condition in use. This boundary condition leaves all faces of the core in contact with the wetting fluid, and all production occurs counter-currently as opposed to co-currently.

In a porous medium, the directional flow of the wetting and non-wetting fluid can be both in the same (co-current) and opposite (counter-current) direction (Karpyn et al. 2009). In a reservoir containing fractures with most of the oil stored in matrix blocks, it is often assumed that most of the

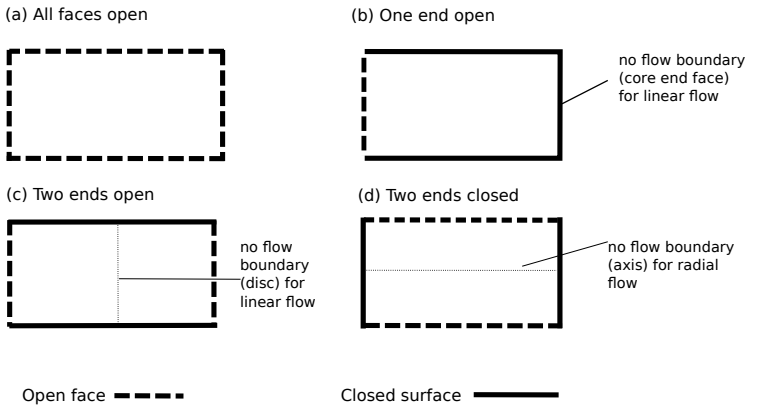

Figure 2.4: Different boundary conditions used for spontaneous imbibition experiments. (Morrow & Mason 2001).

production of oil into the fractures occurs counter-currently (Unsal et al. 2007, Karpyn et al. 2009). Therefore, experiments with the AFO boundary condition have been widely studied. However, Pooladi-Darvish & Firoozabadi (2000) showed that in the case where water only partially covers the matrix block, co-current production dominates the process. This situation can be illustrated by figure 2.5 which shows the case of TEOFSI where one side is exposed to the wetting fluid (water) and the other is exposed to the non-wetting fluid (oil) (Bourbiaux & Kalaydjian 1990, Dong et al. 1998). When spontaneous imbibition occurs counter-currently as opposed to co-currently, the rate of imbibition is much lower (Bourbiaux & Kalaydjian 1990, Pooladi-Darvish & Firoozabadi 2000, Unsal et al. 2007) because in counter-current production it takes a significant positive pressure to overcome the capillary back pressure, which makes a difference to the imbibition rate (Unsal et al. 2007).

TEOFSI was used for all sand packs. For this boundary condition, one face is exposed to the wetting phase, whereas the other is exposed to the non-wetting phase. The capillary back pressure at the face exposed to the non-wetting phase will be zero, as illustrated in figure 2.5. This will stimulate co-current spontaneous imbibition. Both in this thesis and in earlier work, experiments show that the non-wetting phase will produce from both faces using this boundary conditions (Haugen et al. 2014, Føyen 2017). At the beginning of the spontaneous imbibition, the pressure in the non-wetting phase at the saturation front, ($P_{nw,f}$), is higher than the capillary back pressure, and non-wetting phase produces counter-currently. When the spontaneously imbibing phase has a viscosity, there is a viscous drag associated with the transport of the wetting phase from the wetted face to the saturation front (Haugen et al. 2014). This drag is proportional to the distance between the wetted face and the saturation front, thus a higher pressure gradient is needed to transport it to the front. At the same time, the pressure needed to transport the non-wetting phase to the face exposed to non-wetting phase decreases. At some point, the pressure in the non-wetting

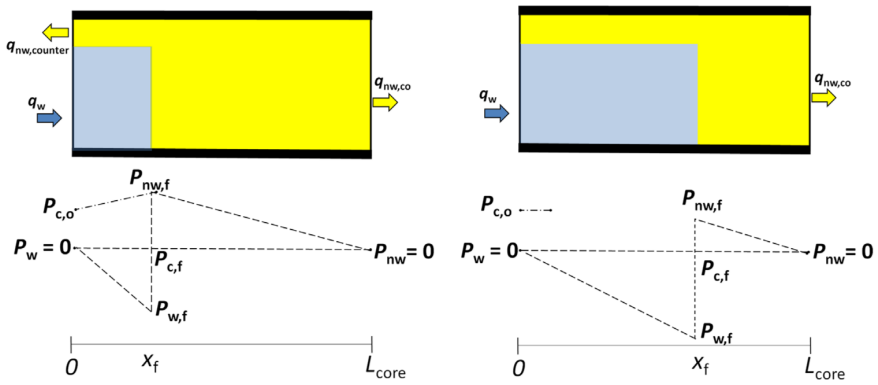

Figure 2.5: The pressure in the non-wetting (P_{nw}) and wetting (P_w) phase at two different time steps during TEOFSI with one end face exposed to the wetting fluid (left face), and the other end face exposed to the non-wetting fluid (right face). Left figure: Combination of co- and counter-current imbibition. Right figure: Purely co-current imbibition. (Haugen et al. 2014).

phase will become lower than the capillary back pressure (illustrated by the right side of figure 2.5), and counter-current production will cease. The pressure distribution during the spontaneous imbibition is illustrated in figure 2.5, showing the distribution when counter-current production occurs (left) and when it does not occur (right).

2.4 Wettability measurement

There are many different ways to indicate the wettability of a porous medium. Anderson (1986*b*) listed these methods divided into two sub-categories; quantitative methods, and qualitative methods. For this thesis, the Amott-Harvey method (quantitative), the imbibition test (qualitative), and the flotation method (qualitative) was used to indicate the wettability of sand and sand packs. The Amott method (Amott 1959) consists of a procedure involving spontaneous- and forced displacement. This should be done with both fluids involved, and the volumes displaced by each is to be recorded. The results are presented by the Amott oil index (δ_o), and the Amott water index (δ_w):

$$\delta_o = \frac{V_{wsp}}{V_{wt}} \tag{2.9}$$

where V_{wsp} is the volume of water spontaneously displaced by oil, and V_{wt} is the volume of water displaced by oil in total.

$$\delta_w = \frac{V_{osp}}{V_{ot}} \tag{2.10}$$

where V_{osp} is the volume of oil spontaneously displaced by water, and V_{ot} is the volume of oil displaced by water in total.

As a porous medium tends towards strongly water-wet, the Amott water index approaches 1, and the oil index approaches 0. For oil-wet samples, the water index approaches 0, and the oil index approaches 1.

Boneau & Clampitt (1977), Trantham & Clampitt (1977) used a revised edition of the Amott wettability test where the Amott-Harvey index, I_{AH}, is calculated. The core is saturated in brine before oil is injected until the irreducible water saturation is reached. Then δ_w and δ_o from equation 2.10 and 2.9 are measured. The Amott-Harvey index is then given by:

$$I_{AH} = \delta_w - \delta_o \tag{2.11}$$

According to Cuiec (1984) the value of I_{AH} indicates the wettability of the porous medium. I_{AH}=1 indicates strongly water-wet, I_{AH}=-1 indicates strongly oil-wet, -0.3>I_{AH}>-0.1 indicates slightly oil-wet, -0.1>I_{AH}>0.1 indicates neutral wet, and 0.1>I_{AH}>0.3 indicates slightly water-wet.

There are also qualitative ways of evaluating the wettability of a porous medium. Evaluating spontaneous imbibition gives an idea of the wettability, i.e. measuring the rate and amount of non-wetting fluid displaced during spontaneous imbibition. According to Anderson (1986*b*), the porous medium is strongly water-wet if large volumes of water imbibe at a high rate. In the case where smaller volumes of water imbibe at a lower rate, the medium is more weakly wetted.

The flotation method, suggested by API (Anderson 1986*b*), was used to test the wettability of the sand grains used in the sand pack. In this method, water, oil, and sand are placed in a container and shaken (Nutting 1925, Bartell & Osterhof 1932, Rust 1957). If the sand grains settle to the bottom of the container, they are considered water-wet. If the grains are suspended in the oil/water contact, and grains in the water clump together, they are considered to be oil-wet. This test gives good indications in case of a strongly wetted sand.

The Amott-Harvey index is insensitive near neutral wettability (Anderson 1986*b*) because it measures the amount of wetting fluid spontaneously imbibed. However, when the contact angle is roughly 60 to 120°, neither fluid will imbibe spontaneously. For the sand packs used in this thesis, which are assumed strongly water-wet, the Amott-Harvey index will define whether they are strongly water-wet as assumed.

2.4.1 Wettability alteration

In its original state, most reservoir minerals are strongly water-wet. By adsorption of polar compounds, in crude or mineral oil, and deposition of organic matter, wettability can be changed towards oil-wet (Anderson 1986*a*). The polar compounds contain a hydrocarbon end so that when the polar end adsorbs to the rock surface, it exposes its hydrocarbon side making the surface oil-wet. For a reservoir core, the wettability can change when it is transported from the subsurfaces (Anderson 1986*a*). It is therefore often necessary to restore its wettability to its original state. This can be done by static aging or dynamic aging (Fernø et al. 2010).

In static aging, a stagnant level of crude oil saturates the core at an elevated temperature. It has been shown that it can take up to 1000 hours for the process to reach equilibrium (Wendell et al. 1987). Fernø et al. (2010) also showed that when aging statically, the Amott water index, δ_w, never reached values lower than 0.25. When aging dynamically, the core is continuously flooded with crude oil at an elevated temperature (Fernø et al. 2010). This method uses less time to age the core compared to static aging. For example, static aging required 3 times as long to age the core to δ_w=0.25 compared with dynamic aging (Fernø et al. 2010).

For the preliminary studies performed on sandstone cores, it was observed that the wettability changed as a function of time stored in paraffinic lamp oil. The cores were kept in a stagnant volume of paraffinic lamp oil, i.e. they were subject to static aging.

2.5 Viscosity

The viscosity of a fluid is a quantification of its resistance to flow. The resistance occurs because the molecules of the flowing fluid interact with each other. In general, fluid viscosity is dependent on temperature (Seeton 2006). When the temperature is increased, the molecular energy increases, leading to a greater distance between the molecules, which in turn reduces the intermolecular forces causing a reduction in viscosity. The Newton model quantifies viscosity, μ, as the proportionality constant between the applied shear stress τ, and the velocity gradient du/dy of a linear flow:

$$\tau = \mu \frac{du}{dy} \tag{2.12}$$

u is the fluid flow velocity and y is the direction normal to the flow direction.

In a hydrocarbon reservoir, a waterflood is affected by the viscosity of both the injected and the

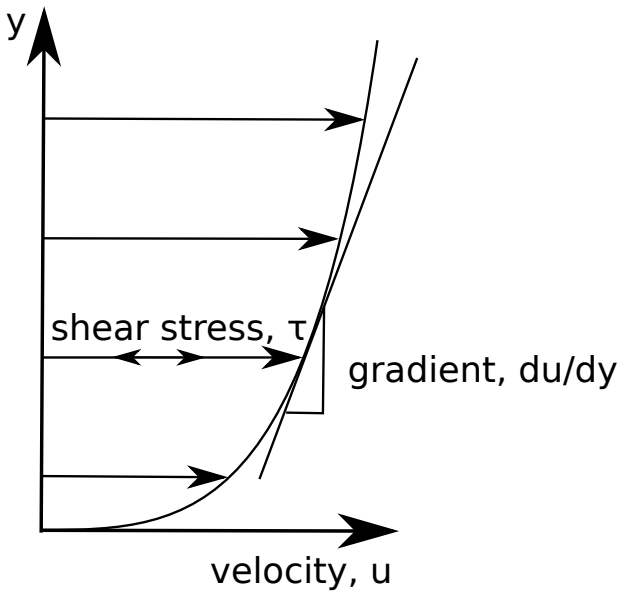

Figure 2.6: Flow velocity increases with distance from the wall at y=0. The velocity gradient, $\frac{du}{dy}$, is proportional to the shear stress, τ, by the viscosity, μ.

displaced fluid. The efficiency of an injection strategy can be evaluated by the fractional flow of water, f_w, which quantifies the fraction of water being produced from a production well. f_w is directly affected by the mobility ratio, M, between the water injected and the oil/gas displaced, which in turn is affected by the viscosity of the fluids. The higher the viscosity of a fluid, the lower its mobility is. If the injected water has a lower viscosity than the displaced fluid, i.e. a higher mobility, it can lead to earlier water breakthrough (Anderson 1987*c*). The mobility ratio was defined by Aronofsky (1952) as:

$$M = \frac{\left(\frac{k_r}{\mu}\right)_w}{\left(\frac{k_r}{\mu}\right)_o} \tag{2.13}$$

For spontaneous imbibition, both Haugland (2016) and Meng et al. (2016) showed that the rate of imbibition decreases as the wetting phase viscosity increases. At the beginning of the imbibition, oil with low viscosity saturates the porous medium. When a wetting fluid of high viscosity imbibes, the rate of spontaneous imbibition rapidly decreases, as shown in figure 2.7. This happens because the resistance of transporting the viscous wetting fluid to the front increases as the front propagates away from the face exposed to the wetting fluid Haugen et al. (2014). This causes the imbibition rate to decrease.

The viscosity of brine can be increased by adding glycerol or polymers. In this thesis, both glycerol and a partially hydrolyzed polyacrylamide (HPAM) polymer was used to increase brine viscosity during spontaneous and forced imbibition. This was done to study the effect of elevated pressures on the stability of the sand packs, as well as the impact viscosity has on ultimate recovery and recovery rate during spontaneous imbibition. When the volumetric flow is kept constant, the pressure gradient through the sand pack increases as the viscosity of the displacing fluid is increased. This possibly has a bigger effect on the stability of the sand packs and has been investigated.

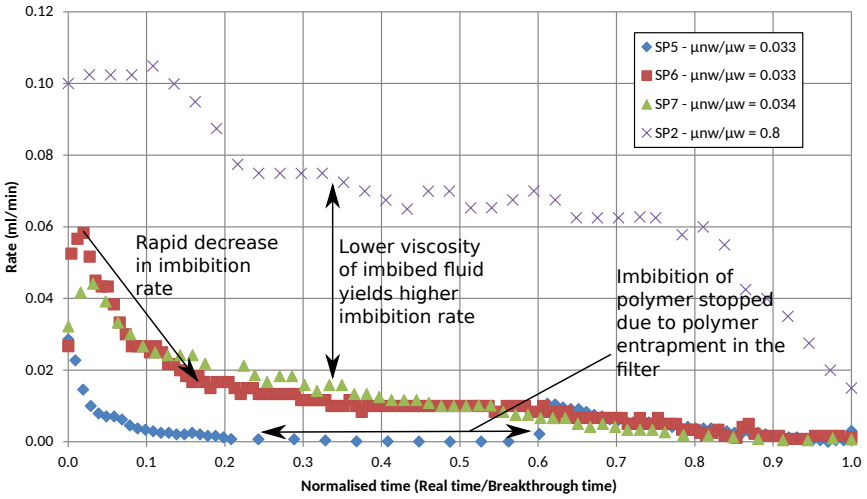

Figure 2.7: Spontaneous imbibition rate during experiments with varying wetting fluid viscosity performed by Haugland (2016). The viscosity of the non-wetting fluid was held constant, whereas the wetting-fluid viscosity was altered by adding glycerol (SP7) and a partially hydrolyzed polymer (SP5, SP6).

2.5.1 Polymers

Polymers are used to increase the viscosity of water and improve waterflood mobility during a flooding of a hydrocarbon reservoir. This gives a more efficient displacement. Both synthetic polymers and biopolymers are commonly used (Sheng et al. 2015), and the synthetic HPAM is, by far, the most applied (Sorbie 1991, Sheng et al. 2015). For this reason, HPAM was used in the experimental work of this thesis.

HPAM is made by partially hydrolyzing polyacrylamide molecules. Acrylamide monomers are stringed together, making long-chain molecules (polyacrylamide). These molecules are then hydrolyzed, forming anionic carboxyl groups that replace some of the amide groups along the backbone chain (Lake et al. 2014). The process is illustrated in figure 2.8. The HPAM molecule is very

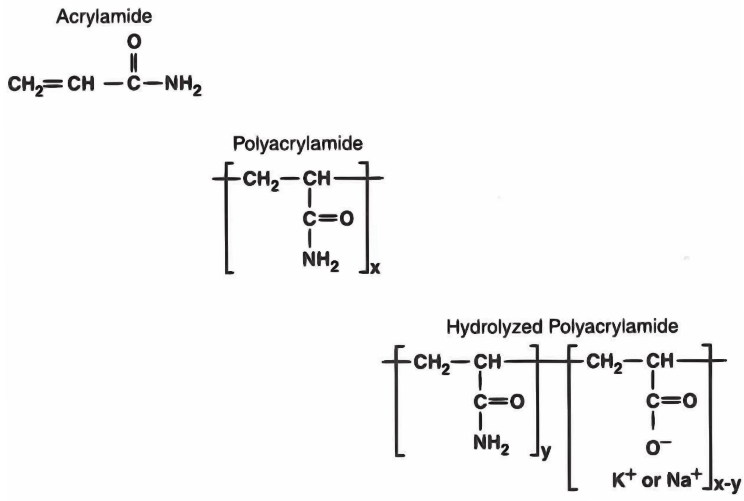

Figure 2.8: Polyacrylamide synthesis and molecular structure, where y indicates the number of amide groups (for HPAM) an x-y the number of carboxylic groups. The degree of hydrolysis is given by the ratio of the moles of carboxylic groups to amide groups. If anions or cations are present, they may shield the carboxylic groups as shown. (Lake et al. (2014)).

flexible, and has a high molecular weight. These large molecules are subject to anionic repulsion both internally and to other molecules, which make them effectively larger. This characteristic is what makes them increase the viscosity of the solution where they are present. For HPAM, the molecular weight and degree of hydrolysis affect properties such as solubility in water, viscosity, and retention, and should be chosen specifically for each case. The degree of hydrolysis is specifically important, as the polymer will be insoluble in water at a very low degree, and too sensitive to salinity and hardness at a high degree (Shupe 1981).

HPAM solutions have non-Newtonian characteristics, which means that there is a non-linear relationship between the viscosity of the solution and the shear-rate as illustrated in figure 2.9. This means that when the flow rate of the polymer is high, the polymer solution will be less viscous. In addition to this, HPAM is particularly susceptible to mechanical degradation (Lake et al. 2014). This means that if the solution is subject to some maximum shear rate, the solution looses some of its low shear rate viscosity as illustrated in figure 2.9. When the polymer molecules are subject to these high shear rates, they break and become shorter, making the solution less viscous.

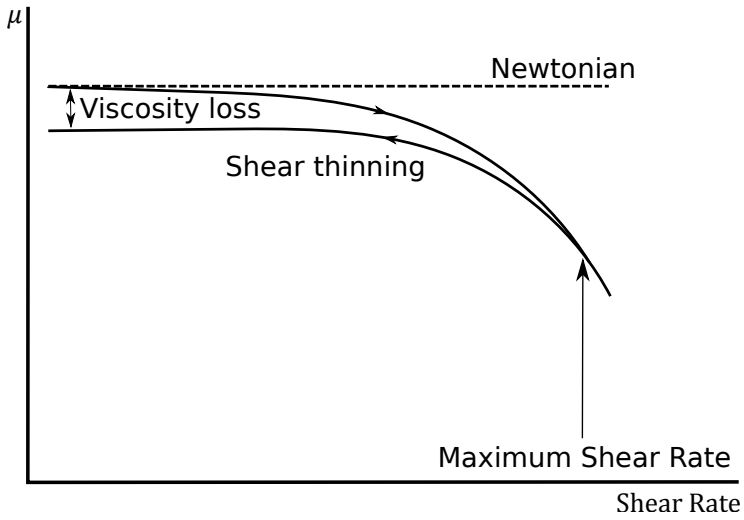

Figure 2.9: Mechanical degradation of polymer solution. The arrows show the direction of shear rate acceleration. (Lake et al. (2014)).

Many studies have shown that the adsorption of polymers in a porous medium can dramatically reduce the relative permeability to water, compared to the relative permeability to oil (Sparlin 1976, Zaitoun et al. 1991, Barreau et al. 1997). This behavior was observed during experimental work with HPAM polymer solutions, as further discussed in section 9.3.1.

2.5.2 Glycerol

Glycerol has been used to increase the viscosity of aqueous solutions in experiments earlier (Rapoport & Leas 1953, Kyte & Rapoport 1958, Fischer & Morrow 2006). Fischer & Morrow (2006) report that glycerol of >99.5% purity has a viscosity of 1647 cP at 20 °C and is highly sensitive to temperature. The viscosity decreases when brine or distilled water is added, and viscosity as a function of glycerol concentration in a brine solution can be expressed by a modified expression of the viscosity of dispersions of spherical particles by van de Ven (Fischer & Morrow 2006), as shown in figure 2.10.

Takamura et al. (2012) showed that aqueous glycerol solutions have a contact angle of zero against refined oils on quartz surfaces. This means that glycerol will imbibe spontaneously in a porous medium containing quartz. Both the sandstone cores and the sand used in the experimental work has a high degree of quartz content, further discussed in section 4 and 5. Thus, it is expected that the porous media will have a strong wettability towards both glycerol solutions and brine.

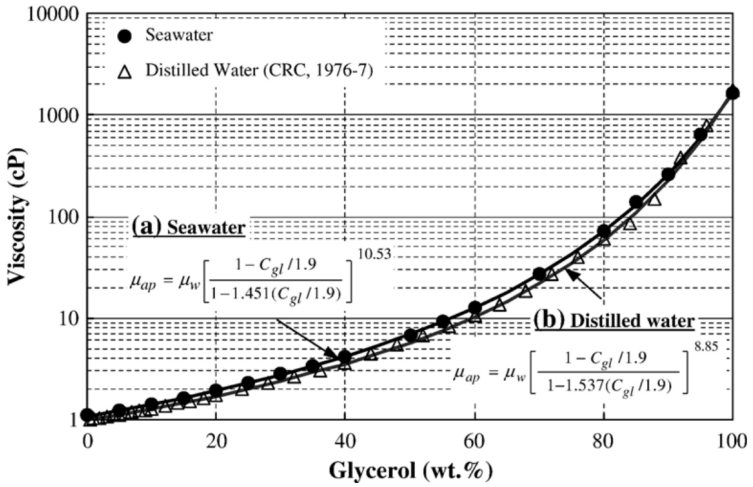

Figure 2.10: Viscosity of aqueous solutions as a function of glycerol consentrations (a) glycerol and brine solution, (b) glycerol and distilled water solution. μ_{ap} is the aqueous phase viscosity, μ_w is the brine/distilled water viscosity, and C_{gl} is the concentration of glycerol in wt%. (Fischer & Morrow 2006).

This makes it possible to study the effect of viscosity alone since other fluid properties are kept constant.

2.6 Scaling of spontaneous imbibition

In fractured reservoirs, most of the hydrocarbon volume is stored in the rock matrix in between fractures (Choi et al. 1997, Fernø 2012). The fractures have high permeability compared to the rock matrix and, in many cases, injected aqueous phase will flow straight past the matrix and only produce volumes originally in the fractures. This leaves large volumes of hydrocarbon behind. Because of this, spontaneous imbibition is an important recovery mechanism in such reservoir (Morrow & Mason 2001, Mason & Morrow 2013, Mirzaei-Paiaman & Masihi 2013, Schmid & Geiger 2013, Meng et al. 2016). This addresses the need for predicting spontaneous imbibition behavior in a reservoir. Many researchers have worked with developing scaling equations of spontaneous imbibition (Morrow & Mason 2001, Mirzaei-Paiaman et al. 2017) from laboratory experiments to reservoir scale.

Mirzaei-Paiaman & Masihi (2013) and Mirzaei-Paiaman & Masihi (2014) made extensive reviews of scaling equations for counter-current spontaneous imbibition and co-current spontaneous imbibition respectively. In both cases, new universal scaling equations were developed by correlating experimental data from earlier work. For this thesis, both the TEOFSI boundary condition (sand

packs) promoting co-current imbibition and the AFO boundary condition (sandstone cores) promoting counter-current imbibition were used. Capillary pressure and relative permeability data are needed to utilize the general scaling equations developed by Mirzaei-Paiaman & Masihi (2013) and Mirzaei-Paiaman & Masihi (2014). These data are generally hard to obtain (Meng et al. 2016), and because of this, scaling equations taking only routine core and fluid properties will be used in this thesis.

For counter-current imbibition, the scaling equation developed by Mason et al. (2010) will be used. It only takes routine core and fluid properties. The scaling equation scales production data to a dimensionless time considering sample shape and size, boundary conditions, and the viscosity of the wetting and non-wetting phase. It is expressed as:

$$t_{D,MFMR} = \frac{2}{L_c^2}\sqrt{\frac{K}{\phi}}\frac{\sigma}{\mu_w\left(1+\sqrt{\mu_{nw}/\mu_w}\right)}t \tag{2.14}$$

where K is the absolute permeability of the core, ϕ is the porosity, σ is the interfacial tension between the wetting and non-wetting phase, μ_{nw} and μ_w are the non-wetting and wetting phase viscosities, and t is the time. L_c is the characteristic length, compensating for different boundary conditions defined by Ma et al. (1995) as:

$$L_c = \sqrt{\frac{V_{total}}{\sum_{i=1}^{i=n}\frac{A_i}{x_i}}} \tag{2.15}$$

where V_{total} is the total volume of the core, A_i is the area open to imbibition in the ith direction, x_i is the distance between the open surface i to the no-flow boundary, and n is the number of surfaces exposed to the wetting fluid. The characteristic length for the boundary condition AFO was derived by Zhang et al. (1996) as:

$$L_c = \frac{L_s d_s}{2\sqrt{d_s^2 + 2L_s^2}} \tag{2.16}$$

where L_s is the core sample length and d_s is the core sample diameter.

It must be mentioned that this scaling equation does not account for variations in wettability. When scaled production data are plotted against each other with dimensionless time on the x-axis and recovery on the y-axis, production data of weakly wetted porous media would systematically be plotted to the right of strongly wetted media (Mirzaei-Paiaman & Masihi 2013).

For co-counter spontaneous imbibition, Mirzaei-Paiaman & Masihi (2014) proposed a simplified

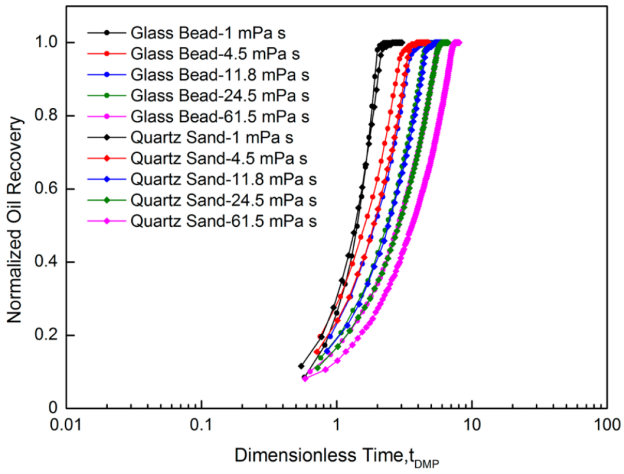

Figure 2.11: Scaled production data for TEOFSI spontaneous imbibition in glass bead and quartz sand porous media. Figure from Meng et al. (2016).

equation for scaling production data to dimensionless time:

$$t_{D,MPM} = \sqrt{\frac{2\sigma\sqrt{\frac{K}{\phi}}}{\left(\mu_{nw} + \sqrt{\mu_w \mu}\right) L_s^2}} t^{1/2} \tag{2.17}$$

where L_s is the sample shape of the sand pack. Mirzaei-Paiaman & Masihi (2014) stresses that the scaling equation might not scale well for systems with different initial saturations of the wetting phase. Later, Meng et al. (2016) showed that the scaling equation did not correlate well between porous media of regular and irregular porous structure. In this case, production data would fall into different groupings when plotting against dimensionless time, as seen in figure 2.11.

3 The progress of spontaneous imbibition in unconsolidated sand

There are big experimental challenges in working with sand packs. This has been shown through the work of Vabø (2016), Haugland (2016), and Føyen (2017). When such challenges are present, sand packs cannot be used in the investigation of more complex phenomena. For example, if polymers impact on wettability is to be investigated, all sand pack properties needs to be constant such that the sand pack wettability can be drawn out specifically. If for example, the pore structure changes between floodings because of bad compaction, a reduction in wetting phase spontaneous imbibition cannot specifically be tied to a wettability change. It can also be because of a wider pore size distribution, or other pore structure irregularities. There are some significant experimental challenges associated with sand packs. This has been shown through the work of Vabø (2016), Haugland (2016), and Føyen (2017). Sand packs can add valuable knowledge to the effect of wettability altering chemicals on capillary pressure, relative permeability, and spontaneous imbibition Føyen (2017). To investigate these effects, uniform and stable unconsolidated sand packs are needed. Vabø (2016) had problems with irregular saturation fronts, which, in turn, led to bypassed oil (see figure 3.1). The problem was allocated to the inlet filter, causing a restricted flow of wetting phase at the inlet. Haugland (2016) solved the problem by changing to a paper filter with lower flow resistance, obtaining piston-like displacement fronts. His experimental set-up enabled measurement of counter-current production. Haugland (2016) used glycerol and polymer

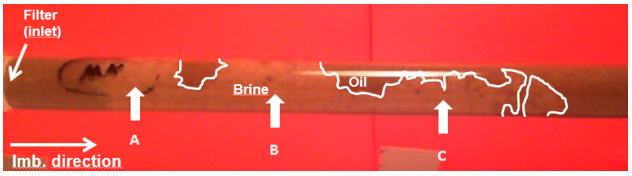

Figure 3.1: Problems with irregular saturation front and bypassed oil during spontaneous imbibition. One can clearly observe bypassed oil as the darker areas of the sand pack. (Vabø 2016).

to increase the viscosity of the aqueous phase. During spontaneous imbibition with an HPAM polymer solution, polymer retained in the inlet filter caused a reduction of the imbibition area at the exposed face, which stopped the imbibition of the polymer solution. After the inlet filter was removed, production started again as seen in figure 3.2. The experimental set-up did not allow forced displacement, and permeability measurements or re-drainage of the system could not be performed. Føyen (2017) developed a new experimental set-up allowing forced displacement and better control of the inlet pressure. This thesis utilized this set-up, and it will be elaborated in the next chapter on methods and experimental set-up. Føyen (2017) observed problems related to the

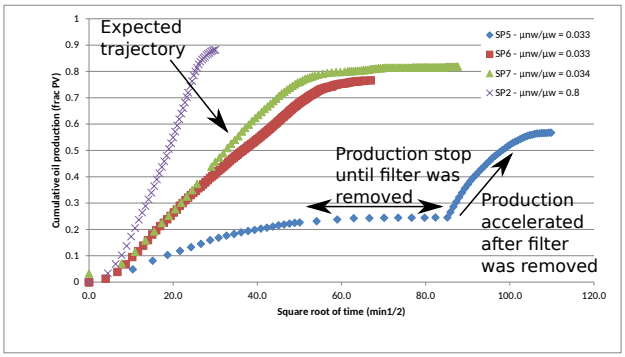

Figure 3.2: Production curves from spontaneous imbibition in unconsolidated sand. The aqueous (wetting) phase viscosity was altered by adding glycerol or HPAM polymer. Notice the production stop (blue diamonds) due to polymer retention in the inlet filter. (Haugland 2016).

compaction of the sand in the imbibition tubes. During experiments, a dye was added to the wetting and non-wetting phase to visualize the saturation front during spontaneous imbibition with initial water saturation. He observed local wettability alterations, causing sequential layers of oil and brine saturated pores (see figure 3.3). It was proposed that the dye added to the non-wetting phase caused the sand to change its wettability. The sequential nature of the wettability alteration can be explained by the method used for packing the sand packs. The imbibition tube was shaken between each sand filling sequence to compact the sand. This caused granular convection leading to size segregation where the larger sand grains moved upwards relative to the smaller grains. By this, separated layers of large and small grains occurred. Because pore size is proportional to grain size in a well-sorted sand, the sand packs had sequential layers of smaller and larger pores. In a mixed-wet sand, wettability depends on the pore size, showing that the pores were segregated by size. Føyen (2017) also had challenges with the stability of the sand packs. In many of his experiments, the sand packs collapsed during forced displacement, causing an alteration of the porous structure. This is critical, because it indirectly affects properties like capillary pressure, wettability, and permeability. With the end pieces and the associated modification of the imbibition glass tubes, the tubes were easily shattered.

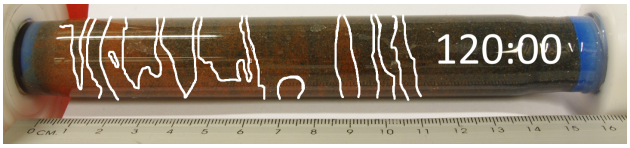

Figure 3.3: Heterogeneous pore size distribution due to compaction method of sand caused mixed-wettability in sand pack. Red colored phase is brine, blue colored phase is n-Decane. The white stripes indicate the separation between the layers of different wettability. (Føyen 2017).

This thesis builds on the experiences made by Vabø (2016), Haugland (2016), and Føyen (2017), and addresses the problems related to sand packs to establish homogeneous and stable sand packs for spontaneous imbibition investigations. This was done by developing a new method to compact the sand, and by developing a new end piece.

Part II

Methods and Experimental Set-Up

4 Sandstone core plugs

Experimental work on sandstone core plugs was conducted in collaboration with Simon Reite as a preliminary to the work on the unconsolidated media. These experiments were conducted to investigate if paraffinic lamp oil had an impact on the wettability of the sand, and to work as a baseline for the experiments conducted on sand packs. The cores used were of Bentheimer Sandstone from the Gildenhausen quarry in Germany. Bentheimer is ideal for reservoir studies because it is homogeneous in terms of grain size distribution, porosity, and permeability (Peksa et al. 2015). It contains approximately 91.7 wt% quartz (Peksa et al. 2015), which is a strongly water-wet mineral (Anderson 1986*a*). This makes it possible to compare experimental results from different core plugs directly, and gives good conditions for spontaneous imbibition of aqueous phases. Cylindrical cores of approximately 6 cm length where diameter varied between 4.7 and 5.2 cm were used. 10 core plugs were prepared and labeled SSxx, where xx is a number between 1 and 10.

4.1 Porosity measurements

Porosity was measured by saturating the core plugs with a fluid. The core plugs were weighed before and after saturation. The porosity was calculated by equation 2.1:

$$\phi = \frac{m_{sat} - m_{dry}}{\rho_i} \frac{1}{V_b}$$

All core plugs were directly saturated with a degassed fluid. The core plugs were placed in a sealed container connected to a vacuum pump. The fluid was degassed in a separate fluid container directly connected to the vacuum pump and the container of the core plug. When both fluid and core plug was evacuated, the core plugs were exposed to the fluid by opening the valve between the two containers, and the core plug was completely saturated. The set-up is shown in figure 4.1.

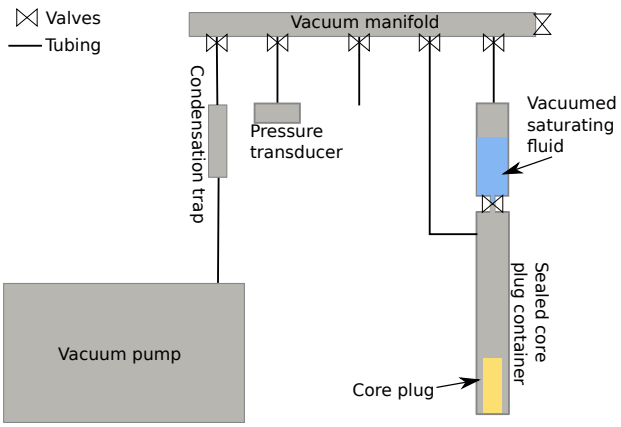

Figure 4.1: Set-up for saturating sandstone core plugs.

9 core plugs were directly saturated with paraffinic lamp oil, whereas one was saturated with brine.

4.2 Permeability measurements

After saturation, absolute permeability was measured by injecting the core plugs with the saturating fluid. The core plugs were placed in a Hassler Core Holder connected to a high precision Pharmacia pump. On the inlet side, an ESI pressure transducer was connected to measure the differential pressure over the core plug during constant volumetric injection. The volumetric flow was sequentially changed between 200 and 499 ml/h. By Darcy's law (equation 2.2), absolute permeability was calculated.

Pressure was recorded every second, and the absolute permeability was taken as the average of calculated absolute permeability from all recordings. The error was taken as the standard deviation of these calculations. An example of the pressure reading during absolute permeability measurement is represented in figure 4.2.

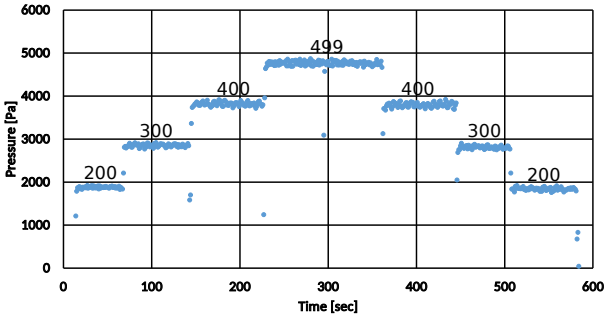

Figure 4.2: Pressure recordings during absolute permeability measurement. The numbers above the graph indicates the injection rate in ml/h when the recordings were taken.

4.3 Spontaneous imbibition

Seven of the core plugs were exposed to spontaneous imbibition. The core plug initially saturated with brine was drained by injecting paraffinic lamp oil before spontaneous imbibition was conducted. The 6 remaining core plugs were stored in paraffinic lamp oil to investigate the effect of storage time on core plug wettability. As will be discussed later, an effect was observed. Different aqueous solutions were used as the wetting imbibing fluid. An experimental overview of the core plugs can be found in table 4.1.

The core plugs were placed in imbibition cells for spontaneous imbibition as seen in figure 4.3. The imbibition cell was saturated with a wetting aqueous phase, leaving the core plugs exposed for spontaneous imbibition with the boundary condition AFO. The imbibition cell contained a bulk volume, for placing the core plugs, connected to a graduated cylinder for recording produced volumes during the spontaneous imbibition. The volume of non-wetting phase produced was recorded at different time steps during the spontaneous imbibition.

Table 4.1: Experimental overview of Bentheimer sandstone core plugs. S_{wi} is the inital water saturation before initializing spontaneous imbibition (the volume fraction of water in the total pore volume of the core plug)

Core	Fluids WF=Wetting fluid NWF=Non-wetting fluid	S_{wi} $\left[\frac{V_w}{V_p}\right]$	Storage time [Days]	Spontaneous imbibition P=Performed NP=Not performed
SS01	WF=Glycerol solution NWF=Lamp oil	0	>6 days	P
SS02	WF=Brine NWF=Lamp oil	0	>6 days	P
SS03	WF=Glycerol solution NWF=Lamp oil	0	>6 days	P
SS04	WF=N/A NWF=Lamp oil	0	N/A	NP
SS05	WF=N/A NWF=Lamp oil	0	N/A	NP
SS06	WF=N/A NWF=Lamp oil	0	N/A	NP
SS07	WF=Glycerol solution NWF=Lamp oil	0	2 days	P
SS08	WF=Brine NWF=Lamp oil	0	2 days	P
SS09	WF=Polymer solution NWF=Lamp oil	0.223	1 day	P
SS10	WF=Polymer solution NWF=Lamp oil	0	1 day	P

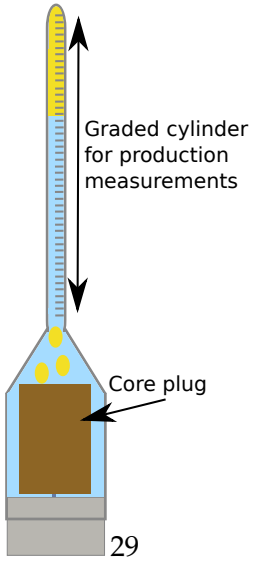

Figure 4.3: Imbibition cell saturated with aqueous wetting phase. Sandstone core plug is placed in the bottom bulk volume, and produced oil is recorded in the graded cylinder above.

5 Sand packs

For this thesis, sand was used for preparing an unconsolidated porous medium. The work conducted builds on the progress and experiences made by Vabø (2016), Haugland (2016), and Føyen (2017). This chapter lists and describes the parts and procedures needed to prepare the sand as an unconsolidated porous medium, hereafter called a sand pack. In total, 19 sand packs were prepared and 60 experimental steps were performed.

5.1 Sand

Investigations made with a microscope by Vabø (2016) showed that the sand contained a high amount of quartz. This makes the sand comparable to Bentheimer sandstone with strong water-wettability. The biggest difference being the cementation of the sand grains in the Bentheimer sandstone.

The sand was previously prepared. It was first flushed with tap water for 48 hours to remove organic content and impurities. Then it was sieved using geological sieves by a sequential procedure until the grain size ranged from 150 μm to 212 μm. After drying the sand at 60°C it was burned, as proposed by Brown & Fatt (1956), at 500°C for at least five hours to ensure that all organic material was removed, rendering the sand strongly water-wet. The full process of preparing the sand is extensively covered by Vabø (2016), Haugland (2016), and Føyen (2017). The sand wettability was qualitatively checked by the flotation method described in chapter 2.4. The sand grains settled to the bottom of the container, indicating they were water-wet.

Two sand packs were made with sand washed in 65 wt% nitric acid and treated with HMDS, an organosilicon compound, in an attempt to alter the sands wettability. The sand was boiled in nitric acid for 30 minutes to oxidize and clean the surface of the grains. The sand was then covered in distilled water, and concentrated sodium hydroxide was added to neutralize the diluted acid solution to a pH of between four and nine. The sodium nitrate salt was removed by changing the distilled water several times before the sand was dried in a heating cabinet. Then sand and HMDS were placed in separate vacuum chambers connected to the same system (see figure 5.1). Both HMDS and sand was dehydrated and deoxygenated by purged N_2-vacuum cycles at 90°C. The valves between the two containers were opened, and the pressure of the system was lowered to approximately 0.5 Torr before the valve to the pump was closed, leaving the system closed. HMDS vaporized, and the sand was left at rest in the vapor for two hours at 90°C. At last, the system was evacuated by 3 purge cycles with N_2-vacuum to remove excess HMDS. This process

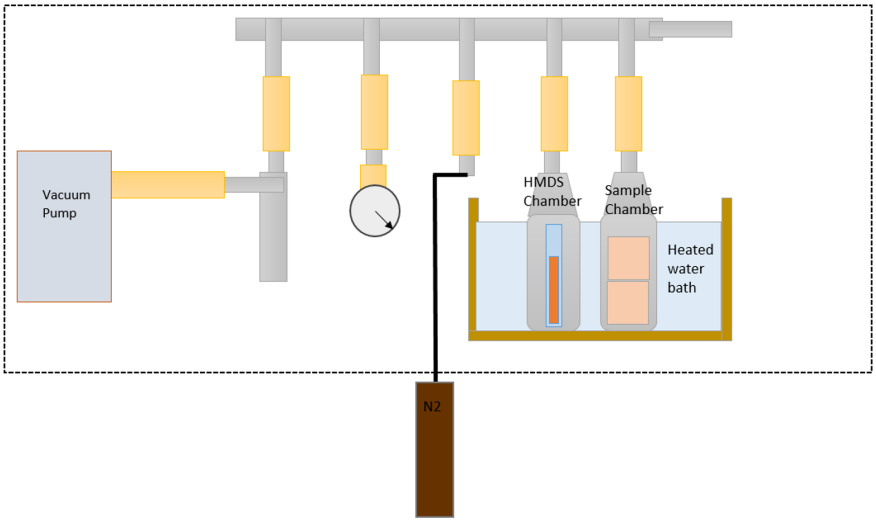

Figure 5.1: Set up for treating sand with HMDS. (Made by PhD candidate Tore Føyen).

was carried out by professor Martin Fernø and Ph.D. candidate Tore Føyen, and the complete procedure is presented in appendix D.

5.2 Glass tubes

For the sand to behave like a porous medium it needs to be contained. This was done by filling the sand into cylindrical glass tubes with an inner diameter of 2.05 cm and length between approximately 10 and 20 cm. By using glass tubes, a cheap and simple method to observe the saturation front development was achieved. This gives valuable information on the spontaneous imbibition and helps to decide if the displacement is piston-like or not.

Two different glass tubes were used. One with threaded ends, and one without threaded ends (see figure 5.2). Note that the inner diameter of the glass tubes with threaded ends narrows down at the threads.

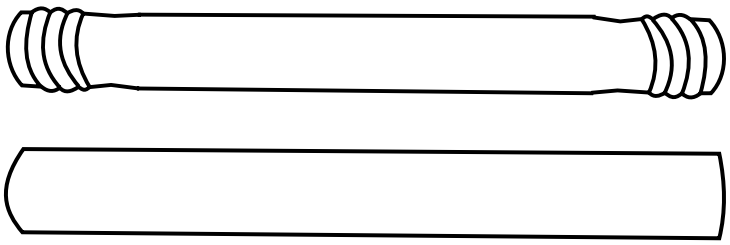

Figure 5.2: Scethces of the two glass tube designs used. The upper was with threaded ends, whereas the lower was without.

5.3 End pieces

An end piece is a construction that helps to contain the sand inside the glass tube. An inlet end piece was attached to one side of the glass tube, whereas an outlet end piece was attached to the other. During a TEOFSI, the inlet is the face of the porous medium exposed to the wetting phase. The outlet is the face exposed to the non-wetting phase. The end pieces were constructed such that they kept a paper filter to contain the sand inside the glass tube. The construction of the end pieces was critical because it needed to ensure that the sand packs were sealed from the atmosphere. It also needed to allow both fluids and filters to be in direct contact with the sand, or else, spontaneous imbibition would not initialize. The end pieces were constructed such that they could be connected to tubing. The inlet end piece needed to be connected to a pump for three reasons: so that the sand pack could be evacuated before saturation, so that the wetting fluid could be vented through the inlet end piece during spontaneous imbibition, and so that the sand packs could be flooded during forced imbibition and drainage. The outlet end piece needed to be connected to a valve so that the sand pack could be evacuated and saturated. The end pieces were machined from polyoxymethylene (POM). Two designs have been used, both containing inlet and outlet: end piece A and end piece B, further described below.

5.3.1 End piece A

End piece A was designed to fit the threaded glass tubes (see figure 5.2). The inlet and outlet end piece each contained two parts. One part to support the paper filter and connection to pumps and valves, and one part with inner threads connected directly to the glass tube. The design is shown in figure 5.3. Stainless steel tubing was pulled through the back of the end piece to the position of the slot for supporting the paper filter, as seen from the figure. The stainless steel

tubing was attached by filling epoxy resin between the inner wall of the end piece and the tubing. This ensured that the end piece was sealed from leakage caused by the tubing. All tubing attached to the end pieces had an outer diameter of ¼ “. For the outlet end piece, a single tube running through the center of the end piece was attached. For the inlet end piece, two stainless steel tubings were attached. This enabled circulation of the imbibing fluid through the inlet end piece during spontaneous imbibition (further described in section 5.6).

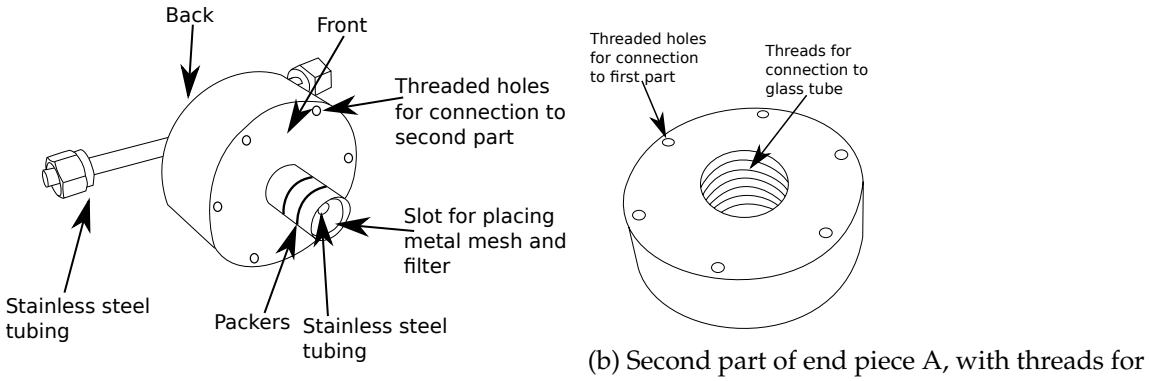

(a) Main part of inlet end piece A, with tubing.

(b) Second part of end piece A, with threads for assembling end piece on glass tube.

Figure 5.3: End piece A. Note that the outlet end piece is similar only with one centralized 1/4" tubing as opposed to the two as shown here.

The use of end pieces, although necessary, presented several challenges. The end pieces were attached to the glass tubes by threads, as described. The glass tube threads were handmade, thus the diameter of the opening and threads varied slightly. Because of this, the uniformly shaped end pieces did not fit each glass tube perfectly. This could cause challenges with insufficient sealing (i.e. leakage of fluids in the void between the end piece and the glass tube), or shattering of the glass tube (force was required for the end piece to enter the opening of the glass tube). Several sand packs were destroyed before experiments could be conducted due to the latter challenge. In addition, experimental results further described in section 9.2 indicated that the use of epoxy should be avoided. Because of these challenges a second end piece was designed.

5.3.2 End piece B

End piece B was designed to avoid the use of epoxy and the need for glass tubes with threaded ends. Sketches of the inlet end piece can be seen in figure 5.4. The inlet end piece was 3D-printed, but due to the density of the material, it did not seal sufficiently. Therefore, the end pieces were machined from polyoxymethylene (POM). These end pieces were machined with internal tubing to avoid stainless steel tubing. At the back of the end pieces, coning threads were machined to the

internal tubing to connect it to NPT-to-Swagelok connectors. The end pieces were designed such that both paper filter and fluid was in contact with the sand. The inlet end piece was designed with two internal tubes to enable circulation of the imbibing fluid through it (further described in section 5.6). The narrower tube of the inlet was machined at an angle to avoid conflict between two NPT-to-Swagelok connectors. The narrow tube had a diameter of 1.5 mm, whereas the second tube had a diameter of 0.635 mm. The outlet end piece was designed with one internal tube with a diameter of 0.635 mm running through the center of the end piece. By eliminating the threads, challenges related to varying glass tube-opening diameters was avoided.

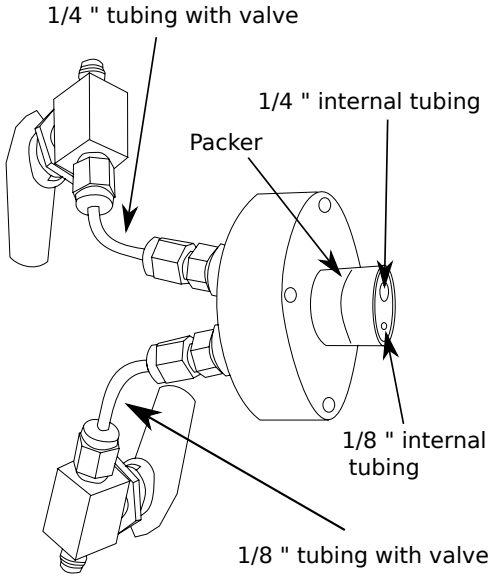

Figure 5.4: Inlet end piece B. Note that it does not include a second part with inner threads. Outlet end piece B is similar, only with one single centralized 1/4" tube.

5.4 Filters

A paper filter was placed in its designated slot of the end piece to keep sand from leaking into the end pieces and tubing. For mechanical support, a coarse metal mesh was placed behind the paper filter. The filter helped contain the sand, keeping the sand pack stabile during experiments, and promoted co-current imbibition by increasing the capillary back pressure. Vabø (2016) showed that the filter affects spontaneous imbibition by adding an additional resistance to flow. Meng et al. (2015) suggests a filter no thicker than 1 mm to avoid additional flow resistance. For this reason, thin paper filters were chosen. Three different filters were used:

- Whatman micropore (WM μ), with a pore size of 5 μm and thickness between 7 and 20 μm. Hydrophobic.
- Whatman quantitative filter paper, grade 589/2 (WM 589/2), with a pore size between 4 and 12 μm and thickness of 180 μm. Water-wet.
- Paper filter of unknown character (paper filter), earlier used by Haugland (2016) and Føyen (2017), showing good performance during spontaneous imbibition. Water-wet.

Experimental results further described in section 9.2.7 suggested that the Whatman micropore, being hydrophobic, affected the spontaneous imbibition, and it is suggested to avoid usage of this filter.

5.5 Packing procedure

A new packing procedure was developed because Føyen (2017) suggested challenges related to the packing procedure used by Vabø (2016), Haugland (2016), and Føyen (2017), as discussed in section 3. The packing procedure produced sand packs with a heterogeneous pore size distribution. Because of this, a packing rig was developed to enable sand compaction by applying pressure instead of shaking, eliminating the challenges with size segregated grains. The packing rig was designed so that a piston could be smoothly lowered and raised inside the glass tube. The rig is shown in figure 5.5.

When the sand was filled into the glass tube, the outlet end piece was attached to the glass tube as can be seen in figure 5.5. The glass tube was sequentially filled with approximately 3 grams of sand. The piston was then lowered, and a weight of 6.1 kg was added on top of the piston for 10 seconds to compact the sand. The sequence was repeated until sand filled the height of the glass tube. Then, a weight of 8.4 kg was placed on top of the piston, and the sand was compacted for an additional 17-18 hours. Finally, the inlet end piece was attached to the open end of the glass tube, fully containing the sand. The entire list of parts needed to assemble the sand packs are shown in figure 5.6.

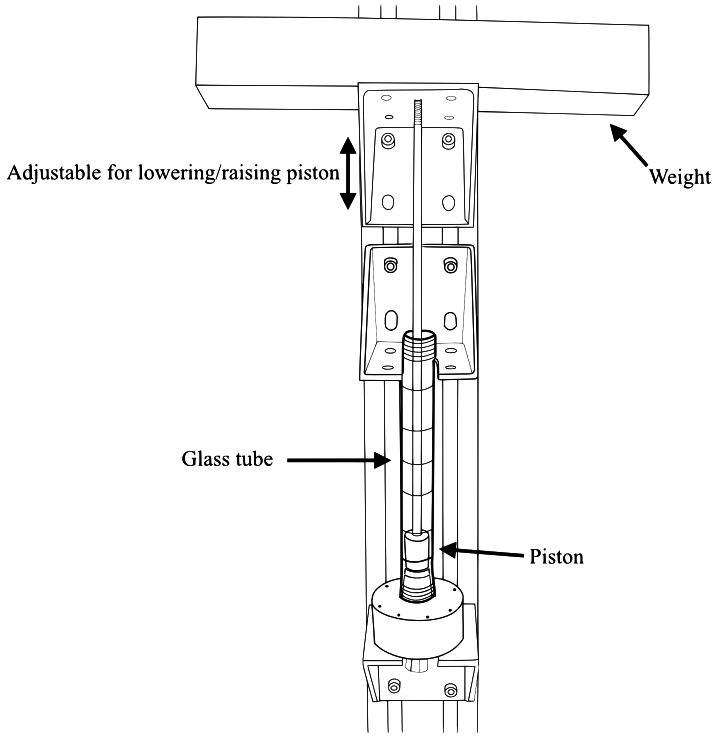

Figure 5.5: Packing rig used to compress sand inside the glass tubes.

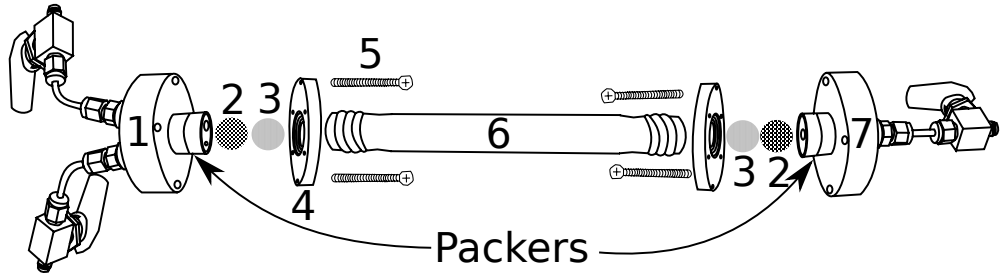

(a) Parts for assembling glass tube with threads and end piece A

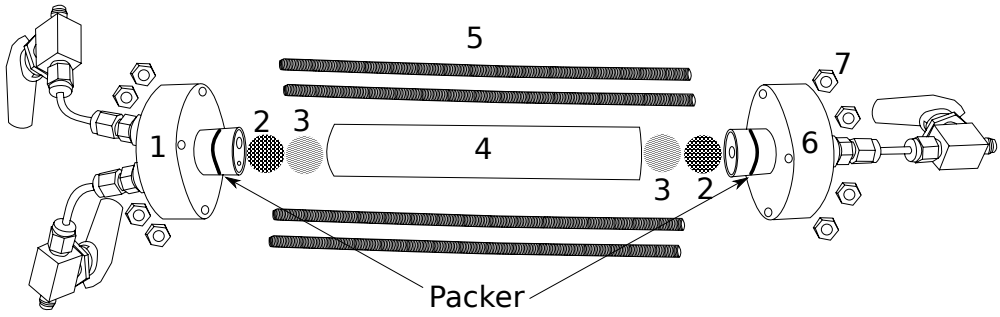

(b) Parts for assembling glass tube without threads and end piece B

Figure 5.6: Parts needed for assembling sand packs.

Table 5.1: List of parts needed to assemble the sand packs. See figure 5.6.

Glass tube with threads	Glass tube without threads
1. Inlet end piece A	1. Inlet end piece B
2. Metal mesh	2. Metal mesh
3. Filter	3. Filter
4. Threaded inlet end piece	4. Glass tube without threads
5. Screws	5. Threaded steel rods
6. Glass tube with threads	6. Outlet end piece B
7. Outlet end piece A	7. Nuts

As discussed, end piece A was designed for the glass tubes with threaded ends. The glass tubes without threaded ends were secured to end piece B by running four threaded steel rods between the two end pieces, securing them by nuts. There were no limiting factors controlling how tight the nuts were secured, possibly causing a high confinement pressure on the sand as discussed further in section 9.1.

After the sand packs were assembled, they were saturated by a degassed fluid. One tubing attached to the inlet end piece was connected to a vacuum pump, and the sand pack was evacuated from air. The degassed fluid was poured into a funnel connected to the outlet end piece. When the sand pack was evacuated, the valve between the sand pack and the vacuum pump was closed. The valve between the sand pack and the column of degassed fluid was opened, and the fluid rushed into the sand pack, completely saturating it. The weight of the sand packs was measured before and after to calculate the porosity by equation 4.1, subtracting the dead volume of the inlet and outlet end piece. An overview of all inlet and outlet end pieces used is presented in table 5.2.

Table 5.2: List of all end-pieces used in experiments with sand-packs. EPI are the inlet end-pieces whereas EPO are the outlet end-pieces. Inlet end piece A has two 1/4" tubes, whereas all inlet end piece B has one 1/4" tube and one 1/8" tube. The connection describes how the end-pieces were connected to tubing.

Inlet end pieces			Outlet end pieces			
End piece	DV [cm^3]	Design	End piece	DV [cm^3]	Tubing diameter [inch]	Design
EPI-1	6.9	A	EPO-1	3.0	1/4	A
EPI-2	7.6	A	EPO-2	2.7	1/4	A
EPI-3	3.1	B	EPO-3	1.4	1/8	B
EPI-4	3.1	B	EPO-4	1.9	1/8	B
EPI-5	4.4	B	EPO-5	1.9	1/8	B
EPI-6	4.1	B	EPO-6	2.1	1/8	B
EPI-7	3.4	B	SPO-7	2.9	1/4	B

5.6 Experimental set-ups

When the sand packs were completely saturated, they were connected to a pump to enable forced displacements and circulation of the wetting fluid through the inlet end piece during spontaneous imbibition. Two different set ups were used, set up A and set up B, further described below.

5.6.1 Set up A

Set up A was developed by Føyen (2017), and a sketch is shown in figure 5.7. The inlet was connected to a Pharmacia pump, and the second tubing of the inlet end piece was connected to a vertically held imbibition cell. The imbibition cell worked as a production trap for counter-currently produced non-wetting phase. The produced fluid was transported to the imbibition cell, collected, and registered by a camera. The production trap had an outlet opening so the wetting fluid could circulate freely. The outlet opening of the production trap was leveled with the outlet of the sand pack, minimizing the differential pressure across the sand pack. A second production collector was placed under the outlet of the sand pack, where co-currently produced fluid was collected and registered by a camera. Because a sensitivity to the height of the outlet of the sand pack and the outlet of the production trap caused a hydrostatic pressure through the sand pack, a second set up was designed.

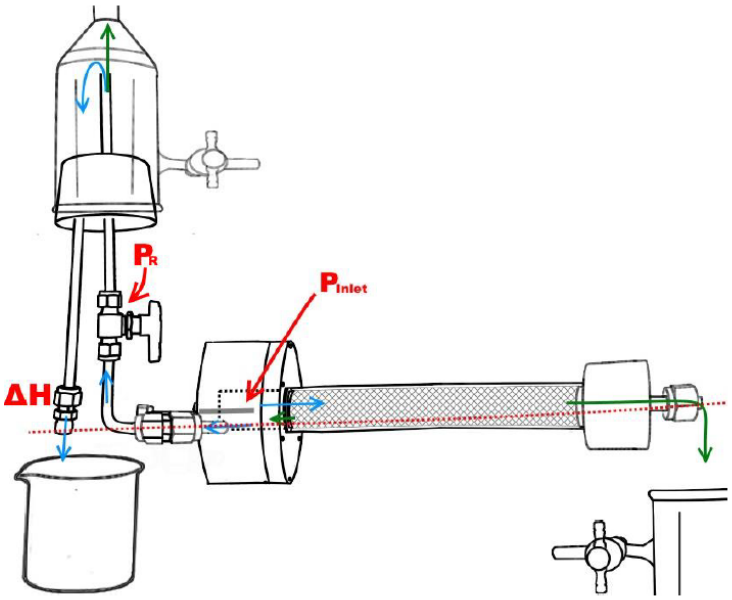

Figure 5.7: Experimental set up A scetched by Føyen (2017).

5.6.2 Set up B

In set up B, the sand packs were submerged in the wetting fluid, ensuring zero differential pressure across the sand pack. The set up is sketched in figure 5.8. An imbibition cell was connected to the tubing between the sand pack and the pump, working as a trap for the counter-currently produced non-wetting fluid. Counter-currently produced volumes would be transported by the flowing wetting fluid to the production trap, collected, and registered by a camera. A second production collector was placed above the sand pack outlet, where co-currently produced non-wetting fluid was collected and registered by a camera. A layer of mineral oil covered the bath of imbibing fluid to stop it from evaporating. The tubing was connected in a way such that an accumulator easily could be tied in, enabling forced flooding by glycerol or polymer solution. By lowering the sand pack in the wetting fluid, the hydrostatic pressure at both inlet and outlet side of the sand pack is ensured equal, eliminating any differential pressure across the sand pack during spontaneous imbibition.

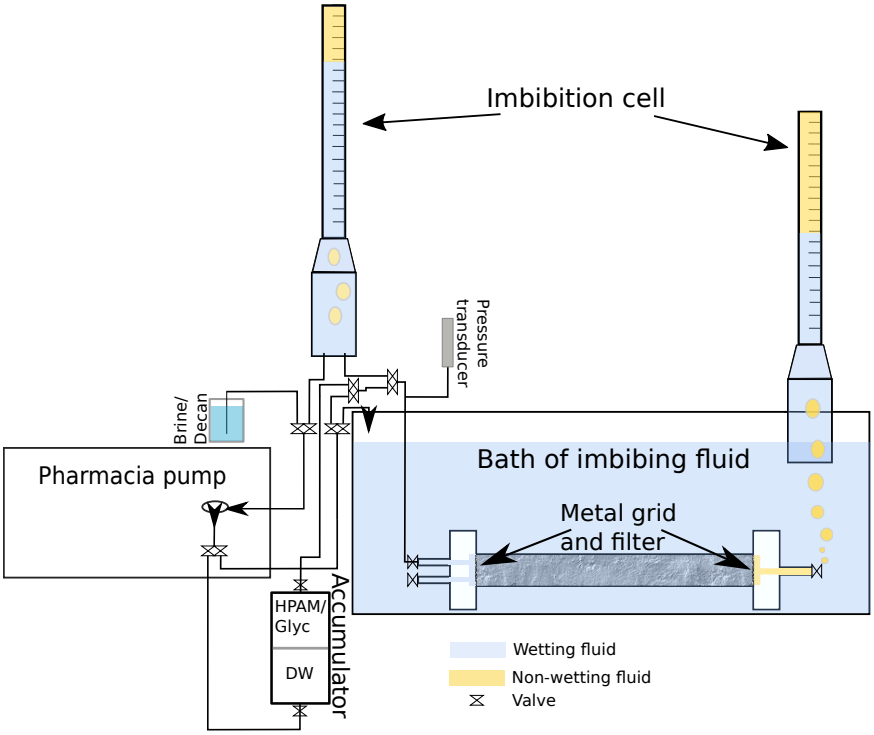

Figure 5.8: Experimental set up B scetched. Sand pack is submerged in the wetting fluid.

5.7 Sand pack overview

19 sand packs were prepared for experiments, all labeled SPxx, where xx is a number between 01 and 19. In table 5.3 all sand packs prepared are listed with end piece, experimental set up, and filter used for the sand pack.

Table 5.3: Overview of sand packs prepared including which end piece, experimental set up, and filter was used.

Sand pack	End piece	Experimental set up	Filter
SP01	A	A	WM μ
SP02	A	A	Paper filter
SP03	A	A	Paper filter
SP04	A	A	Paper filter
SP05	A	A	Paper filter
SP06	A	A	Paper filter
SP07	B	A	WM 589/2
SP08	B	A	WM 589/2
SP09	B	A	WM 589/2
SP10	B	A	WM 589/2
SP11	B	A	WM 589/2
SP12	B	A	WM 589/2
SP13	B	A	WM 589/2
SP14	B	A	WM 589/2
SP15	B	A	WM 589/2
SP16	B	A	WM 589/2
SP17	B	A	WM 589/2
SP18	B	B	WM 589/2
SP19	B	B	WM 589/2

5.8 Permeability measurements

Absolute permeability measurements were conducted by the same method as for the Bentheimer sandstone cores. A forced displacement was conducted by closing the valve on the second tubing of the inlet end piece. The constant volumetric flow was varied between 200 ml/h and 499 ml/h. The pressure was registered by an ESI pressure transducer, and the absolute permeability was calculated as the average for each volumetric flow step by Darcy's law. The error was taken as the standard deviation.

5.9 Spontaneous imbibition

Spontaneous imbibition was initiated by venting the wetting fluid through the inlet end piece, exposing the filter and the sand at the inlet side to the wetting fluid. The spontaneous imbibition was characterized by the boundary condition TEOFSI with the inlet side exposed to the wetting fluid and the outlet side exposed to the non-wetting fluid. For experimental set up A, the Pharmacia pump vented the wetting fluid through the inlet end piece, via the production trap, and out of the outlet of the production trap. For experimental set up B, the Pharmacia pump circulated the imbibing fluid from the bath of imbibing fluid, through the inlet end piece, via the production trap, and back into the bath of imbibing fluid. Spontaneous imbibition experiments were conducted on all sand packs. A forced start was needed to initiate spontaneous imbibition in several sand packs. The sand packs were exposed to the wetting fluid for several hours without any volumes imbibing. In these cases, the valve on the second tubing of the inlet end piece was closed, and wetting fluid was imbibed in the sand pack at a rate of 30 ml/h for 1 minute before opening the valve again.

The initial plan was to conduct several rounds of spontaneous imbibition on all sand packs, but due to unforeseen experimental challenges like leakage and shattered glass tubes, 10 of the sand packs were disposed of before secondary spontaneous imbibitions were conducted.

5.10 Forced imbibition and drainage

The experimental set ups were designed so that the second tubing of the inlet end piece could be closed, so that forced imbibition and drainage could be conducted on the sand packs. After spontaneous imbibition, forced imbibition was conducted until residual oil saturation (S_{or}) was reached. During the forced imbibition, pressure was monitored, and residual oil saturation was reached when the pressure leveled off and kept constant. At residual oil saturation, relative permeability of water ($k_{r,\bar{w}}(S_{or})$) was measured. The procedure for measuring the absolute permeability was followed, using the generalized Darcy's law (2.4) to calculate the relative permeability.

Drainage was conducted until irreducible water saturation (S_{iw}) was reached. For a strongly water-wet porous medium such as the sand pack, this water saturation is hard to obtain. During a drainage, there will be an early breakthrough of the non-wetting fluid, and the wetting fluid will produce for several injected poor volumes after breakthrough (Anderson 1987*c*). Therefore, it was decided that the irreducible water saturation was reached when the pressure during

drainage seemingly leveled off. The procedure for measuring $k_{r,w}$ was followed to measure the relative permeability of oil ($k_{r,o}(S_{iw})$). After drainage, some of the sand packs were used for a second spontaneous imbibition experiment, with an initial water saturation present.

6 Fluids

Mineral oils were used as the non-wetting fluid, whereas aqueous solutions were used as the wetting fluid. In this thesis, the viscosity of the wetting fluid has been varied by the addition of glycerol and polymers to the aqueous phase. Polymers are widely used to increase the viscosity of brine, and one object of the experimental work was to investigate if polymers affected spontaneous imbibition. The viscosities of the polymer and glycerol solutions were measured by a rotational viscometer (Brookfield DV-II+ Pro) with a laboratory bath to regulate the temperature. One mL of sampled fluid was placed in the viscometer cup. The viscosity was measured at different spindle rotational speeds given by rounds per minute (RPM).

6.1 Wetting fluids

In the cases where brine additives were used to increase its viscosity, brine was injected after forced imbibition to circulate the increased viscosity wetting fluid out of the sand pack. This was done to ensure similar initial conditions during SSI, with brine saturation for all sand packs.

6.1.1 5 wt% NaCl brine

A sodium chloride brine was prepared by mixing 5 wt% NaCl in distilled water. To prevent bacterial growth, 0.5 ml of a NaN_3 solution (0.2 g NaN_3 per mL solution) was added to every liter of brine. During one spontaneous imbibition, a red dye was added to the brine to visualize the saturation front. The red dye was a simple food coloring containing glycerin, water, and dye E124.

A model was made to calculate the viscosity of the 5 wt% NaCl solution as a function of temperature. Kestin et al. (1981) have collected viscosity data for NaCl solutions of different concentrations in the temperature range 20-150 °C and pressure range 0.1-35 MPa. From these data, a model for the viscosity of a 5 wt% NaCl solution at atmospheric pressure as a function of temperature, T, has been made by regression as seen in figure 6.1:

$$\mu(T) = 0.3919 \cdot T^2 - 41.112 \cdot T + 1745.9 \tag{6.1}$$

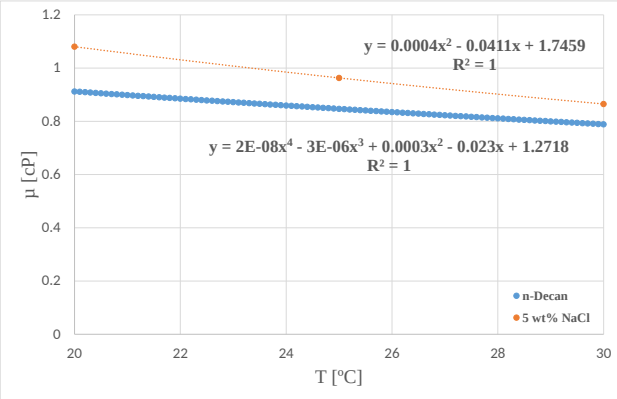

Figure 6.1: Viscosity models of 5 wt% NaCl solution and n-Decane with respect to temperature.

6.1.2 Glycerol solution

Glycerol was added to increase the viscosity of the brine. Glycerol was mixed with brine by using a magnetic stirrer. Three batches with two different concentrations of glycerol were used: 72 wt% glycerol, and 69 wt% glycerol. To keep the salinity of the glycerol solutions equal to the brine salinity, the salt content was kept at 5 wt%. NaN_3 was added to the solution to prevent bacterial growth.

6.1.3 5000 ppm HPAM solution

A polymer was added directly to the premade 5 wt% NaCl brine to increase its viscosity. Acloflood 935, a partially hydrolyzed polyacrylamide polymer, was used. It has a degree of hydrolysis making it soluble in water, but not sensitive to the 5 wt% salinity of the brine. The polymer is commercially available and has a molecular weight of $5{\cdot}10^6$ daltons, and is hydrolyzed to a degree of 5-10 mole% (Sydansk et al. 2004). 4 batches of polymer solution were made, all containing 5000 ppm of Alcoflood 935.

One liter of the 5000 ppm solution was made by mixing 5 grams of Alcoflood 935 powder with 1024.8 grams of pre-made brine using a magnetic stirrer. Brine was stirred at a speed sufficient to make a vortex, as seen in figure 6.2. The polymer powder was gradually added to the side of the vortex by using a funnel to prevent aggregation. When all powder was dissolved in the brine, the speed was reduced to a minimum and the solution was left over night.

Figure 6.2: A vortex was created during mixing of brine and Alcoflood 935 powder. The powder was carefully added to the side of the vortex to avoid aggregation. Picture from Haugland (2016).

Foshee et al. (1977) recommends filtering all polymer solutions to remove microgels and other multimolecular structures before using them in experiments. In his work, Haugland (2016) had challenges with polymer clogging the inlet filter during spontaneous imbibition of a 5000 ppm HPAM solution. Thus, it was decided to filter the polymer solutions. When filtrating the solution, caution should be taken to prevent polymer degradation (Foshee et al. 1977). Jennings et al. (1971) recommend a four feet hydrostatic head (corresponding to appr. 12 kPa) giving adequate filtration rates, and minimal degradation.

A set up for filtering the polymer solutions was made by using a tall imbibition glass tube. An end piece where two filters were placed was attached to one end of the tube. The end piece was connected by tubing to a vacuum chamber connected to a vacuum pump. The unfiltered polymer solution was poured through a funnel on top of the glass tube. The vacuum pump was started and the pressure in the system was regulated between 300 and 600 Torr, a level where the

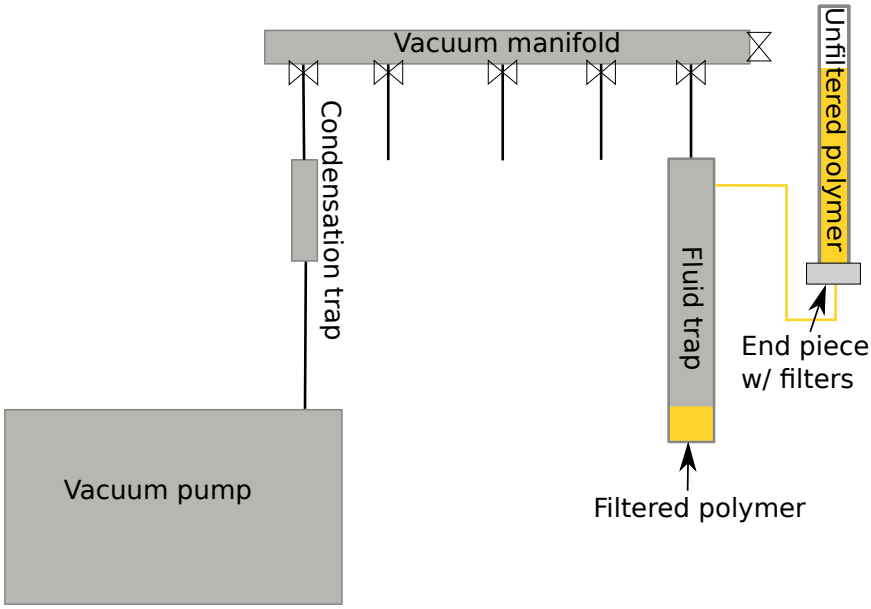

Figure 6.3: Set up for filtering the HPAM solution.

polymer solution did not boil. The filtered polymer solution was collected in the vacuum chamber. Viscosity measurements of the polymer solutions further discussed in section 7.1 suggests that, for some of the solutions, the filtration rate was too high. For later, it is therefore recommended to keep the pressure of the system higher. The filtering set up is schematically presented in figure 6.3.

6.2 Non-wetting fluids

Paraffinic lamp oil and n-Decane were used as the non-wetting fluid. Polar compounds were removed by filtrating the oil through a column of alumina, silica, and glass wool as suggested by Fernø et al. (2013). The compound column was filled inside a separatory funnel, and the mineral oil was gently poured over the column and collected. Experiments on sandstone core plugs further discussed in section 8.2 suggest that paraffinic lamp oil alters the wettability of quartz grains (Bentheimer sandstone contains over 90 % quartz). Because the sand used to construct the sand packs contains a high amount of quartz, it was decided to use n-Decane as the non-wetting phase for all sand packs.

A model for calculating the viscosity of n-Decane as a function of temperature was made. A data sheet for the viscosity of n-Decane as a function of temperature at atmospheric pressure was retrieved from Lemmon et al. (2018). From this data, the viscosity as a function of temperature, T,

was modeled as seen in figure 6.1:

$$\mu(T) = 1.522 \cdot 10^{-8} \cdot T^4 - 2.980 \cdot 10^{-6} \cdot T^3 + 3.074 \cdot 10^{-4} \cdot T^2 - 2.305 \cdot 10^{-2} \cdot T + 1.272 \qquad (6.2)$$

Part III

Results and Discussion

7 Fluid analysis

Different fluids were used as wetting and non-wetting phase during the experimental work. Viscosities for glycerol and polymer solutions were measured, whereas viscosity of brine and n-Decane was calculated from the temperature models made in section 6.1. In addition, interfacial tensions were measured. Density, and calculated and measured viscosity, of all fluids are listed in table 7.1. Density and viscosity of paraffinic lamp oil was retrieved from Haugen et al. (2014), and the values were assumed constant. The HPAM polymer solutions were shear-thinning at increasing shear rate. During spontaneous imbibition, the flow rate is low, i.e. the shear rate applied to the imbibing fluid is low. Therefore, the viscosity listed for the HPAM solutions is the viscosity measured at 2.5 RPM. Ph.D. candidate Arthur Uno Rognmo measured interfacial tension between all fluid couples, except between paraffinic lamp oil and the aqueous solutions. It is assumed that the interfacial tension between n-Decane and 72 wt% glycerol is the same as between n-Decane and 69 wt% glycerol. The measured values are listed in table 7.2.

Table 7.1: Viscosity and density of all fluids used. Note that the HPAM solutions are non-Newtonian and were shear-thinning. HPAM viscosity was taken as the value measured at 2.5 RPM. Glycerol solution viscosity is taken as the average of measurements on all rotational speeds performed, and the error as the standard deviation. Temperature denotes the temperature at which viscosity was measured/calculated.

Fluid	Density, ρ [g/cm^3]	Viscosity, μ [cP]	Temperature [°C]
5 wt% NaCl brine	1.03±0.01	1.08	20
Paraffinic lamp oil	0.74^A	1.47^A	20
n-Decane	0.73±0.01	0.91	20
Glycerol A	1.22±0.01	30.4±0.2	23.5
Glycerol B	1.22±0.01	45.9±2.7 43.0±0.3	23.5 27.9
Glycerol C	1.22±0.01	47.0±0.5	23.2
HPAM A	1.04±0.01	28.0±0.5	23.5
HPAM B	1.04±0.01	30.2±0.5	27.0
HPAM C	1.04±0.01	26.1±0.5	28.0
HPAM D	1.04±0.01	25.3±0.5	27.5

A - Haugen et al. (2014).

Table 7.2: Interfacial tension between the different fluid couples used in experiments. (Measurements conducted by Ph.D. Arthur Uno Rognmo).

Oleic phase	Aqueous phase	σ $[mN/m]$
n-Decane	5 wt% NaCl	47.2±0.9
n-Decane	5k ppm HPAM	45.9±0.4
n-Decane	69 wt% Glycerol	34±0.5[A]

A 72 wt% glycerol solutions is assumed to have the same interfacial tension to decane as the 69 wt% glycerol solution.

7.1 The effect of filtrating the HPAM polymer solutions

All HPAM solutions used in sand pack experiments were filtered by the method described in section 6.1. Samples were taken from HPAM C and HPAM D both before and after filtration to measure and compare the viscosity. These samples showed that HPAM solutions could be subject to mechanical degradation by filtration. The viscosity values are shown in figure 7.1.

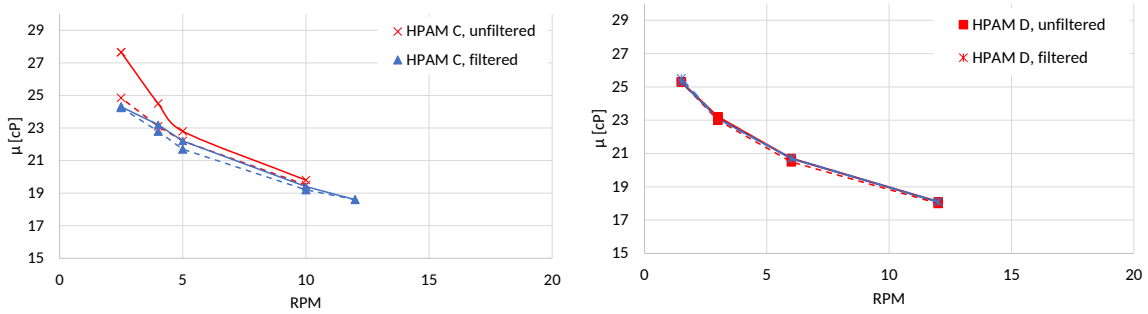

(a) HPAM C (b) HPAM D

Figure 7.1: Viscosity measurements for samples taken before and after filtering HPAM C and HPAM D. Note that the y-axis starts at y=15. The rotational speed was started at the lowest RPM and was increased sequentially (solid line) before it was sequentially lowered (dashed line) to the initial RPM.

For HPAM C, the difference in viscosity between the filtered and unfiltered sample measured at 2.5 RPM was 3.4 cP, a 12% change. This difference could be due to mechanical degradation caused by the shear rate at which the solution was filtered. This effect was not observed for HPAM D, implying it was not mechanically degraded during filtration. When filtering the polymer solutions, a differential pressure between 21 and 61 kPa was applied to force the polymer solution through a filter. The differential pressure applied was not controlled in a close manner, and fluctuated

between the two endpoints. Thus, the applied pressure during filtration of HPAM C could have been higher than the pressure applied to HPAM D, explaining why HPAM C was mechanically degraded and HPAM D was not. Jennings et al. (1971) recommended a maximum differential pressure of approximately 12 kPa during filtration to avoid mechanical degradation. Therefore, more caution should be taken to avoid mechanical degradation. A filtration system including a filter with a larger cross-sectional area should be developed. Then, filtering the same volume of the polymer solution at a lower differential pressure (by Darcy's law, eq. 2.2) takes less time. Thus polymer degradation can be avoided.

8 Preliminary studies on sandstone core plugs

Spontaneous imbibition experiments performed on Bentheimer sandstone core plugs were conducted in addition to the sand pack experiments. Porosity and absolute permeability were measured on all core plugs. Seven of the core plugs were used in spontaneous imbibition experiments with paraffinic lamp oil as the non-wetting fluid and different aqueous solutions as the wetting fluid. Six of the cores used for spontaneous imbibition experiments were directly saturated and stored in paraffinic lamp oil for different times to investigate the effect. In the following, experimental results will be presented and discussed.

8.1 Porosity and permeability

Standard core plug properties are presented in table 8.1. The average porosity of all core plugs was 0.216 with a standard deviation of 0.019. The average permeability was 663 mD with a standard deviation of 44 mD. All core plugs were within one standard deviation of the mean porosity except SS07 and SS10. SS07 was partly crushed between weighing the core plug before and after saturation, causing an underestimated porosity. All core plugs SS01 through SS08 were cut from the same long Bentheimer sandstone core plug. SS09 and SS10 were pre-cut, and it is uncertain if they were from a sandstone block geographically close to where SS01 through SS08 were fetched. This could be the explanation for SS10 being more than one standard deviation from the mean porosity, and that both were outside one standard deviation from the mean permeability of the core plugs. Despite this, the low standard deviations show that the core plugs are very similar, making them good comparisons to the homogeneous sand packs later discussed.

Table 8.1: Standard core properties for all Bentheimer sandstone core plugs.

Core plug	Length [$\pm$0.001 cm]	Diameter [$\pm$0.001 cm]	Pore volume [$cm^3 \pm 2\%$]	Porosity [frac. PV $\pm$ 2%]	Absolute permeability [mD $\pm$ 5%]
SS01	6.112	5.170	28.85	0.225	630
SS02	6.090	5.170	29.09	0.228	647
SS03	6.100	5.168	28.49	0.223	642
SS04	6.128	5.168	28.32	0.220	620
SS05	6.100	5.174	27.08	0.211	648
SS06	6.086	5.175	25.74	0.201	657
SS07*	6.086	5.171	22.32	0.175	666
SS08	6.088	5.170	26.04	0.204	633
SS09	6.090	4.785	24.76	0.227	522
SS10	6.140	4.773	26.08	0.237	737

* Partly crushed between weighing the core plug before and after saturation.

8.2 The effect of paraffinic lamp oil on quartz grain wettability

The 6 sandstone cores initially saturated with paraffinic oil were stored for different periods of time before they were submerged in the wetting fluid for spontaneous imbibition. This was done to investigate the paraffinic lamp oils effect on quartz grain wettability. The wetting fluids were varied, but it was assumed that these variations did not have any effect. Because forced imbibition data are not available, the imbibition test was used to estimate wettability. The imbibition test uses the rate and amount of non-wetting phase displaced during spontaneous imbibition to qualitatively estimate the wettability of a porous medium Anderson (1986*b*). If large volumes are displaced at a high rate, the porous medium is strongly wetted towards the imbibing fluid. SS09 was not stored in paraffinic lamp oil and will not be included in the further discussion.

8.2.1 Storing for 6 days or more

SS01, SS02, and SS03 (group 2) were stored for more than six days and had recovery factors after spontaneous imbibition lower than 3%. All other core plugs (group 1), stored two days or less, had recovery factors larger than 44%, as showed in figure 8.1. The recovery decreased when the core plugs were stored in paraffinic lamp oil for 6 days or more. Bentheimer sandstone is a homogeneous porous media with high amounts of quartz (Peksa et al. (2015)) which is naturally strongly water-wet. It was therefore expected that the wettability was similar for all cores and

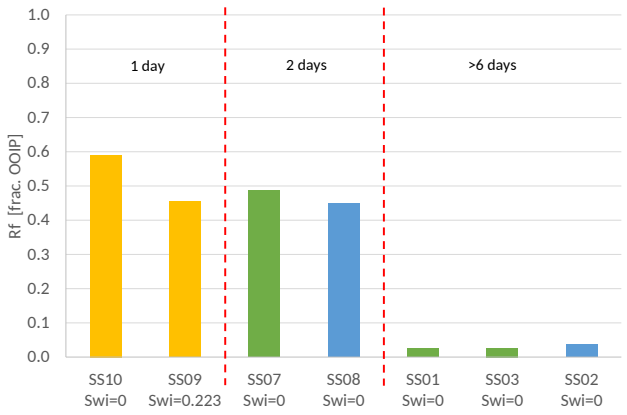

Figure 8.1: The relationship between time stored and recovery factor during spontaneous imbibition. Swi denotes the initial water saturation when imbibition started. The color coding shows which aqueous phase acted as the wetting fluid: Blue=5 wt% NaCl, Green=69 wt% Glycerol, Yellow=5k ppm HPAM.

would perform similarly during spontaneous imbibition - this was, however, not the case. Larger amounts of oil were produced during spontaneous imbibition in group 1 core plugs compared with group 2. Hence, the wettability estimated by the imbibition test was different between the two groups. The wettability of a porous medium can be altered by deposition of polar components or organic matter from mineral oils (Anderson 1986*a*), thus the wettability change can be assigned to the paraffinic lamp oil. It is therefore not recommended to store quartz-rich porous media in paraffinic lamp oil for more than six days.

8.2.2 Storing for 2 days or more

SS10 and SS08 were stored in paraffinic lamp oil for 1 and 2 days respectively before initiating spontaneous imbibition with the aqueous phase. The wetting phase for spontaneous imbibition in SS10 was an HPAM polymer solution, whereas it was brine in SS08. It is assumed that the wetting phase has no effect on wettability. The imbibition rate was higher in SS10 than in SS08, as seen in figure 8.2 with a 6 times higher average imbibition rate. For similar porous media, imbibition rate normally decreases as wetting phase viscosity increases (Meng et al. (2016) and Haugland (2016)), however not the case for SS10 and SS08. This indicates, by the imbibition test, that SS10 had a stronger preference to water than SS08 because, under equal wettability, imbibition rate would be highest in SS08. This further indicates that the wettability of porous media containing quartz may be altered by storing it in paraffinic lamp oil for as short as 2 days.

SS10 and SS08 differ slightly in core properties. These properties affect spontaneous imbibition in

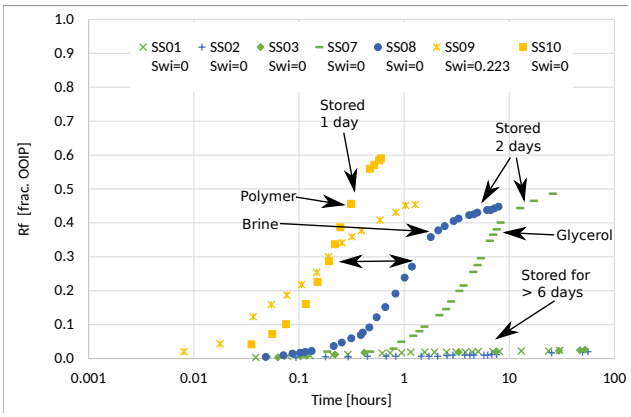

Figure 8.2: Recovery factor as a function of time for sandstone cores during spontaneous imbibition. Note that the x-axis is in logarithmic scale. Color coding: Blue=Brine, Green=69 wt% Glycerol, Yellow=5k ppm HPAM.

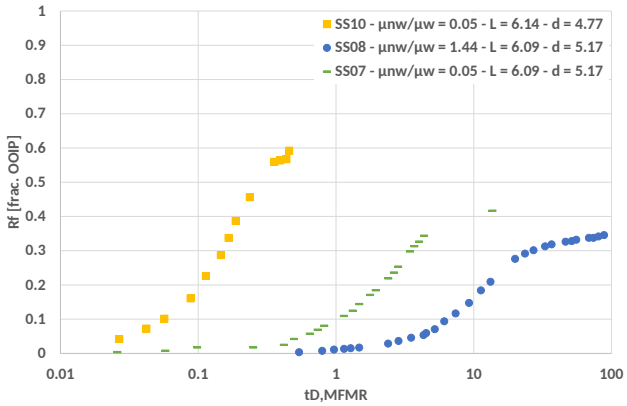

Figure 8.3: Production data for SS07, S08, and SS10 scaled against Mason et al. (2010) dimensionless time. The x-axis is in logarithmic scale. The colors indicate the wetting aqueous phase used: blue=brine, green=glycerol, yellow=polymer.

porous media, and could possibly cause the difference in spontaneous imbibition discussed in the previous paragraph. Production data of SS08 was plotted further to right when plotted against dimensionless time (eq. 2.14), as seen in figure 8.3. This equation scales spontaneous imbibition production data accounting for core properties and fluid viscosities. However, it does not scale well for different wettabilities, and production data for weekly wetted porous media would systematically lie to the right of production data for stronger wetted porous media (Mirzaei-Paiaman & Masihi 2013). Thus, SS10 has a stronger wettability than SS08, and quartz grain wettability is altered after storing it in paraffinic lamp oil for as short as 2 days.

From the observations discussed above, there is a clear indication that quartz grain wettability will be altered if it is stored in paraffinic lamp oil. Because of this, it was decided to use n-Decane

instead of paraffinic lamp oil as the non-wetting phase for sand pack experiments.

9 Sand packs

A new methodology for packing sand packs has been developed through experiences made during this thesis. Experiments conducted on sand packs during this thesis, together with earlier work conducted by Vabø (2016), Haugland (2016), and Føyen (2017) indicate that sand pack performance in terms of reproducible results and sand stability, e.g. collapsing sand, is extremely sensitive to the methodology. The choice of filter to contain the sand, the construction of the end pieces, and confinement pressure applied to the sand to name a few, affect performance. In the following, sand pack stability will be evaluated by analyzing experimental data. From this, recommendations for constructing stable and uniform sand packs for core scale analysis will be given. In addition, experiments conducted with HPAM polymer solutions and spontaneous imbibition in sand packs with initial water saturation will be analyzed.

9.1 Porosity and permeability

Sand pack properties such as porosity and absolute permeability data are presented in table 8.1 and visualized in figure 9.1. Average porosity for 19 sand packs was 0.42 with a standard deviation of 0.04, whereas average absolute permeability was 12.1 Darcy with a standard deviation of 2.3 Darcy.

It was found that SP01 through SP06 (hereafter called group A) had a 15% higher permeability than SP07 through SP19 (hereafter called group B). Group A were constructed with glass tubes having constricted openings (ref. chapter 5.2). Group B were constructed using glass tubes without constricted openings (ref. chapter 5.2). For group A, a piston with a smaller diameter than the diameter of the glass tube body was used to compact the sand, due to the constricted opening. This was not the case for group B. It is believed that the difference in piston diameter between the two groups caused the average absolute permeability of group A (13.2 Darcy) to be higher than for group B (11.5 Darcy). The smaller piston used in group A left a ring of sand between the piston and the glass wall not directly contacted by the piston. There was a small deviation between the piston diameter and inner wall diameter for group B as well, but the area of the ring in group A was 5.4 times bigger. This could have caused an outer ring of less compressed sand in group A and, since decreased compression gives increased permeability (Gobran et al. 1987), given them a higher average permeability. However, the stress yielded on the sand grains in the outer ring increases as it is buried deeper, thus the overall compression increases.

Another possible explanation could be that the sand in group B was subject to higher confine-

Table 9.1: Standard sand pack properties for all sand packs. If NM is stated, it means the value was not measured.

Sand pack	Group	Diameter [cm]	Length [±0.1 cm]	Porosity [frac. PV ±2%]	Absolute permeability [D ±2%]
SP01	A	2.05	14.97	0.412	14.3
SP02	A	2.05	14.80	0.382	13.2
SP03	A	2.05	15.18	0.370	13.0
SP04	A	2.05	15.05	0.338	11.4
SP05	A	2.05	14.57	0.397	14.4
SP06	A	2.05	14.74	0.391	13.2
SP07	B	2.05	9.97	0.398	9.2
SP08	B	2.05	9.72	0.406	9.6
SP09	B	2.05	9.81	0.424	10.5
SP10	B	2.05	9.85	0.445	NM
SP11	B	2.05	9.90	0.435	9.5
SP12	B	2.05	9.87	0.456	13.1
SP13	B	2.05	9.9	0.495	7.0
SP14	B	2.05	9.79	0.426	11.4
SP15	B	2.05	9.88	0.470	12.2
SP16	B	2.05	16.73	0.434	16.9
SP17	B	2.05	16.3	0.423	11.3
SP18	B	2.05	9.94	0.473	14.7
SP19	B	2.05	9.68	0.418	12.7

ment pressure because of the method used to secure the end pieces to glass tube (ref. 5.5). The pressure induced from the nuts on the end pieces was transferred to the sand pack, elevating the confinement pressure. For group A, the confinement pressure was limited by the strength of the glass threads. If the end pieces were tightened too hard, the glass tube would shatter. Thus, confinement pressure of group B was, on average, higher, giving a more compressed sand, leading to higher absolute permeability.

The lack of limiting factors to the confinement pressure for group B resulted in larger variations in absolute permeability, with a standard deviation of 2.7 Darcy. Group A had a standard deviation of 1.1 Darcy. Because group A had a limiting factor in the glass threads, they were more consistent in terms of confinement pressure and absolute permeability. Because of the higher deviation in absolute permeability for group B, it is recommended to use a torque when attaching the end pieces to the glass tubes without constricted openings. This will give better control regarding the confinement pressure, yielding reproducible absolute permeability.

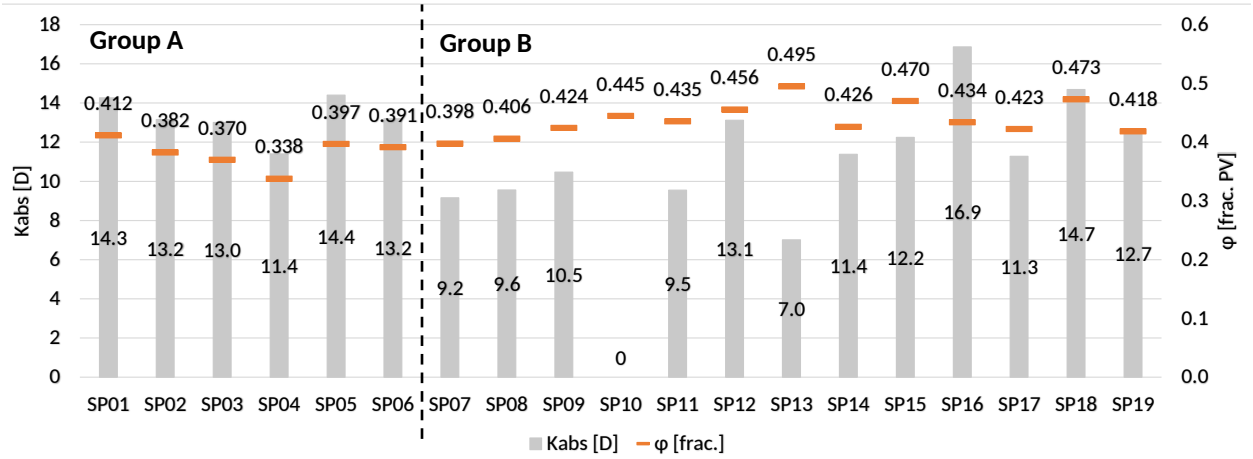

Figure 9.1: Absolute permeability and porosity of all sand packs visually presented. Note that the Kabs-axis goes to 18 and the ϕ-axis goes to 0.6.

9.1.1 Absolute permeability measurements as and indicator of sand pack stability

The sand packs were found to be stable in terms of sand grain arrangement and pore structure during absolute permeability measurements. One object of this thesis was to establish homogeneous and stable sand packs. By this, the sand packs should stay stable during experiments and not change its properties, e.g. no migration or restructure of sand grains and no collapsing of sand packs. Føyen (2017) observed a channel widening through his sand pack during absolute permeability measurement causing a change in sand pack properties. He also observed several sand packs collapsing during measurements. No such observations were made during absolute permeability measurements on sand packs during this thesis, indicating that the sand packs were stable. The stability can be further assessed by analyzing pressure data during absolute permeability measurements. During absolute permeability measurements, volumetric flow was sequentially increased from 200 ml/h to 499 ml/h and lowered again (ref. section 4.2). By controlling the change in pressure measured at the same volumetric flow rate before and after it had been raised to 499 ml/h, it can be evaluated if any major changes have occurred in the sand pack. If the pressure readings differ by a lot, it would indicate some structural change. A limit was set to the change in pressure equal to the uncertainty of the ESI pressure transducer, equal to 300 Pa. If the absolute change exceeded this, the sand pack was considered unstable. For the analysis, SP11 was secluded and will be discussed below. For the 17 sand packs that were included in this analysis, the absolute pressure change between two equal flow rates never exceeded 300 Pa (see figure 9.2). The sand packs constructed by the new packing method were therefore considered stable during absolute permeability measurements.

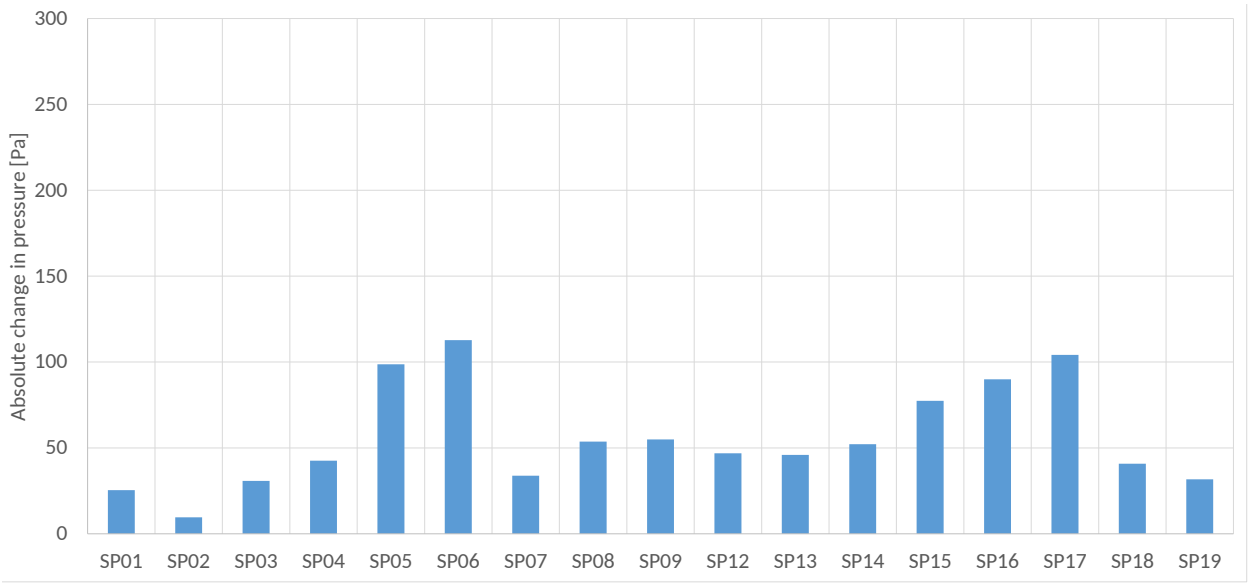

Figure 9.2: Maximum recorded change in pressure between two equal flow rates before and after increasing volumetric flow to 499 ml/h. Change never exceeded 300 Pa for any of the sand packs, and they were considered stable.

Pressure recordings during absolute permeability measurements in SP11 fluctuated severely compared to other sand packs (see figure 9.3). SP11 was treated with HMDS, an organosilicon compound, in an attempt to alter the sands wettability. One possible explanation could be that excess HMDS in the sand pack was mobilized and rearranged during absolute permeability measurements. However, no further tests were done to confirm this theory. Another possibility is that the sand pack was, in fact, unstable causing sand grains to restructure. Again, no further tests were performed to confirm this.

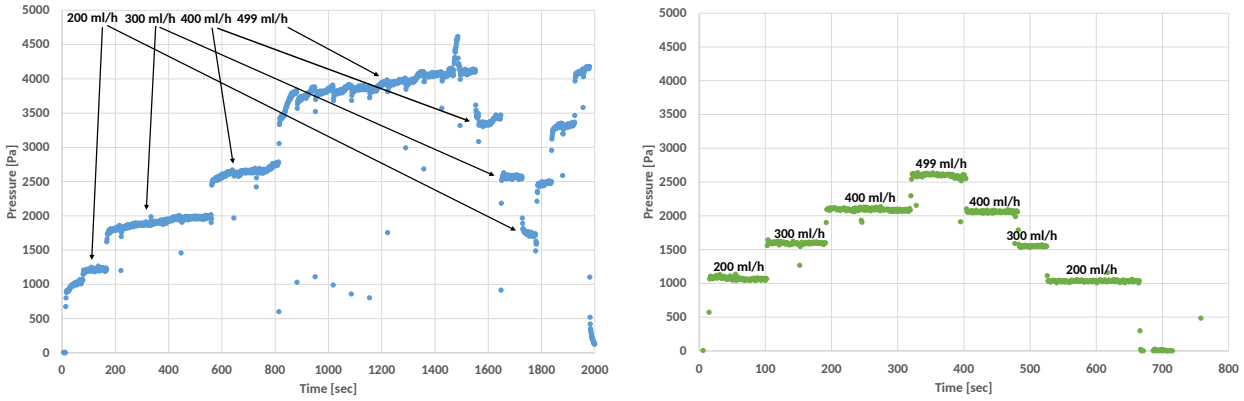

(a) SP11 (b) SP12

Figure 9.3: Pressure during absolute permeability measurement on SP11 and SP12, visualizing the fluctuating pressure in SP11 compared to other sand packs.

After absolute permeability measurements, the sand packs were exposed to the wetting aqueous phase to initiate spontaneous imbibition.

9.2 Spontaneous imbibition

Spontaneous imbibition experiments were conducted on all sand packs. The viscosity of the aqueous wetting phase during spontaneous imbibition was increased by adding glycerol or Alcoflood 935 (HPAM polymer) to the 5 wt% brine to investigate the different effects of glycerol and HPAM polymer on spontaneous imbibition. Adding HPAM polymer to increase wetting phase viscosity was of specific interest because Haugland (2016) encountered challenges with polymer retention in the inlet filter during spontaneous imbibition with a 5000 ppm HPAM solution as the wetting phase. Seven of the sand packs initially saturated with n-Decane were oil flooded after the first spontaneous imbibition and used for a second spontaneous imbibition experiment to investigate the effect of initial water saturation on spontaneous imbibition. SP10 and SP11, which were initially saturated with brine and contained sand treated with HMDS, were initially assumed oil-wet. Spontaneous imbibition with n-Decane was initially conducted on these sand packs. In the following, results from spontaneous imbibition experiments will be presented and discussed. Spontaneous imbibition conducted on sand packs with no initial water saturation will be termed primary spontaneous imbibition, whereas spontaneous imbibition conducted on sand packs with initial water saturation will be termed secondary spontaneous imbibition. Additional production curves that will not be presented in this section are included in appendix B.

9.2.1 Primary spontaneous imbibition overview

Primary spontaneous imbibition (PSI) experiments were conducted on all sand packs except SP10 and SP11 (because they were initially saturated with brine). PSI never initialized in SP06 despite several attempts with forced initialization (by the method described in section 5.9). Key experimental results from PSI experiments are presented in table 9.2.

Table 9.2: Key data from primary spontaneous imbibition experiments. S_{wi} denotes the initial water saturation at PSI start, $S_{w,sp}$ denotes the water saturation after PSI, WF=wetting fluid, R_f=recovery factor, $\frac{N_{cou}}{N_p}$ is the fraction of oil produced counter-currently to total oil volume produced. In the case where PSI needed to be forcefully initialized, initial water saturation was unequal to zero because a certain volume of water was forcefully imbibed to initiate PSI.

	WF	$\frac{\mu_{nw}}{\mu w}$ [frac.]	S_{wi} [frac. PV]	$S_{w,sp}$ [frac. PV $\pm$0.01]	R_f [frac. OOIP $\pm$0.01]	$\frac{N_{cou}}{N_p}$ [frac.]
SP01^{A,B,C}	Brine	0.87	0.03	0.82	0.82	0
SP02^{A}	Brine	0.87	0.08	0.79	0.77	0
SP03^{A}	Brine	0.87	0.04	0.84	0.84	0.05
SP04^{A}	Glyc. A	0.03	0.01	0.84	0.83	0
SP05^{A,D}	Glyc. B	0.02	0.02	0.59	0.58	0
SP07	Brine	0.89	0	0.86	0.91	0
SP08^{A}	Glyc. B	0.02	0.04	0.88	0.87	0
SP09	HPAM B	0.03	0	0.93	0.93	0
SP12^{D}	HPAM C	0.03	0	0.61	0.61	0
SP13^{A,D}	HPAM C	0.03	0.09	0.42	0.36	0
SP14	HPAM C	0.03	0	0.90	0.90	0
SP15	HPAM C	0.03	0	0.88	0.88	0.18
SP16	HPAM D	0.03	0	0.85	0.85	0.01
SP17	HPAM D	0.03	0	0.85	0.85	0.07
SP18^{E}	Glyc. C	0.02	0	NM	NM	NM
SP19^{E}	Glyc. C	0.02	0.07	0.97	0.97	0.15

A - Forced initialization, B - Oil-wet filter, C - Hydrostatic pressure during PSI, D - Front never reached outlet, E - Submerged in wetting fluid

9.2.2 Secondary spontaneous imbibition overview

After primary spontaneous imbibition, forced imbibition and drainage was performed on the sand packs. Experimental results from these processes will be presented and further analyzed in section 9.3. The impact of initial water saturation on spontaneous imbibition was evaluated during

secondary spontaneous imbibition (SSI). Key experimental results from SSI experiments are presented in table 9.3.

Table 9.3: Key data from secondary spontaneous imbibition experiments. $\frac{\mu_{nw}}{\mu_w}$ is the ratio of non-wetting fluid viscosity to wetting fluid viscosity, $S_{w,i}$ is the initial water saturation at SSI start, $S_{w,sp}$ is the water saturation after SSI, WF=wetting fluid, R_f is the recovery factor (produced oil volume divided by initial oil volume), and $\frac{N_{cou}}{N_p}$ is the fraction of oil produced counter-currently to total oil volume produced.

	WF	$\frac{\mu_{nw}}{\mu w}$ [frac.]	S_{wi} [frac. PV]	$S_{w,sp}$ [frac. PV $\pm$10%]	R_f [frac. OOIP $\pm$10%]	$\frac{N_{cou}}{N_p}$ [frac.]
SP01[A,B]	Brine	0.87	0.46	0.85	0.72	0.37
SP02[A,D]	Brine	0.87	0.18	0.33	0.18	0.06
SP03[A]	Brine	0.87	0.12	0.58	0.52	0.3
SP06[A]	Glyc. B	0.02	0.23	0.67	0.57	0.18
SP09	HPAM B	0.03	0.29	0.48	0.26	0
SP10[E]	Brine	0.90	0.24	N/A	N/A	N/A
$SP11_1$[E]	Brine	0.90	0.20	0.83	0.78	0.26
$SP11_2$[A,C,E]	Brine	0.90	0.27	0.91	0.87	0.08
SP15[F]	HPAM C	0.03	0.18	0.62	0.38	1
SP17	HPAM D	0.03	0.12	0.62	0.56	0.08

A - Forced initialization, B - Oil-wet filter, C - Hydrostatic pressure during PSI, D - Dyed brine, E - Sand treated with HMDS to render it oil-wet, F - Boundary condition changed to OEO

9.2.3 Reproducible primary spontaneous imbibitions

The sand packs constructed by using the new packing methodology (compression by pressure) were found to give more reproducible primary spontaneous imbibitions than sand packs constructed by using the old packing method (compression by shaking). This is important for the development of sand pack investigations because effects such as wettability alteration can be investigated. In the following, sand packs used in this thesis will be referred to as new sand packs, and sand packs used in previous thesis' (Vabø 2016, Haugland 2016, Føyen 2017) will be referred to as old sand packs.

By comparing scaled PSI production data from old sand packs with new sand packs, it was indicated that PSI was more reproducible in the new sand packs compared with the old. When scaled against dimensionless time (Mirzaei-Paiaman & Masihi 2014), PSI production data from the new sand packs all grouped together, whereas old sand packs separated into two groups (Føyen 2017)

(see figure 9.4). This gives an indication that PSI in the new sand packs give reproducible experiments independent of sand pack properties. Meng et al. (2016) suggested that spontaneous imbibition production data will scale differently to Mirzaei-Paiaman & Masihi (2014) scaling equation (eq. 2.17) depending on the regularity of the pore structures of the porous media. The different grouping of the old sand packs indicate that the pore structures in the sand packs of the two groupings had different pore structure regularity. The fact that the new sand packs scale similarly to each other indicates that the sand packs have more similar pore structure regularity. The similar regularity gives reproducible PSI, making it possible to investigate more complex behaviors and impacts to spontaneous imbibition.

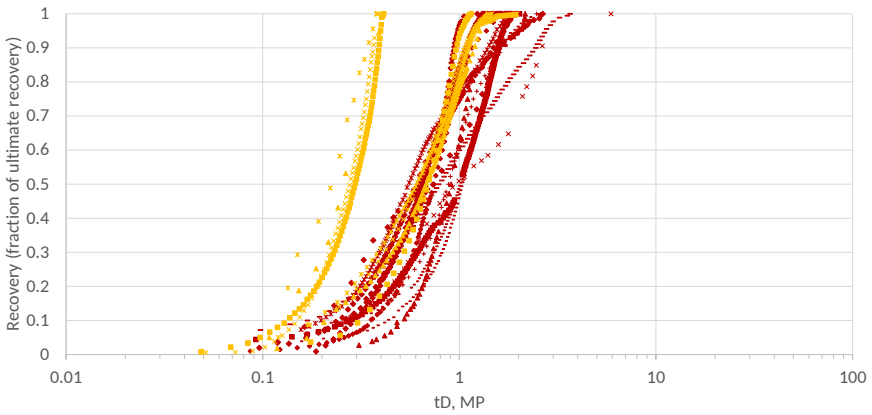

Figure 9.4: PSI production data from old sand packs (Føyen 2017) and new sand packs plotted against dimensionless time. The yellow series are production data from Føyen (2017). Note that these are The red group is production data from the experiments related to this thesis. x-axis is in logarithmic scale.

9.2.4 The effect of initial water saturations on spontaneous imbibition

SSI (spontaneous imbibition with initial water saturation) was found to be less efficient yielding lower recovery factors and production rates compared with PSI (spontaneous imbibition with no initial water saturation). When conducting SSI with brine as the wetting fluid a larger fraction of production occurred counter-currently during SSI compared with PSI (spontaneous imbibition with no initial water saturation). Over 30% of all production occurred counter currently during SSI compared to 2% during PSI.

On average, recovery factor was 40% higher during PSI compared to SSI. In addition, water saturation was brought to an average of 79% during PSI compared to 68% during SSI. The reason for this could be that pores were restructured during forced imbibition and drainage, as will be dis-

cussed in section 9.3.1. This restructuring caused a change in the conditions for the spontaneous imbibition, giving lower relative recovery.

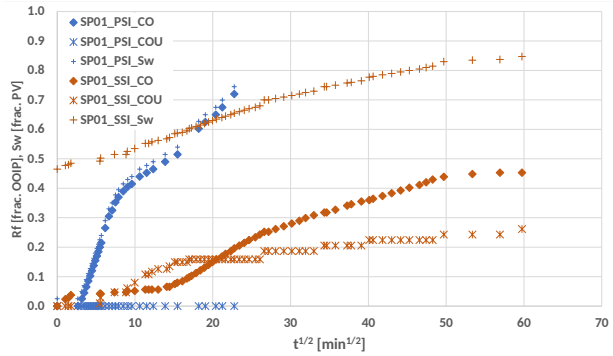

(a) SP01 - WF=Brine

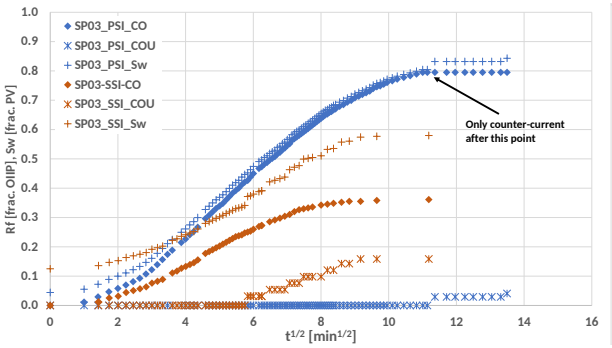

(b) SP03 - WF=Brine

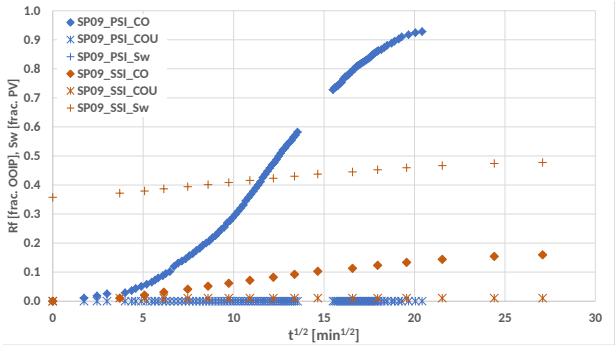

(c) SP09 - WF=HPAM solution

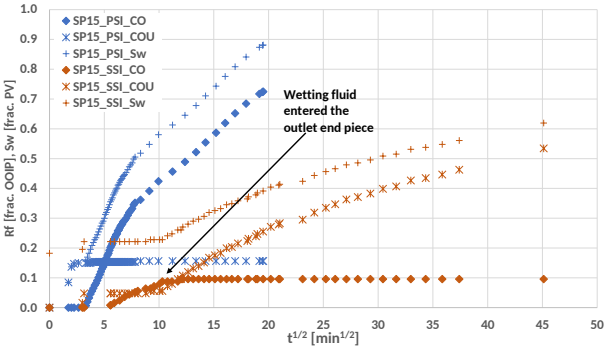

(d) SP15 - WF=HPAM solution

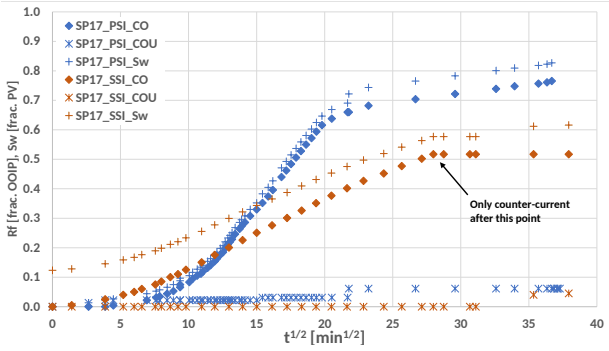

(e) SP17 - WF=HPAM solution

Figure 9.5: Co-current and counter-current production as a fraction of initial oil volume (Rf on the y-axis), and water saturation (Sw on the y-axis) plotted against the square root of time. In the legend: PSI denotes primary spontaneous imbibition, SSI denotes secondary spontaneous imbibition, CO denotes co-current production, COU denotes counter-current production, and Sw denotes water saturation.

SSI took longer to finish for all sand packs except for SP3, as seen in figure 9.5. When saturating SP03, the sand pack was not brought to a pressure low enough to saturate the sand pack entirely. This caused air to be present, as observed close to the inlet in figure 9.6. When air is present, the displacement becomes a three-phase flow process which is much more complicated than two-phase flow. This could cause the spontaneous imbibition to slow down because the area available for the wetting fluid to flow through is lowered, thus a higher capillary pressure is needed to maintain the flow rate. Some of the air that was observed during PSI could have been displaced out of the sand pack during forced imbibition and drainage performed between PSI and SSI. Because of this, SSI was not limited by air, and the process was more time efficient compared to PSI.

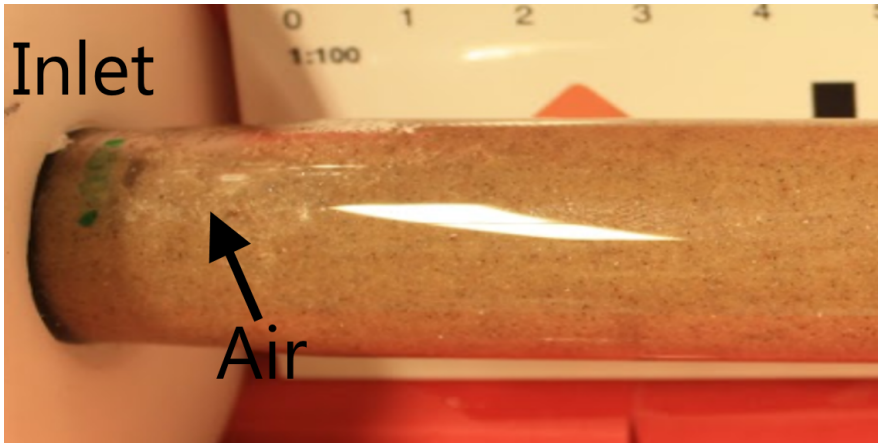

Figure 9.6: Air observed close to the inlet in SP03 during PSI.

In SP15, more oil was produced counter-currently than co-currently (see figure 9.5d). This was believed to be caused by a change in boundary conditions. As discussed in section 9.2.6, wetting fluid was observed to enter the outlet end piece during spontaneous imbibition. During forced imbibition after SSI in SP15, a volume of n-Decane smaller than the dead volume was produced, proving that wetting fluid must have been present in the end piece during PSI. This caused a change in the boundary conditions to a situation similar to the one-end-open boundary condition, thus oil produced only counter-currently from this point.

When brine was the wetting fluid, a higher amount was produced counter-currently during SSI compared to when glycerol or HPAM was the wetting fluid (see table 9.3). Haugen et al. (2014) reported that, during spontaneous imbibition with brine in a core with no initial water present, counter-current production only occurred at the beginning of the process, and that 93% of the oil was produced co-currently. Similar results were produced in this thesis. When conducting PSI with brine, over 95% of the oil was produced co-currently. In SP01 and SP03 (imbibed with brine),

only 70% was produced co-currently showing there is a difference between SSI and PSI when the wetting fluid is brine. During SSI in SP01 and SP03, oil was observed being produced counter-currently for the whole period SSI was running. Thus, the pressure in the oil phase was kept at a level adequate to overcome the capillary back pressure through the whole process. The reason for this to occur during SSI with brine is that brine and n-Decane have approximately the same mobility. When the mobility of the wetting fluid is much lower than of the non-wetting fluid, less will be produced counter-currently (Haugen et al. 2014). But the reason for the additional counter-current production during SSI compared to PSI is unknown and more experiments should be conducted to investigate physical processes during spontaneous imbibition with the TEOFSI boundary condition and an initial water saturation present.

9.2.5 The effect of glycerol and HPAM polymer on spontaneous imbibition

Spontaneous imbibition with HPAM solution yielded higher recovery than with glycerol solutions during PSI. On average, PSI using HPAM polymer yielded a recovery factor of 88.3%, whereas using glycerol yielded a recovery factor of 85.6%. The final recovery varies for both HPAM polymer and glycerol with standard deviations of 3.4% and 2.7% respectively. Thus it can not be concluded that HPAM polymer gives higher recovery, but for 3 out of 5 experiments (SP09, SP14, and SP15) it did, indicating that there is some correlation.

Earlier, Haugland (2016) reported that using HPAM polymer during PSI gave 5% less recovery compared to glycerol. He reported challenges with retention of polymer in the inlet filter and reasoned that this could have been the cause of the lower recovery. In this thesis, HPAM polymer solutions were filtered to remove microgels and other multimolecular structures to avoid challenges with retention. No indications of retention in the inlet filter were observed, and HPAM polymer could imbibe freely. The spontaneous imbibition process became more effective and resulted in 3% higher recovery compared to when glycerol was used. The recovery factors for PSI with HPAM polymer and glycerol solution are presented in figure 9.7.

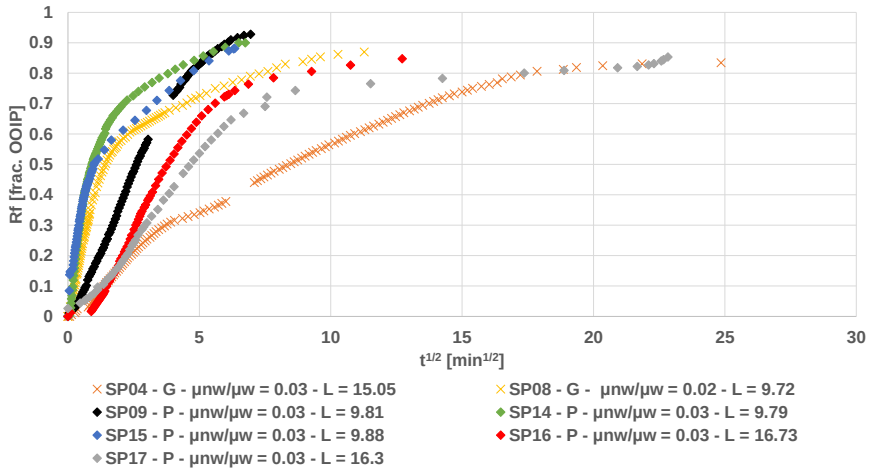

Figure 9.7: Oil recovery during PSI with HPAM polymer and glycerol solutions as a fraction of original oil in place plotted against the square root of time ($\sqrt{min}$). Production data for HPAM polymer solutions are plotted as diamonds, whereas glycerol solutions are plotted as crosses. In the legend, N_{cou}/N_p gives the fraction of oil produced counter-currently to the total oil production.

Haugland (2016) also speculated that the cause of reduced recovery using HPAM polymer could be due to wettability alterations of the sand pack. By taking advantage of the possibility to conduct forced imbibition and drainage in the sand packs, the Amott-Harvey wettability index (I_{AH}) was calculated by equation 2.11. Because quartz grains are naturally strongly water-wet, it was assumed that no n-Decane would spontaneously displace brine in the sand packs. The Amott-Harvey oil index was therefore assumed to be zero. The Amott-Harvey water index was calculated by equation 2.10 as $\delta_w = \frac{S_{w,sp} - S_{wi}}{S_{w,fi} - S_{wi}}$. The results showed that for the sand packs where spontaneous imbibition was conducted with HPAM polymer, the average I_{AH} was 0.92 compared to 0.97 for the other sand packs. In 4 measurements I_{AH} was less than 0.9 for the sand packs where HPAM polymer had been present compared to 1 measurement where it had not been present. This indicates that the sands wettability was altered by the HPAM polymer, and the reason for the lower recovery reported by Haugland (2016) could be wettability alteration. All wettability indices measured are given in table 9.4.

Table 9.4: Amott-Harvey wettability indices. For sand packs where two rounds of spontaneous imbibition/oil flooding were conducted, the index was calculated twice. The sand packs where HPAM polymer was used as wetting fluid are marked by *. S_{wi} is the initial water saturation, $S_{w,sp}$ is the water saturation after spontaneous imbibition, and $S_{w,fi}$ is the water saturation after forced imbibition.

	1st cycle				2nd cycle			
	S_{wi}	$S_{w,sp}$ [frac. PV $\pm$0.01]	$S_{w,fi}$ [frac. PV $\pm$0.01]	I_{AH}	S_{wi} [frac. PV $\pm$0.01]	$S_{w,sp}$ [frac. PV $\pm$10%]	$S_{w,fi}$ [frac. PV $\pm$10%]	I_{AH}
SP01	0.03	0.82	0.83	0.99		N/A		
SP02	0.08	0.79	0.79	1.00		N/A		
SP03	0.04	0.84	0.84	1.00		N/A		
SP04	0.01	0.84	0.84	1.00		N/A		
SP05	0.02	0.59	0.65	0.90		N/A		
SP06			N/A		0.23	0.67	0.80	0.78
SP07	0	0.86	0.86	1.00		N/A		
SP08	0.04	0.88	0.88	1.00		N/A		
SP09*	0	0.93	0.93	1.00		N/A		
SP11	0.20	0.83	0.83	1.00	0.27	0.91	0.91	1.00
SP12*	0	0.61	0.69	0.87		N/A		
SP13*	0.09	0.42	0.57	0.71		N/A		
SP14*	0	0.90	0.9	1.00		N/A		
SP15*	0	0.88	0.88	1.00	0.18	0.62	0.71	0.83
SP16*	0	0.85	0.85	1.00		N/A		
SP17*	0	0.85	0.86	0.99	0.12	0.62	0.67	0.90

In some sand packs imbibed with HPAM polymer(SP15, SP16, and SP17), some counter-current production occurred. By analyzing pictures taken of the front during spontaneous imbibition, an initial deviation from a sharp front was observed. This caused some oil close to the inlet to be isolated by HPAM polymer solution in the co-current direction (see figure 9.8). Thus, the oil could only be produced counter-currently. The front development in SP15 is shown in figure 9.8. Similar development was observed in SP16 and SP17. After 10 minutes, HPAM polymer imbibed into the lower parts of the sand pack causing a tongue to develop. After 15 minutes, HPAM polymer imbibed vertically and covered the whole cross-sectional area of the sand pack approximately 1 cm from the inlet. This immobilized the oil behind the imbibed area in the co-current direction. After 30 minutes, HPAM polymer had started to spontaneously imbibe counter-currently towards the inlet, producing oil counter-currently. For the other sand packs, the wetting fluid did not imbibe a distance into the sand pack before it was able to saturate the whole cross-section, as seen in figure 9.9. Thus, no oil was immobilized in the co-current direction, and no oil was produced counter-currently.

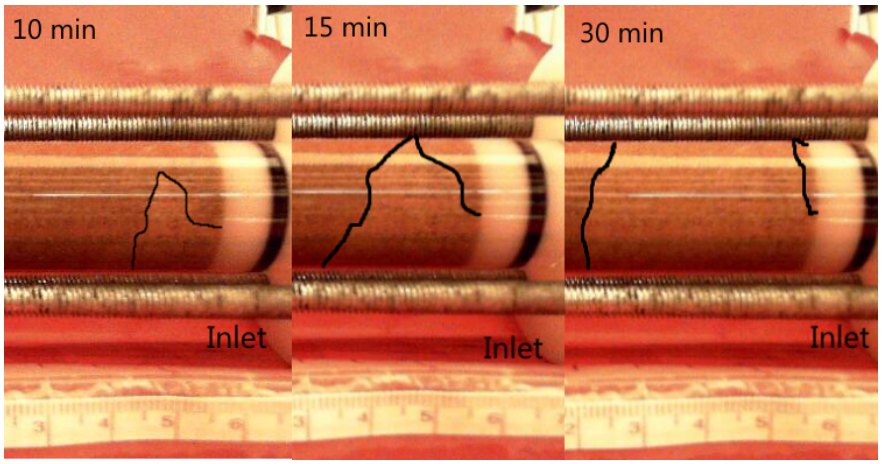

Figure 9.8: Front development in SP15 during PSI. After 15 minutes, the front saturates the cross-section of the sand pack a distance of 1 cm from the inlet, making oil behind the front immobile in the co-current direction.

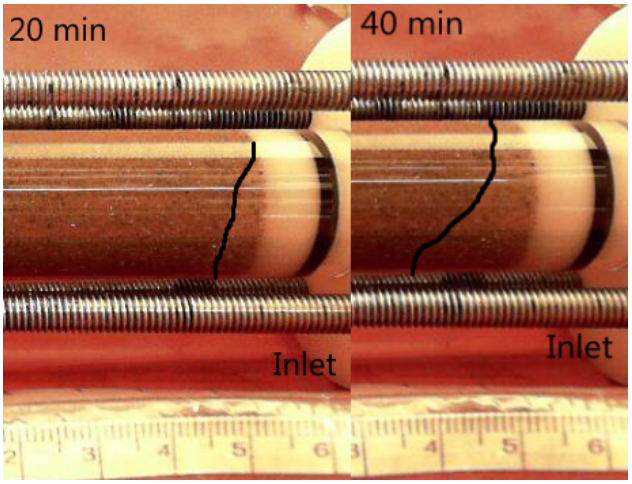

Figure 9.9: Front development in SP09 during PSI. The front develops and saturates the entire cross-section of the sand pack close to the inlet, and no oil is trapped behind the front.

9.2.6 Wetting fluid entering the outlet end piece during spontaneous imbibition

Using experimental set up A (ref. section 5.6) yielded unlikely high recovery during PSI in some sand packs. A closer analysis showed that wetting fluid entered the outlet end piece during PSI in these sand packs. For these cases, time and produced volumes were extrapolated back to when wetting fluid first entered the outlet end piece. The challenge with wetting fluid entering the outlet end piece was confirmed during forced imbibition after spontaneous imbibition. Normally, a

volume of n-Decane equal to the dead volume would be produced before breakthrough of the wetting fluid. However, not the case for those sand packs where unlikely high recovery factors were observed. The experimental challenge was initially attributed to a small hydrostatic pressure caused by height differences in the outlet tubing of the sand pack and outlet tubing of the production trap (ref. experimental set up A, section 5.6). Because of this, experimental set up B was suggested. Analyzing production data for the sand packs where wetting fluid entered the outlet end piece indicated, however, that there was no hydrostatic pressure present.

In experimental set up B, measures were taken to avoid any differential pressure over the sand packs during spontaneous imbibition (ref. section 5.6). However, SP19, which used experimental set up B (ref. section 5.7), also had an unlikely high recovery factor (0.97) after PSI. Unfortunately, forced imbibition was not performed to confirm that wetting fluid had entered the outlet end piece. With only one measurable experiment performed in experimental set up B, it can not be confirmed whether SP19 was a special case and if the problem would occur in other sand packs. Therefore, more tests are recommended to analyze if experimental set up B eliminates the problem with wetting fluid entering the outlet end piece during spontaneous imbibition.

Because wetting fluid could have entered the outlet end piece using experimental set up B, there could be other explanations than hydrostatic pressure for this to occur. Therefore, an assessment of whether a hydrostatic pressure was present during PSI in the sand packs using experimental set up A was performed. An analysis was performed by scaling production data of the sand packs to dimensionless time (Mirzaei-Paiaman & Masihi 2014). The scaled production data was compared to scaled production data for a sand pack where wetting fluid did not enter the outlet end piece. The scaled production data for all sand packs followed approximately the same trajectory, as seen in figure 9.10. This implies that there was no additional hydrostatic pressure present in the sand packs where it was suspected (SP03, SP07, SP14, and SP15). The scaling equation scales production data to account for different sand pack size, absolute permeability, porosity, fluid viscosity, and interfacial tension. It does, however, not account for additional applied pressures. Thus if a hydrostatic pressure was present during spontaneous imbibition, the production data would scale differently compared to production data with no hydrostatic pressure present. The hydrostatic pressure would speed up the process, and production data would therefore be plotted further left against dimensionless time. Thus, production data for the sand packs where a hydrostatic pressure was suspected, would be plotted further left compared with SP02. This was, however, not the case, and it was concluded that no hydrostatic pressure was present in the sand packs. Because of this, it was suspected that there could be an additional pressure in the inlet end piece caused by the flow of wetting fluid through it. Therefore, a model was built using Comsol Multiphysics to estimate the pressure caused by the flowing fluid. An additional pressure of 3 Pa was estimated. The model built in Comsol Multiphysics is presented in appendix C.

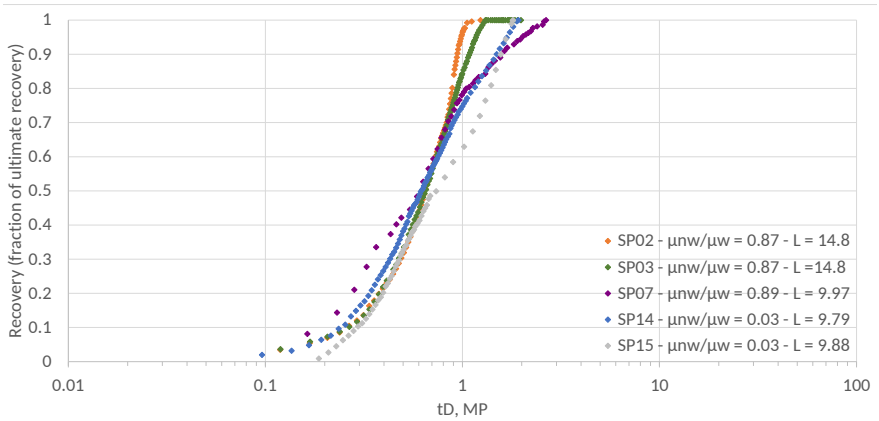

Figure 9.10: Production data normalized to ultimate production scaled to dimensionless time (Mirzaei-Paiaman & Masihi 2014). If a hydrostatic pressure was present in SP03, SP07, SP14, and SP51, the scaled production data would be moved further to the left compared to SP02, however, not the case.

The pressure in the inlet end piece during spontaneous imbibition was estimated by Føyen (2017) by simplifying the shape and size properties of the connected tubing. He found that the pressure caused by the flow of wetting phase through the inlet was insignificant, and did not influence spontaneous imbibition. The insignificance of the pressure from the viscous flow was confirmed in this thesis by modeling the inlet end piece using Comsol Multiphysics. The pressure due to viscous flow in the inlet was estimated to be less than 3 Pa for all wetting fluids used. This corresponds to a water column of 0.3 mm. Therefore, it was assumed that the wetting fluid did not enter the outlet end piece because of the viscous flow through the inlet, and more tests are recommended to determine the reason to control and avoid it in the future.

When the additional pressure from viscous flow in the inlet was modeled, an evaluation of its significance on the spontaneous imbibition was conducted. Haugland (2016) estimated the capillary pressure at the front during spontaneous imbibition in sand packs to be higher than 26 Pa. Therefore, the additional pressure of 3 Pa from viscous flow in the inlet was considered not to affect the spontaneous imbibition in the sand packs.

9.2.7 The effect of the inlet filter on spontaneous imbibition

The filter used for containing sand in SP01 (WM μ) was considered to be hydrophobic by submerging it in brine. No brine spontaenously imbibed, and therefore it was considered to be hydrophobic. The filter impacted spontaneous imbibition by extending the onset period and reducing the

imbibition rate. Thus, the oil-wet filter was not used in further spontaneous imbibition experiments.

Primary spontaneous imbibition in SP02 and SP03 were comparable to SP01, having similar sand pack properties and the same wetting and non-wetting fluid. A hydrostatic pressure was observed in SP01, but it was assumed to be insignificant compared to the capillary pressure occurring from intermolecular forces, and will therefore not be accounted for in the following. Approximately the same amount of brine imbibed into the, giving a first indication that the sand packs performed equally (with recovery factors between 0.7 and 0.8). However, a longer onset period was observed in SP01. This is observed by the slow incline in recovery factor during the initial period of spontaneous imbibition (see figure 9.11). This could be explained by the brine having limited access to the cross-section of the sand pack where it imbibed from, i.e. the inlet filter. A possible reason for this could be an insufficient flushing of the non-wetting fluid originally in the inlet end piece when initializing spontaneous imbibition. This would be observed by the displaced dead volume from the inlet end piece being less than the measured dead volume, but this was not the case. This indicates that the brine had access to the total area of the inlet boundary of the sand pack, and the extended onset period for SP01 can therefore not be explained by limited access. A second possible explanation is that the boundary between the imbibing brine and the sand pack, i.e. the filter, was different in SP01. The filter in SP01, being hydrophobic, could have provided an additional resistance for the brine to contact the sand pack, leading to the extended onset period.

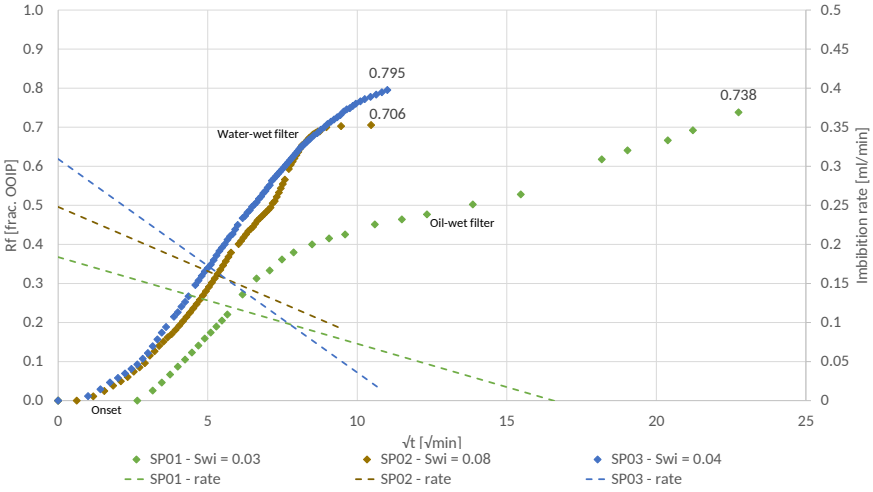

Figure 9.11: PSI production data plotted against the square root of time. Note the extended onset period and lower imbibition rate in SP01.

Brine imbibes at a lower rate in SP01 after the onset period. This can be seen from the linear approximation of the imbibition rate plotted in figure 9.11. An alteration of the wettability in SP01

could explain the lower imbibition rate, but the Amott water index, δ_w, was equal to one in all cases indicating similar wettabilities. It is therefore believed that the deviation in spontaneous imbibition behavior in SP01 was caused by an additional resistance in the hydrophobic inlet filter and it was decided not to use it any further.

9.2.8 The packing methods effect on pore size distribution

A wettability altered sand pack was used as an indicator to show that the sand packs compressed by the new method (compression by pressure) had a more homogeneous pore size distribution compared with the sand packs compressed by the old method (compression by shaking). A dye added to the brine during SSI in SP02 caused wettability alteration in the sand pack, thus it was decided not to use it for further experiments. The technique was adopted from Føyen (2017) to visualize the saturation front during SSI. SSI was considerably slower, and less water imbibed in SP02 compared with SP03 as seen in figure 9.12.

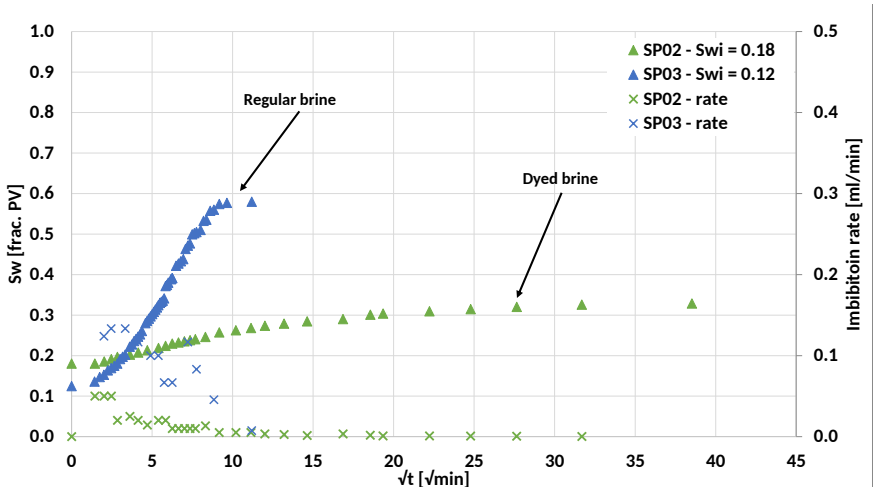

Figure 9.12: Water saturation and imbibition rate during SSI in SP02 and SP03 plotted against the square root of time. Dye was added to the imbibing brine in SP02.

One explanationfor the slower SSI in SP02 compared with SP03 could be that the dye altered the sand pack wettability. Føyen (2017) observed a slow SSI using dyed fluids and attributed it to local wettability alterations. He reasoned that the sand pack had a mixed wettability because he observed that wettability alteration occurred in distinct layers separated by pore size (ref. section 3). A heterogeneous pore size distribution was not observed in SP02. Assuming that SP02 was mixed wet, there would be a distinct pattern to the brine distribution if the pores were size segregated. However, in SP02, dyed brine was observed saturating the sand pack from the inlet to the position of the saturation front except for a small pocket of bypassed oil at the inlet (see figure

9.13). Thus, given that SP02 had a mixed wettability, shows that it had a more homogeneous pore size distribution.

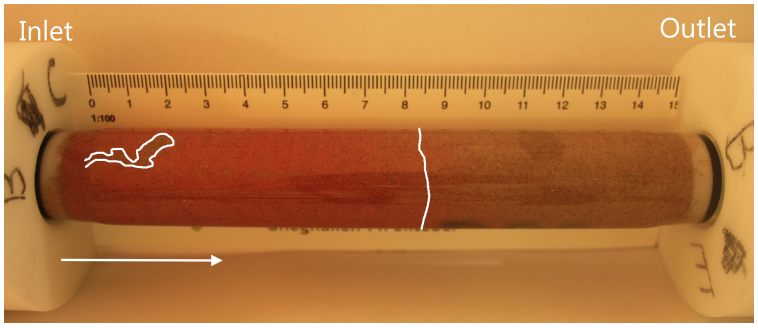

Figure 9.13: Saturation front in SP02 at ended SSI. The front is indicated by the white line to the right. The bypassed oil is indicated by the white lines at the inlet position. The arrow indicates the imbibition direction.

To further test whether the dyed brine could have altered the wettability of the sand grains, a simple test was performed. Dyed brine, n-Decane, and sand were added to a small beaker. The sand grains initially settled to the bottom of the glass indicating they were water-wet. The beaker was left for 20 minutes before it was shaken again. This time, some sand grains clustered together with globules of oil surrounding them (see figure 9.14). By the flotation method (ref. section 2.4), these sand grains were considered oil-wet. This indicates that the dyed brine did, in fact, alter the wettability of some sand grains after only a short period of time (20 minutes). This could have caused a situation of mixed or fractional wettability in the parts of the sand pack that was contacted by the dyed brine. Proving that SP03 had an altered wettability implies that SP02 had a more homogeneous pore size distribution compared with the old sand packs, showing that the new packing method yields more homogeneous sand packs. Because the dyed brine altered the wettability of the sand pack, it was decided not to use it in any further experiments.

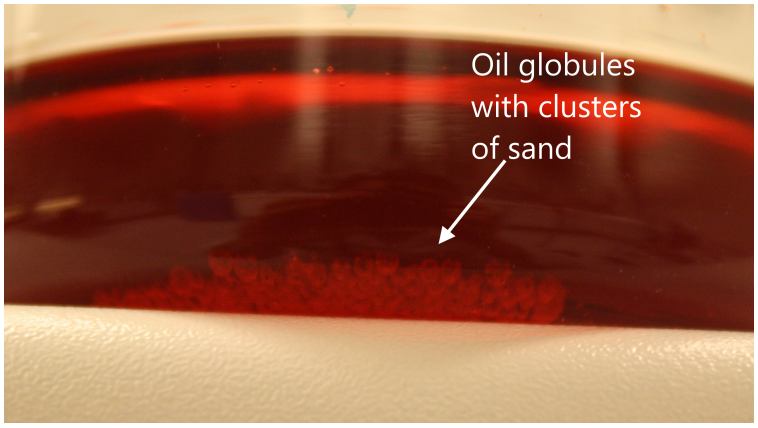

Figure 9.14: Picture taken after sand grains, dyed brine, and n-Decane had been contained in the beaker for 20 minutes. Sand grains were observed in clusters surrounded by oil globules.

9.2.9 The effect of epoxy on spontaneous imbibition initialization

The presence of epoxy resin in the inlet end piece (end piece A) resulted in challenges with initializing spontaneous imbibition due to local wettability changes. Because of this, end piece B was designed to avoid the use of epoxy, giving self-initializing spontaneous imbibitions.

Forced initialization was needed for all spontaneous imbibitions performed in SP01 through SP06 (end piece A), whereas it was only needed for 4 out of 17 spontaneous imbibitions in SP07 through SP19 (end piece B. Morrow & Xie (2001) showed that if epoxy resin was present in an oil volume that was in contact with a porous medium, interactions between the resin and the oil caused a wettability alteration. In end piece A, epoxy resin came in direct contact with n-Decane during saturation and drainage of the sand packs, which could have caused a local wettability alteration close to the inlet. The local wettability alteration caused a restriction for the wetting fluid to spontaneously imbibe into the sand pack. When wetting fluid was forcefully imbibed, it passed this obstacle and spontaneous imbibition initiated.

9.2.10 The effect of HMDS treatement on quartz sand grains

Two sand packs were packed using sand treated with HMDS, an organosilicon compound, in an attempt to alter the sands wettability. The effect of the treatment was found to be insufficient. In the following, SP10, which contained treated sand, will not be included because of in-

sufficient drainage before initializing spontaneous imbibition. Two spontaneous imbibitions were conducted in SP11, but the second will not be included due to detection of a hydrostatic pressure present. The following will show that the treatment was not effective in altering quartz sand grain wettability.

SP11 was directly saturated with brine and exposed to n-Decane because it was expected that the sand was oil-wet. The oil did not spontaneously displace any brine, indicating that the sand was not oil-wet. Therefore, n-Decane was injected to the sand pack before it was exposed to brine to investigate if it spontaneously displaced any oil.

By spontaneous imbibition of brine, more oil was recovered from the sand pack treated with HMDS (SP11) compared with the sand pack not treated with HMDS (SP03), as seen in figure 9.15. 78% of the initial oil was produced from SP11, whereas 52% was recovered from SP03. It could be expected that more oil would be produced at a higher rate in SP03 if SP11 had an altered wettability. In addition, spontaneous imbibition occurs at a higher rate in SP11. However, the sand packs had slightly different sand pack properties, as seen in table 9.1. Therefore, production data was scaled to dimensionless time (Mirzaei-Paiaman & Masihi 2014) for comparison. The two sand packs correlated well, as seen in figure 9.16, meaning that, accounting for different sand pack properties, they performed similarly. Thus the two sand packs should have similar wettability. In addition to this, the Amott-Harvey wettability index was equal to one for both sand packs, proving that the treated sand pack (SP11) contained strongly water-wet sand.

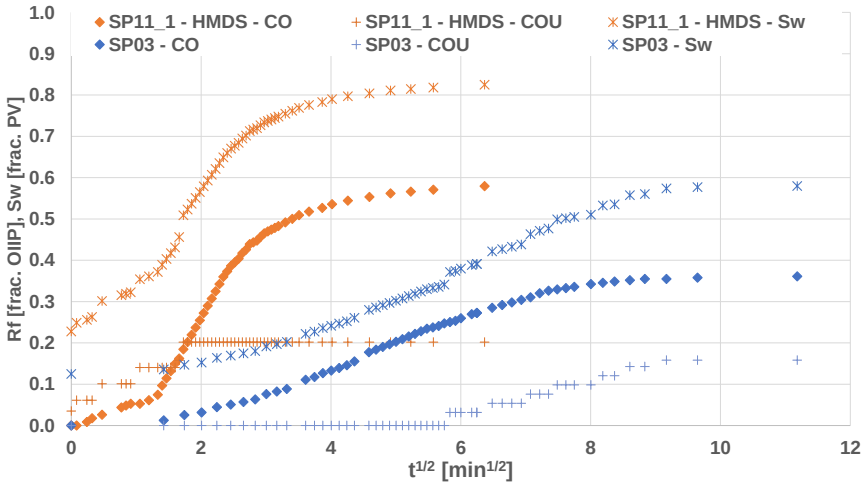

Figure 9.15: Production data plotted against the square root of time ($\sqrt{min}$) for one sand pack with treated sand, and one sand pack with untreated sand.

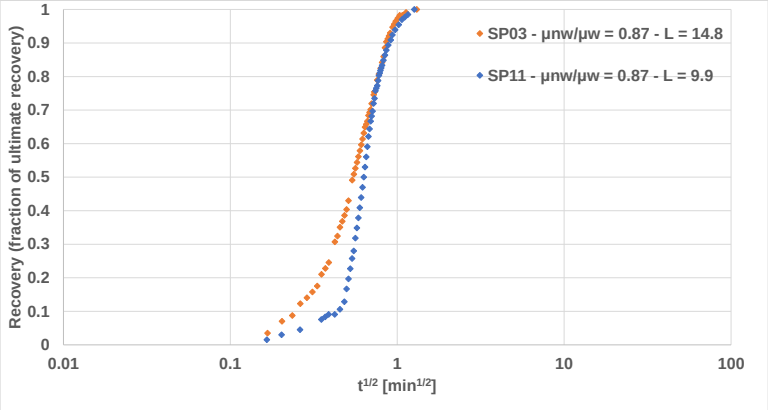

Figure 9.16: Production data for SSI in SP03 and SP11 plotted against dimensionless time (Mirzaei-Paiaman & Masihi 2014).

9.3 Forced imbibition and drainage

Forced imbibition and drainage was performed after spontaneous imbibition experiments to calculate relative permeabilities, Amott-Harvey wettability indices, and to oil flood the sand packs for a new spontaneous imbibition experiment. Relative permeability data is presented in figure 9.17. On average, the relative permeability of water was 0.59 with a standard deviation of 0.15 at a water saturation of 85%, whereas relative permeability of oil was 0.41 with a standard deviation of 0.13 at a water saturation of 21%. As stated in section 2.1, the non-wetting fluid will usually have the largest relative permeability, i.e. oil relative permeability was expected to be largest in the strongly water-wet sand packs. Relative permeability in sand packs used by Føyen (2017) agreed more with literature. He reported average relative permeabilities equal to 0.46 (S_w=0.87%) and 0.69 (S_w=0.21%) to water and oil respectively. The reason for the discrepancy in the sand packs prepared for this thesis could be that sand grains were mobilized and pores got restructured during forced imbibition and drainage.

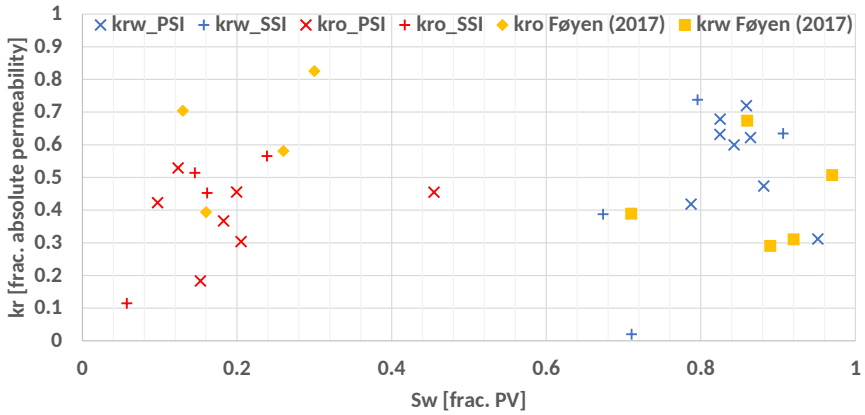

Figure 9.17: Calculated relative permeability values. Relative permeabilities taken after primary spontaneous imbibition are marked PSI, relative permeabilities taken after secondary spontaneous imbibition are marked SSI.

9.3.1 Relative permeability as an indicator of sand pack stability

No sand packs gave reproducible relative permeability measurements within the error margin, as seen in figure 9.18. Relative permeability measurements were taken twice on 4 sand packs. SP15 and SP17 were not included in the analysis because they were imbibed with HPAM polymer, which has been shown to reduce relative permeability, especially to water (Sparlin (1976) and Zaitoun et al. (1991)).

The reason for the lack of reproducible results could be that pores got restructured during forced imbibition and drainage. The pressure during relative permeability measurements varied during volumetric flow (see figure 9.19), indicating that sand grains were mobilized and restructured, i.e. leading to new pore structures. Because relative permeabilities depend on pore geometry (Anderson 1987*b*), it resulted in different values between the two measurements. This gives an indication that the sand packs are not stable during forced imbibition and drainage. During measurement of relative permeability, a maximum flow rate of 499 ml/h was used. This caused higher differential pressures (by a factor of minimum 1.5) than during absolute permeability measurements and could have contributed to a mobilization of sand grains. Thus, the sand packs were not stable at the elevated pressures, and it it recommended to use a lower flow rate to reduce the pressure during relative permeability measurements.

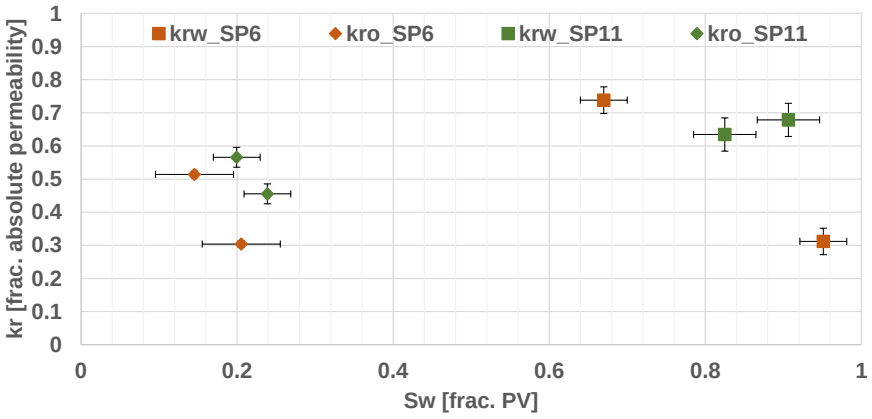

Figure 9.18: Relative permeability for SP06 and SP11 after PSI and after SSI. SP11 gave reproducible relative permeability values, indicating that the sand grains were stable and did not migrate during forced imbibition or drainage.

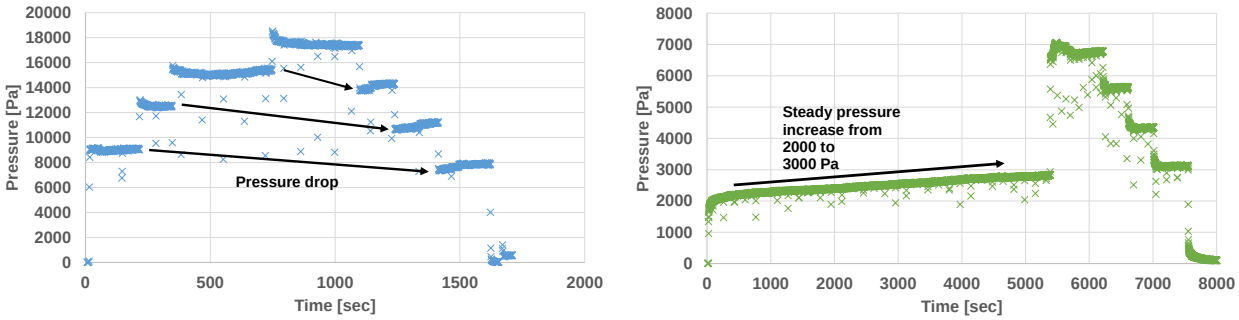

(a) SP06

(b) SP11

Figure 9.19: Recorded pressure during relative permeability to water measurements in SP06 and SP11. Pressure varies, indicating that sand grains were redistributed.

Part IV

Conclusion and Further Work

10 Conclusion

During this thesis, work has been conducted to establish a methodology to produce homogeneous and stable unconsolidated sand packs for spontaneous imbibition investigations. Equipment used for packing the sand packs have been improved to overcome previous challenges such as sand pack leakage, shattered glass during experiments, and heterogeneous pore size distribution. Experiments have been conducted to validate the improvement of the designs developed. New end piece designs and experimental set up allowed for forced displacements in the sand packs, giving the possibility to measure relative permeability and oil flood the sand pack to repeat spontaneous imbibition experiments. This gave the possibility to confirm sand pack stability through multiple cycles of displacement processes. In addition, successful spontaneous imbibition with HPAM polymer added to brine for increased viscosity was performed. Following conclusions were made:

- A new packing methodology gave homogeneous and stable sand packs. The sand packs had a uniform pore size distribution with similar pore structure regularity making it possible to conduct reprodusible spontaneous imbibitions. This was confirmed by experiments and comparison with previous work. The sand packs were stable and sand grains did not redistribute under flow rates up to 499 ml/h, proven by stable and consistent pressure measurements during cycles of increased and lowered flow rates.
- Recovery from spontaneous imbibition was less efficient when initial water saturation was present. Recovery of original oil in place in sand packs with no initial water was on average 40% higher compared to sand packs with initial water. By comparing sand packs where spontaneous imbibition was performed both with and without initial water, it was shown that the imbibition process was slower when initial water was present. It was also observed that 30% of production occurred counter currently during spontaneous imbibition with brine in sand packs where initial water was present. This is different from spontaneous imbibition without initial water where only 5% was produced counter-currently.
- Spontaneous imbibition with HPAM solution yielded higher recovery than glycerol/brine. Recovery was on average 3% higher for HPAM polymer compared to glycerol. This contradicts earlier findings by Haugland (2016) who reported that using HPAM polymer yielded 5% less recovery than glycerol. Haugland (2016) reported challenges with retention of polymers in the inlet filter, and reasoned that it could be the reason for the lower recovery. The HPAM polymer solution used in this thesis was filtered to remove microgels and other multimolecular structures, and no challenges with polymer retention were observed. Thus, the HPAM polymer solution yielded higher recoveries. In addition, Amott-Harvey indices (I_{AH} indicated that HPAM polymer altered the wettability of the sand packs. Average I_{AH} for

sand packs where HPAM polymer had been present was 0.92, whereas for sand packs where it had not been present, the value was 0.97.

- Relative permeability was on average higher for brine than for oil. Average relative permeability to brine was 0.59 at a water saturation of 85%, whereas relative permeability to oil was 0.41 at a water saturation of 21%. This contradicts common theory and findings in earlier sand packs where relative permeability was highest for oil. No sand packs produced reproducible relative permeability values within the error margin. This could be due to sand grain migration and restructuring of the pores due to the higher pressure generated during forced imbibition and drainage. It is therefore recommended to flood the sand packs on flow rates lower than 499 ml/h.

11 Further work

The work in this thesis is built on the experimental development carried out by Vabø (2016), Haugland (2016), and Føyen (2017). The experimental challenges they encountered have been addressed, and a sturdy framework for producing homogeneous and stable sand pack has been developed. The sand pack set up and packing method gives the opportunity to conduct reproducible experiments, and to use sand packs in several cycles of spontaneous imbibition and oil flooding cycles. Spontaneous imbibition in strongly water-wet sands with polymer and initial water saturation has been studied. For future work, a recommendation of altering the sands wettability is given. This gives the opportunity to study spontaneous imbibition in weakly wetted sands. In addition, the effect of HPAM polymer on sand grain wettability should be studied more in depth. In addition, more spontaneous imbibition should be carried out with initial water saturation to confirm findings in this thesis. For future work, some recommendations are given:

- Paraffinic lamp oil was shown to shift quartz grain wettability towards neutral wettability. It is therefore recommended not to use paraffinic lamp oil in sand packs containing large amounts of quartz.
- The filter used was shown to affect spontaneous imbibition immensely. An oil-wet filter was used in one sand pack. It slowed down the process by lowering the imbibition rate. It is therefore recommended to use water-wet filters for strongly water-wet sand packs.
- Adding dye to the imbibing wetting fluid to visualize the saturation front was shown to alter the wettability of the sand pack. This has been proposed earlier and was further confirmed by a simple test. It is therefore not recommended to use dye in any further sand pack experiments.
- Using glass tubes with threaded ends has proved to increase the risk of leakage in the sand pack. The glass tubes are also very fragile and shatter easily. A new end piece was designed so that the use of threaded glass tubes could be eliminated, giving less leakage and a safer working environment.
- Using epoxy resin in the inlet end piece was shown to prohibit initialization of spontaneous imbibition. It is therefore recommended not to use epoxy resin when preparing sand packs.

Abbreviations

PV Pore volume.

AFO All Faces Open.

AP Aqueous phase.

Brine 5 wt% NaCl brine.

D Drainage.

EPI-x Inlet End-Piece number x {x=1, 2,..., 7}.

EPO-x Outlet End-Piece number x {x=1, 2,..., 7}.

FI Forced Imbibition.

HPAM Hydrolyzed Polyacrylamide.

N/A Not applicable.

NM Not measured.

NPT National Pipe Taper.

NWF Non-Wetting Fluid.

OEO One end open.

OOIP Original oil in place.

OP Oleic phase.

POM Polyoxymethylene.

ppm Parts per million.

PSI Primary spontaenous imbibition.

SI Spontaneous Imbibition.

SP Sand pack.

SPxx Sand pack number xx {xx=01, 02,..., 19}.

SSI Secondary spontaenous imbibition.

SSxx Sandstone core number xx {xx=01, 02,..., 10}.

TEOFSI Two Ends Open Free Spontaneous Imbibition.

WF Wetting Fluid.

WM Whatman.

wt% Weight percent.

Nomenclature

δ_i The Amott index for fluid i.

λ_{ri} Mobility of fluid i.

μ_i Viscosity of fluid i.

ϕ Porosity.

ρ Density.

σ Interfacial tension.

τ Shear stress.

θ Contact angle.

D Flow diameter.

E_A Areal sweep efficiency.

E_V Vertical sweep efficiency.

E_{vol} Volumetric sweep efficiency.

f_i Fractional flow of fluid i.

g The gravitational acceleration [$9.81 m/s^2$].

I_{AH} Amott-Harvey wettability index.

K Absolute permeability.

$k_{ri}(S_w)$ Relative permeability of fluid i at a given water saturation S_w.

L Length of sample.

L_c Characteristic length.

L_s Sample length.

M Mobility ratio.

N_g^0 Gravity number.

N_p Accumulative volume of oil produced.

N_{cou} Accumulative volume of oil produced counter-currently.

P Pressure.

P_c Capillary pressure.

P_F Pressure due to viscous flow.

P_H Pressure due to height difference.

P_{atm} Atmospheric pressure.

$P_{c,f}$ Capillary pressure at the saturation front.

P_i Pressure in the fluid i.

q Volumetric flow $[cm^3/h]$.

R_f Recovery factor.

r_s Principal radii of spherical interface between two phases in a capillary tube.

r_t Radius of capillary tube.

Re Reynolds number.

S_{iw} Irreducible water saturation.

S_{or} Residual oil saturation.

$S_{w,d}$ Water saturation after drainage.

$S_{w,f}$ Water saturation after forced imbibition.

$S_{w,i}$ Initial water saturation.

$S_{w,sp}$ Water saturation after spontaneous imbibition.

T Temperature $[^\circ C]$.

$t_{D,MFMR}$ Scaling equation for counter-current spontaneous imbibition (Mason et al. 2010).

$t_{D,MPM}$ Scaling equation for co-current spontaneous imbibition (Mirzaei-Paiaman & Masihi 2014).

u Fluid flow velocity $[m/s]$.

V_{isp} Volume of fluid i displaced spontaneously.

V_{it} Total volume of fluid i displaced.

i o (oil), w (water)

Bibliography

Amott, E. (1959), 'Observations Relating to the Wettability of Porous Rock', *Petroleum Transactions, AIME* **216**(1959), 156–162.

Anderson, W. G. (1986*a*), 'Wettability Literature Survey- Part 1: Rock/Oil/Brine Interactions and the Effects of Core Handling on Wettability', *Journal of Petroleum Technology* **38**(10), 1125–1144.

Anderson, W. G. (1986*b*), 'Wettability Literature Survey- Part 2: Wettability Measurement', *Journal of Petroleum Technology* **38**(11), 1246–1262.

Anderson, W. G. (1987*a*), 'Wettability literature survey- part 4: Effects of wettability on capillary pressure', *Journal of Petroleum Technology* **39**(10), 1238–1300.

Anderson, W. G. (1987*b*), 'Wettability literature survey part 5: The effects of wettability on relative permeability', *Journal of Petroleum Technology* **39**(11), 1453–1468.

Anderson, W. G. (1987*c*), 'Wettability literature survey-part 6: The effects of wettability on water-flooding', *Journal of Petroleum Technology* **39**(12), 1605–1622.

Aronofsky, J. S. (1952), 'Mobility ratio - its influence on flood patterns during water encroachment', *Journal of Petroleum Technology* **4**(01), 15–24.

Barreau, P., Bertin, H., Lasseux, D., Glénat, P. & Zaitoun, A. (1997), 'Water control in producing wells: Influence of an adsorbed-polymer layer on relative permeabilities and capillary pressure', *SPE Reservoir Engineering* **12**(04), 234–239.

Bartell, F. E. & Osterhof, H. J. (1932), 'Adhesion Tension. Pressure of Displacement Method.', *The Journal of Physical Chemistry* **37**(5), 543–552.
URL: *http://pubs.acs.org/doi/abs/10.1021/j150347a001*

Boneau, D. F. & Clampitt, R. L. (1977), 'A surfactant system for the oil-wet sandstone of the north burbank unit', *Journal of Petroleum Technology* **29**(05), 501–506.

Bourbiaux, B. J. & Kalaydjian, F. J. (1990), 'Experimental study of cocurrent and countercurrent flows in natural porous media', *SPE Reservoir Engineering* **5**(03), 361–368.

Brown, R. J. & Fatt, I. (1956), Measurements Of Fractional Wettability Of Oil Fields & Rocks By The Nuclear Magnetic Relaxation Method, *in* 'Fall Meeting of the Petroleum Branch of AIME', Society of Petroleum Engineers.
URL: *http://www.onepetro.org/doi/10.2118/743-G*

Choi, E. S., Cheema, T. & Islam, M. R. (1997), 'A new dual-porosity/dual-permeability model with non-darcian flow through fractures', *Journal of Petroleum Science and Engineering* **17**(3), 331–344.
URL: *http://www.sciencedirect.com/science/article/pii/S0920410596000502*

Coskun, S. B., Wardlaw, N. C. & Haverslew, B. (1993), 'Effects of composition, texture and diagenesis on porosity, permeability and oil recovery in a sandstone reservoir', *Journal of Petroleum Science and Engineering* **8**(4), 279–292.
URL: *http://www.sciencedirect.com/science/article/pii/092041059390005Y*

Craig, F. F. (1971), *The reservoir engineering aspects of waterflooding*, Vol. 3 of *Henry L. Doherty series*, Henry L. Doherty Memorial Fund of AIME, New York.

Cuiec, L. (1984), 'Rock/crude-oil interactions and wettability: An attempt to understand their interactions'.

Domenico, S. N. (1977), 'Elastic properties of unconsolidated porous sand reservoirs', *Geophysics* **42**(32), 1339–1368.

Dong, M., Dullien, F. a. L. & Zhou, J. (1998), 'Characterization of waterflood saturation profile histories by the 'complete' capillary number', *Transport in Porous Media* **31**(2), 213–237.
URL: *https://doi.org/10.1023/A:1006565621860*

Fernø, M. A. (2012), *Enhanced Oil Recovery in Fractured Reservoirs*, InTech, pp. 89–110.
URL: *http://www.intechopen.com/books/introduction-to-enhanced-oil-recovery-eor-processes-and-bioremediation-of-oil-contaminated-sites/enhanced-oil-recovery-in-fractured-reservoirs*

Fernø, M. A., Haugen, A. & Graue, A. (2011), 'Wettability effects on the matrix–fracture fluid transfer in fractured carbonate rocks', *Journal of Petroleum Science and Engineering* **77**(1), 146–153.
URL: *http://www.sciencedirect.com/science/article/pii/S0920410511000623*

Fernø, M. A., Haugen, A., Wickramathilaka, S., Howard, J., Graue, A., Mason, G. & Morrow, N. R. (2013), 'Magnetic resonance imaging of the development of fronts during spontaneous imbibition', *Journal of Petroleum Science and Engineering* **101**, 1–11.
URL: *https://www.sciencedirect.com/science/article/pii/S0920410512002562*

Fernø, M. A., Torsvik, M., Haugland, S. & Graue, A. (2010), 'Dynamic laboratory wettability alteration', *Energy & Fuels* **24**(7), 3950–3958.
URL: *https://doi.org/10.1021/ef1001716*

Fischer, H. & Morrow, N. R. (2006), 'Scaling of oil recovery by spontaneous imbibition for wide variation in aqueous phase viscosity with glycerol as the viscosifying agent', *Journal of Petroleum Science and Engineering* **52**(1), 35–53.
URL: *http://www.sciencedirect.com/science/article/pii/S0920410506000568*

Foshee, W. C., Jennings, R. R. & West, T. J. (1977), 'Preparation and testing of partially hydrolyzed polyacrylamide solutions'.

Føyen, T. L. (2017), Onset of Spontaneous Imbibition, Master's thesis, The University of Bergen.
URL: *http://bora.uib.no/handle/1956/16077*

Fraser, H. J. (1935), 'Experimental study of the porosity and permeability of clastic sediments', *The Journal of Geology* **43**(8), 910–1010.
URL: *http://www.jstor.org/stable/30058422*

Gobran, B. D., Brigham, W. E. & Ramey, H. J., J. (1987), 'Absolute permeability as a function of confining pressure, pore pressure, and temperature', *SPE Formation Evaluation* **2**(01), 77–84.

Graton, L. C. & Fraser, H. J. (1935), 'Systematic packing of spheres: With particular relation to porosity and permeability', *The Journal of Geology* **43**(8), 785–909.
URL: *http://www.jstor.org/stable/30058420*

Haugen, A., Fernø, M. A., Mason, G. & Morrow, N. R. (2014), 'Capillary pressure and relative permeability estimated from a single spontaneous imbibition test', *Journal of Petroleum Science and Engineering* **115**, 66–77.
URL: *https://www.sciencedirect.com/science/article/pii/S0920410514000242*

Haugen, A., Fernø, M. A., Mason, G. & Morrow, N. R. (2015), 'The effect of viscosity on relative permeabilities derived from spontaneous imbibition tests', *Transport in Porous Media* **106**(2), 383–404.
URL: *https://link.springer.com/article/10.1007/s11242-014-0406-4*

Haugland, H. K. (2016), Spontaneous Imbibition in Sand - Viscosity Effects on Oil Recovery and Flow Using Polymer and Glycerol, Master's thesis, The University of Bergen.
URL: *http://bora.uib.no/handle/1956/12570*

Jennings, R. R., Rogers, J. H. & West, T. J. (1971), 'Factors influencing mobility control by polymer solutions', *Journal of Petroleum Technology* **23**(03), 391–401.

Karpyn, Z. T., Halleck, P. M. & Grader, A. S. (2009), 'An experimental study of spontaneous imbibition in fractured sandstone with contrasting sedimentary layers', *Journal of Petroleum Science and Engineering* **67**(1), 48–56.
URL: *http://www.sciencedirect.com/science/article/pii/S0920410509000837*

Kestin, J., Khalifa, H. E. & Correia, R. J. (1981), 'Tables of the dynamic and kinematic viscosity of aqueous nacl solutions in the temperature range 20–150°c and the pressure range 0.1–35 mpa', *Journal of Physical and Chemical Reference Data* **10**(1), 71–88.
URL: *http://aip.scitation.org/doi/10.1063/1.555641*

Krumbein, W. C. & Monk, G. D. (1943), 'Permeability as a function of the size parameters of unconsolidated sand', *Transactions of the AIME* **151**(01), 153–163.

Kyte, J. R. & Rapoport, L. A. (1958), 'Linear waterflood behavior and end effects in water-wet porous media', *Journal of Petroleum Technology* **10**(10), 47–50.

Lake, L. W., Johns, R. T., Rossen, W. R. & Pope, G. A. (2014), *Fundamentals of enhanced oil recovery*, 2nd ed. edn, Society of Petroleum Engineers, Richardson, TX.

Lemmon, E., McLinden, M. & Friend, D. (2018), *Thermophysical Properties of Fluid Systems*, National Institute of Standards and Technology, Gaithersburg MD.

Li, Y., Morrow, N. R. & Ruth, D. (2003), 'Similarity solution for linear counter-current spontaneous imbibition', *Journal of Petroleum Science and Engineering* **39**(3-4), 309–326.
URL: *'Similarity solution for linear counter-current spontaneous imbibition'*

Ma, S. X., Zhang, X. Y. & Morrow, N. R. (1995), 'A characteristic length for scaling of mass transfer between rock matrix and fractures'.

Masch, F. D. & Denny, K. J. (1966), 'Grain size distribution and its effect on the permeability of unconsolidated sands', *Water Resources Research* **2**(4), 665–677.
URL: *https://doi.org/10.1029/WR002i004p00665*

Mason, G., Fischer, H., Morrow, N. R. & Ruth, D. W. (2010), 'Correlation for the effect of fluid viscosities on counter-current spontaneous imbibition', *Journal of Petroleum Science and Engineering* **72**(1), 195–205.
URL: *http://www.sciencedirect.com/science/article/pii/S0920410510000628*

Mason, G. & Morrow, N. R. (2013), 'Developments in spontaneous imbibition and possibilities for future work', *Journal of Petroleum Science and Engineering* **110**, 268–293.
URL: *https://www.sciencedirect.com/science/article/pii/S0920410513001939*

Meng, Q., Liu, H. & Wang, J. (2015), 'Entrapment of the non-wetting phase during co-current spontaneous imbibition', *Energy & Fuels* **29**(2), 686–694.
URL: *https://doi.org/10.1021/ef5025164*

Meng, Q., Liu, H., Wang, J. & Liu, H. (2017), 'Effect of fluid viscosity on correlation of oil recovery by linear counter-current spontaneous imbibition', *Journal of Petroleum Science and Engineering* **151**, 341–347.
URL: *http://www.sciencedirect.com/science/article/pii/S0920410517300311*

Meng, Q., Liu, H., Wang, J. & Zhang, H. (2016), 'Effect of wetting-phase viscosity on cocurrent spontaneous imbibition', *Energy & Fuels* **30**(2), 835–843.
URL: *https://doi.org/10.1021/acs.energyfuels.5b02321*

Mirzaei-Paiaman, A., Kord, S., Hamidpour, E. & Mohammadzadeh, O. (2017), 'Scaling one- and multi-dimensional co-current spontaneous imbibition processes in fractured reservoirs', *Fuel* **196**, 458–472.
URL: *http://www.sciencedirect.com/science/article/pii/S0016236117301370*

Mirzaei-Paiaman, A. & Masihi, M. (2013), 'Scaling equations for oil/gas recovery from fractured porous media by counter-current spontaneous imbibition: From development to application', *Energy & Fuels* **27**(8), 4662–4676.
URL: *https://doi.org/10.1021/ef400990p*

Mirzaei-Paiaman, A. & Masihi, M. (2014), 'Scaling of recovery by cocurrent spontaneous imbibition in fractured petroleum reservoirs', *Energy Technology* **2**(2), 166–175.
URL: *http:https://doi.org/10.1002/ente.201300155*

Morrow, N. R., Huppler, J. D. & Simmons, A. B. (1969), 'Porosity and permeability of unconsolidated, upper miocene sands from grain-size analysis', *Journal of Sedimentary Research* **39**(1), 312–321.
URL: *http://dx.doi.org/10.1306/74D71C3F-2B21-11D7-8648000102C1865D*

Morrow, N. R. & Mason, G. (2001), 'Recovery of oil by spontaneous imbibition', *Current Opinion in Colloid & Interface Science* **6**(4), 321–337.
URL: *https://www.sciencedirect.com/science/article/pii/S1359029401001005*

Morrow, N. R. & Xie, X. (2001), 'Oil recovery by spontaneous imbibition from weakly water-wet rocks', *Petrophysics* **42**(04), 313–322.

Nutting, P. G. (1925), 'Chemical Problems in the Water Driving of Petroleum from Oil Sands.', *Industrial & Engineering Chemistry* **17**(10), 1035–1036.
URL: *http://pubs.acs.org/doi/abs/10.1021/ie50190a014*

Peksa, A. E., Wolf, K.-H. A. A. & Zitha, P. L. J. (2015), 'Bentheimer sandstone revisited for experimental purposes', *Marine and Petroleum Geology* **67**, 701–719.
URL: *http://www.sciencedirect.com/science/article/pii/S0264817215300106*

Pooladi-Darvish, M. & Firoozabadi, A. (2000), 'Cocurrent and countercurrent imbibition in a water-wet matrix block', *SPE Journal* **5**(01), 3–11.

Rapoport, L. A. & Leas, W. J. (1953), 'Properties of linear waterfloods', *Journal of Petroleum Technology* **05**(05), 139–148.

Rogers, J. J. W. & Head, W. B. (1961), 'Relationships between porosity, median size, and sorting coefficients of synthetic sands', *Journal of Sedimentary Research* **31**(3), 467–470.
URL: *http://dx.doi.org/10.1306/74D70BA5-2B21-11D7-8648000102C1865D*

Rust, C. (1957), 'A Laboratory Study of Wettability Effects on Basic Core Parameters'.
URL: *https://www.onepetro.org/general/SPE-986-G*

Salathiel, R. A. (1973), 'Oil Recovery by Surface Film Drainage In Mixed-Wettability Rocks', *Journal of Petroleum Technology* **25**(10), 1216–1224.

Schmid, K. S. & Geiger, S. (2013), 'Universal scaling of spontaneous imbibition for arbitrary petrophysical properties: Water-wet and mixed-wet states and handy's conjecture', *Journal of Petroleum Science and Engineering* **101**, 44–61.
URL: *http://www.sciencedirect.com/science/article/pii/S0920410512002598*

Seeton, C. J. (2006), 'Viscosity–temperature correlation for liquids', *Tribology Letters* **22**(1), 67–78.
URL: *https://doi.org/10.1007/s11249-006-9071-2*

Sheng, J. J., Leonhardt, B. & Azri, N. (2015), 'Status of polymer-flooding technology', *Journal of Canadian Petroleum Technology* **54**(02), 116–126.

Shupe, R. D. (1981), 'Chemical stability of polyacrylamide polymers', *Journal of Petroleum Technology* **33**(08), 1513–1529.

Sorbie, K. (1991), *Polymer-improved oil recovery*, Blackie, New York.
URL: *https://books.google.no/books?id=T-8IAQAAMAAJ*

Sparlin, D. D. (1976), 'An evaluation of polyacrylamides for reducing water production (includes associated papers 6561 and 6562)', *Journal of Petroleum Technology* **28**(08), 906–1018.

Standnes, D. C. (2004), 'Experimental study of the impact of boundary conditions on oil recovery by co-current and counter-current spontaneous inhibition', *Energy & Fuels* **18**(1), 271–282.
URL: *https://pubs.acs.org/doi/abs/10.1021/ef030142p*

Sydansk, R. D., Al-Dhafeeri, A. M., Xiong, Y. & Seright, R. S. (2004), 'Polymer gels formulated with a combination of high- and low-molecular-weight polymers provide improved performance for water-shutoff treatments of fractured production wells', *SPE Production & Facilities* **19**(04), 229–236.

Takamura, K., Fischer, H. & Morrow, N. R. (2012), 'Physical properties of aqueous glycerol solutions', *Journal of Petroleum Science and Engineering* **98-99**, 50–60.
URL: *http://www.sciencedirect.com/science/article/pii/S0920410512002185*

Torsaeter, O. (1984), 'An experimental study of water imbibition in chalk from the ekofisk field'.

Trantham, J. C. & Clampitt, R. L. (1977), 'Determination of oil saturation after waterflooding in an oil-wet reservoir the north burbank unit, tract 97 project', *Journal of Petroleum Technology* **29**(05), 491–500.

Unsal, E., Mason, G., Morrow, N. R. & Ruth, D. W. (2007), 'Co-current and counter-current imbibition in independent tubes of non-axisymmetric geometry', *Journal of Colloid and Interface Science* **306**(1), 105–117.
URL: *http://www.sciencedirect.com/science/article/pii/S0021979706009520*

Unsal, E., Mason, G., Morrow, N. R. & Ruth, D. W. (2009), 'Bubble snap-off and capillary-back pressure during counter-current spontaneous imbibition into model pores', *Langmuir* **25**(6), 3387–3395.
URL: *https://doi.org/10.1021/la803568a*

Vabø, T. (2016), Viscosity Effects on Imbibition Rate and Front Behavior during Co-Current Spontaneous Imbibition in Unconsolidated Porous Media, Master's thesis, The University of Bergen.

Wendell, D. J., Anderson, W. G. & Meyers, J. D. (1987), 'Restored-state core analysis for the hutton reservoir', *SPE Formation Evaluation* **2**(04), 509–517.

Zaitoun, A., Kohler, N. & Guerrinl, Y. (1991), 'Improved polyacrylamide treatments for water control in producing wells', *Journal of Petroleum Technology* **43**(07).

Zhang, X., Morrow, N. R. & Ma, S. (1996), 'Experimental verification of a modified scaling group for spontaneous imbibition', *SPE Reservoir Engineering* **11**(04), 280–285.

Appendices

A Uncertainty estimations

Two sources can cause uncertainties in experimental work: uncertainty of instruments used, e.g. pressure transducer or caliper, and uncertainty of the observer or the experiment itself, e.g. pressure contribution from the continuously flushing inlet during spontaneous imbibition.

For all values where the arithmetical of the sample was calculated, the uncertainty was given as the standard deviation given by:

$$S = \sqrt{\frac{1}{N-1}\sum_{i=1}^{N}(x_i - \bar{x})^2} \tag{A.1}$$

where N is the number of sampled values, x_i is sample value i, and $\bar{x}$ is the sample mean.

For all values such as pore volume, saturation, and density of fluids the uncertainty was calculated as the propagation of error in the variable uncertainty (length, mass, volume). All instruments used and their uncertainty is presented in table A.1. When a value R is a function of n variables, the uncertainty of R, S_R is given by the uncertainty of the variables:

$$S_R = \sqrt{\sum_{i=1}^{n}\frac{\partial R}{\partial x_i}^2 S_{x_i}^2} \tag{A.2}$$

where x_i is variable i, and S_{x_i} is the uncertainty of variable i.

Table A.1: Instrumental uncertainties

Instrument	Parameter	Uncertainty
Weight	Mass [gram]	$\pm$ 0.01
Caliper	Length [cm]	$\pm$ 0.02
Graded imbibition tube	Volume [ml]	$\pm$ 0.05
Graded cylinder 50 ml	Volume	$\pm$ 0.5
Erlenmeyer flask 5000 ml	Volume	$\pm$ 5%
Pressure transducer	Pressure [bar]	$\pm$ 0.10 % of full scale
Pump	Volumetric flow rate [ml/h]	$\pm$ 1

B Additional spontaneous imbibition production curves

B.1 Spontaneous imbibition with brine

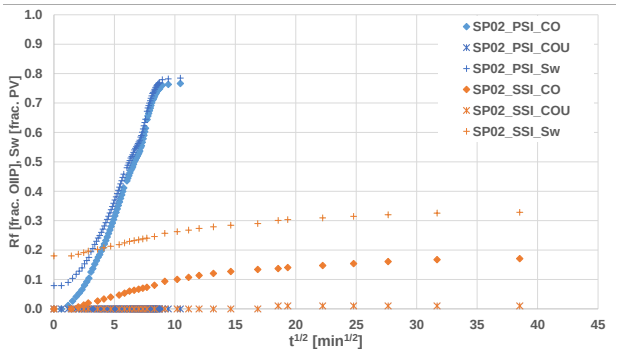

(a) SP02 - L=14.97 cm - K=14.3 D - Dyed brine during SSI

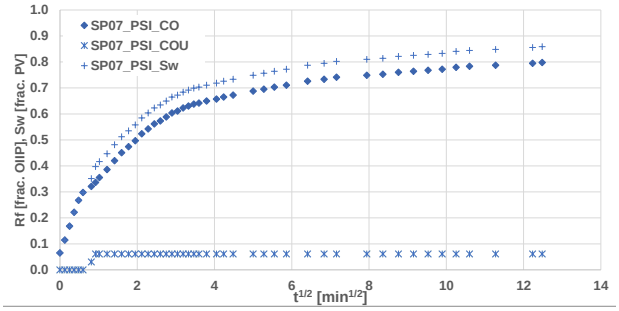

(b) SP07 - L=9.97 cm - K=9.2 D

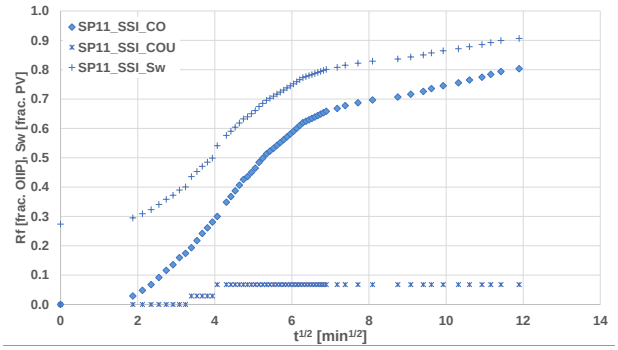

(c) SP11 - L=9.90 cm - K=9.5 D - Treated sand - Forced

Figure B.1: Co-current and counter-current production as a fraction of initial oil volume (Rf on the y-azis), and water saturation (Sw on the y-axis) plotted against square root of time.

B.2 Spontaneous imbibition with glycerol solution

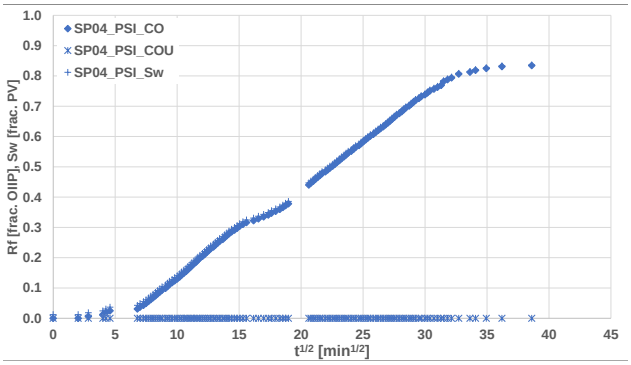

Figure B.2: Glycerol A. SP04 - L=15.05 cm - K=11.4 D - Forced. Co-current and counter-current production as a fraction of initial oil volume (Rf on the y-azis), and water saturation (Sw on the y-axis) plotted against square root of time.

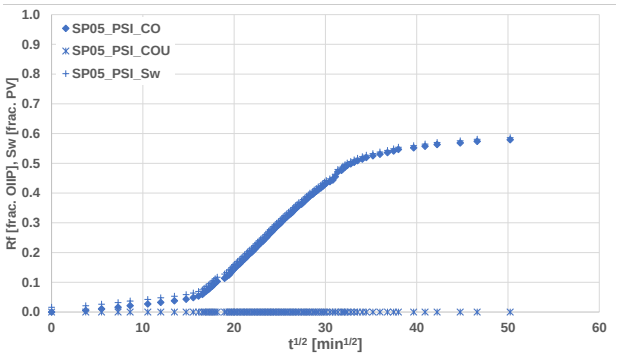

(a) SP05 - L=14.57 cm - K=14.4 D - Forced - Front never reached outlet

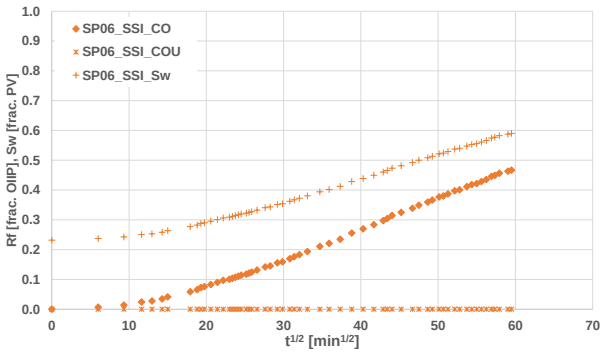

(b) SP06 - L=14.74 cm - K=13.2 D - Forced

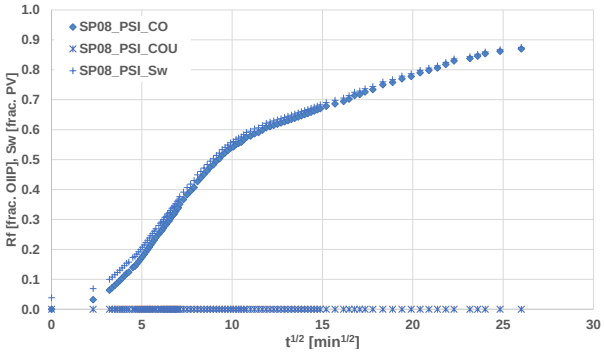

(c) SP08 - L=9.72 cm - K=9.6 D - Forced

Figure B.3: Glycerol B. Co-current and counter-current production as a fraction of initial oil volume (Rf on the y-azis), and water saturation (Sw on the y-axis) plotted against square root of time.

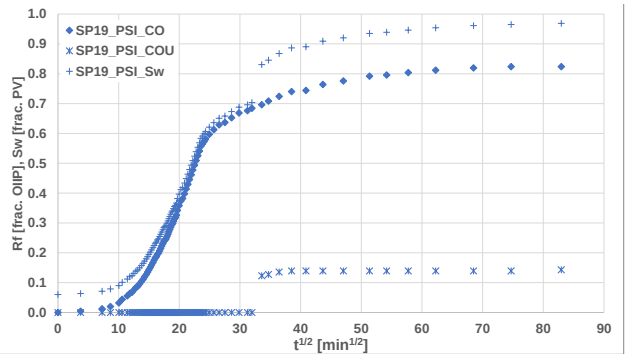

Figure B.4: Glycerol C. SP19 - L=9.68 cm - K=12.7 D - Submerged - Forced. Co-current and counter-current production as a fraction of initial oil volume (Rf on the y-azis), and water saturation (Sw on the y-axis) plotted against square root of time.

B.3 Spontaneous imbibition with HPAM polymer solution

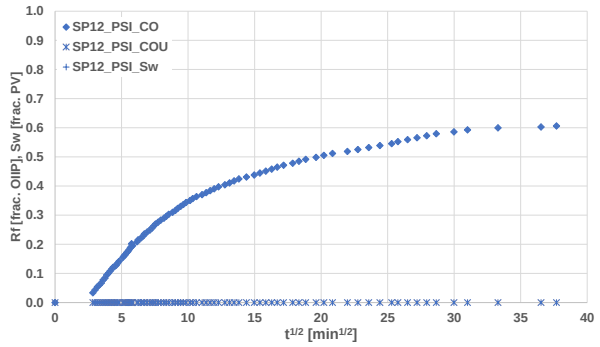

(a) SP12 - L=9.87 cm - K=13.1 D - Front never reached outlet

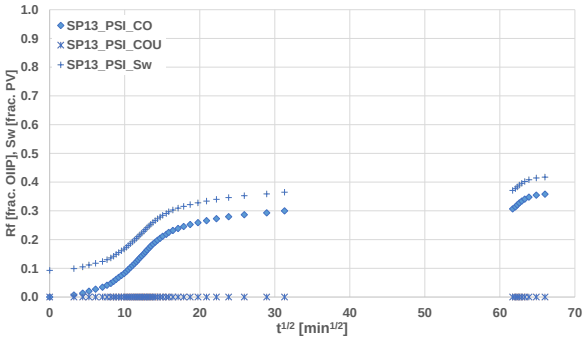

(b) SP13 - L=9.90 cm - K=7.0 D - Front never reached outlet - Forced

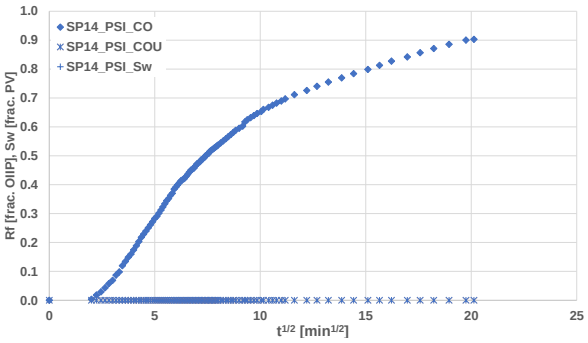

(c) SP14 - L=9.76 cm - K=11.4 D

Figure B.5: HPAM C. Co-current and counter-current production as a fraction of initial oil volume (Rf on the y-azis), and water saturation (Sw on the y-axis) plotted against square root of time.

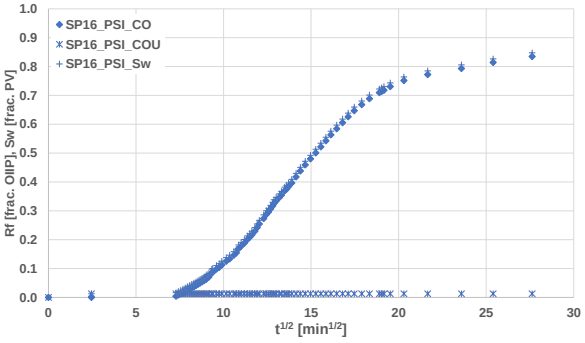

Figure B.6: HPAM D. SP16 - L=16.73 cm - K=16.9 D. Co-current and counter-current production as a fraction of initial oil volume (Rf on the y-azis), and water saturation (Sw on the y-axis) plotted against square root of time.

C Modelling the inlet end piece in Comsol Multiphysics

Table C.1: Pressure contribution from viscous flow in the continuously flushing inlet for all fluid viscosities.

Fluid	**Viscosity [cP]**	ΔP_F **[Pa]**
Brine	1.07	0.1
5k ppm HPAM/69 wt% Glycerol	30	2
72 wt% Glycerol	45	3

A 3D model of the continuously flushing inlet was built using the Comsol Multiphysics software. It was assumed that only the wetting fluid flows in the inlet. Reynolds number was calculated for each fluid and can be seen in table C.2, and the flow was considered laminar for all fluids. It was assumed that only wetting fluid flows in the inlet tubing. Therefore, a model for single-phase laminar flow was used. Because the pressure aggregated by the flow was of interest, the volume force of the fluid was neglected. The viscosity of the circulating fluid was varied between 1.07 and 45 cP, equal to the viscosities of the wetting fluids used in spontaneous imbibition experiments. The volumetric flow was set to 100 cm^3/h, equal to the volumetric flow used to circulate brine through the inlet.

Table C.2: *Calculated Reynolds number for each wetting fluid flushed through the continuously flushing inlet.*

	Brine	5k HPAM	69 wt% Glycerol	72 wt% Glycerol
q $[cm^3/h]$	100	100	100	100
ρ $[g/cm^3]$	1.03	1.04	1.22	1.3
μ $[cP]$	1.07	30	30	45
D $[cm]$	2.05	2.05	2.05	2.05
Re	1.83	0.07	0.08	0.06

The model contained 11 separate parts as seen in figure C.1. Cylinders were added for the straight parts of the tubing (parts 1, 3, 5, 7, 9, and 11), the bulk volume where the wetting fluid contacts the sand pack (part 4), and the counter-current cell (part 10). 90° of a torus was added to simulate the turns of the tubing (part 2, 6, and 8). The measures and position of all parts are presented in table C.3. In the model, the volume force of the fluid was neglected, and only the pressure contribution of the flowing fluid was considered. The output from Comsol Multiphysics is represented in figures C.2 (brine), C.3 (HPAM polymer and 69 wt% glycerol), and C.4 (72 wt% glycerol).

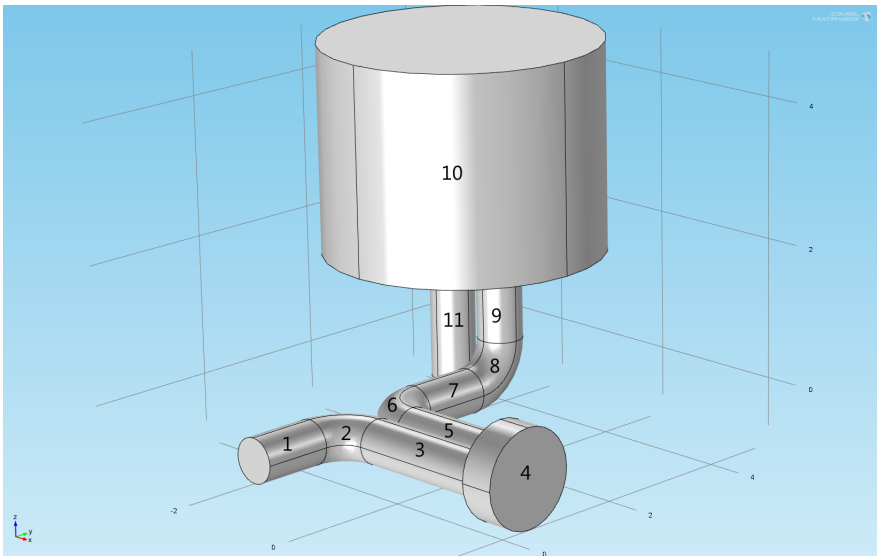

Figure C.1: The model built in Comsol Multiphysics for calculating the pressure caused by flow in the continuously circulating inlet.

Table C.3: *Dimensions and positions of all parts in the Comsol Multiphysics model. The part numbers are stated in figure C.1.*

Straight parts					
Part nr.	Radius [cm]	Length [cm]	Position x	y	z
1	0.3175	1	-0.635	-0.953	0
3	0.3175	2	0	-0.3175	0
4	0.7	0.5	2	0	0
5	0.3175	2	0	0.3175	0
7	0.3175	1	-0.635	0.953	0
9	0.3175	1	-0.635	2.588	0.635
10	2	3	-1.635	2.9055	1.635
11	0.3175	1.9525	-2	3	-0.3175

Bend parts						
Part nr.	Major radius [cm]	Minor radius [cm]	Revolution angle [degrees]	Position x	y	z
2	0.635	0.3175	90	0	-0.953	0
6	0.635	0.3175	90	0	0.953	0
8	0.635	0.3175	90	-0.635	1.953	0.635

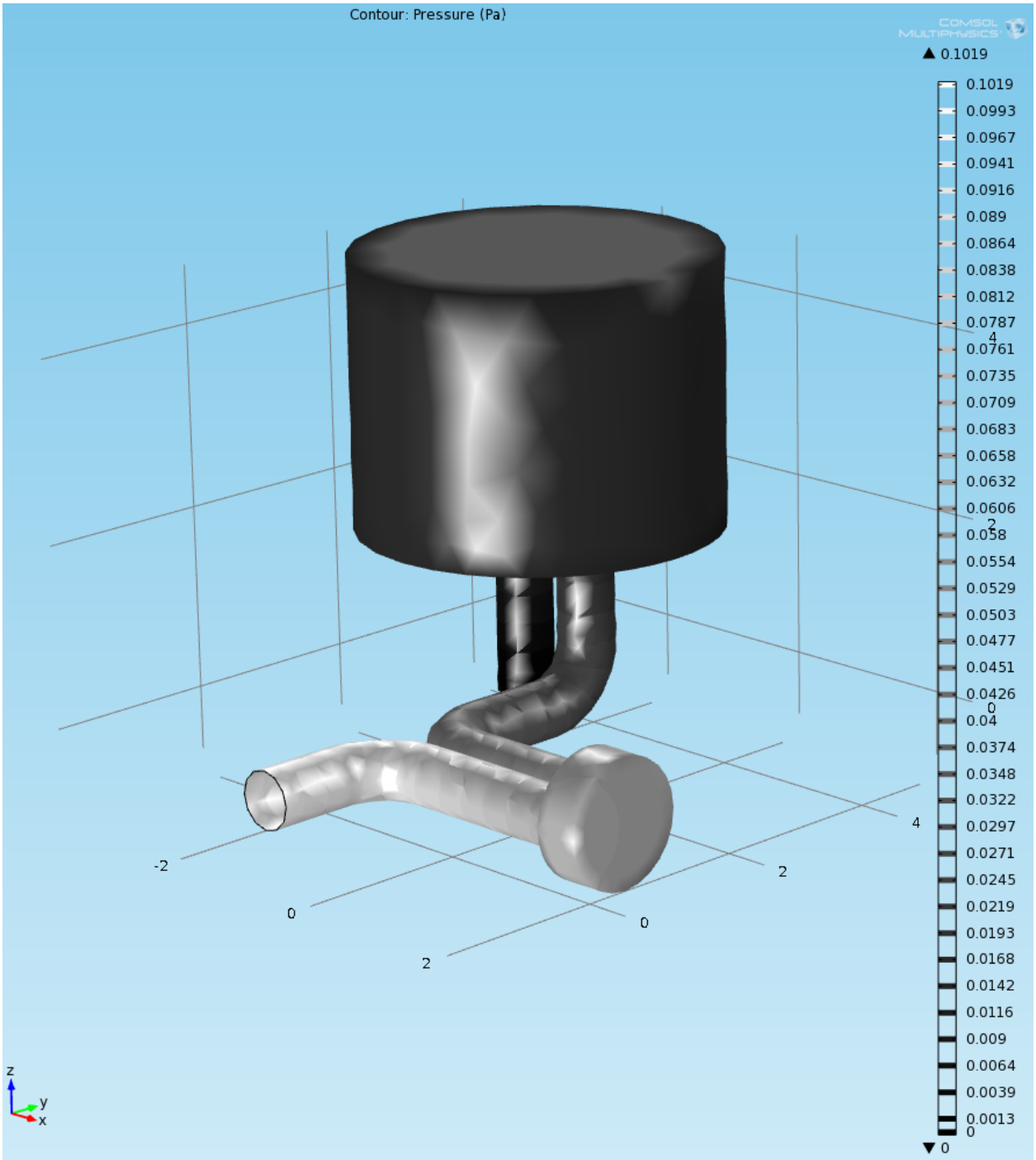

Figure C.2: Pressure in continuously flushing inlet caused by flow of a fluid with viscosity 1.07 cP (Brine)

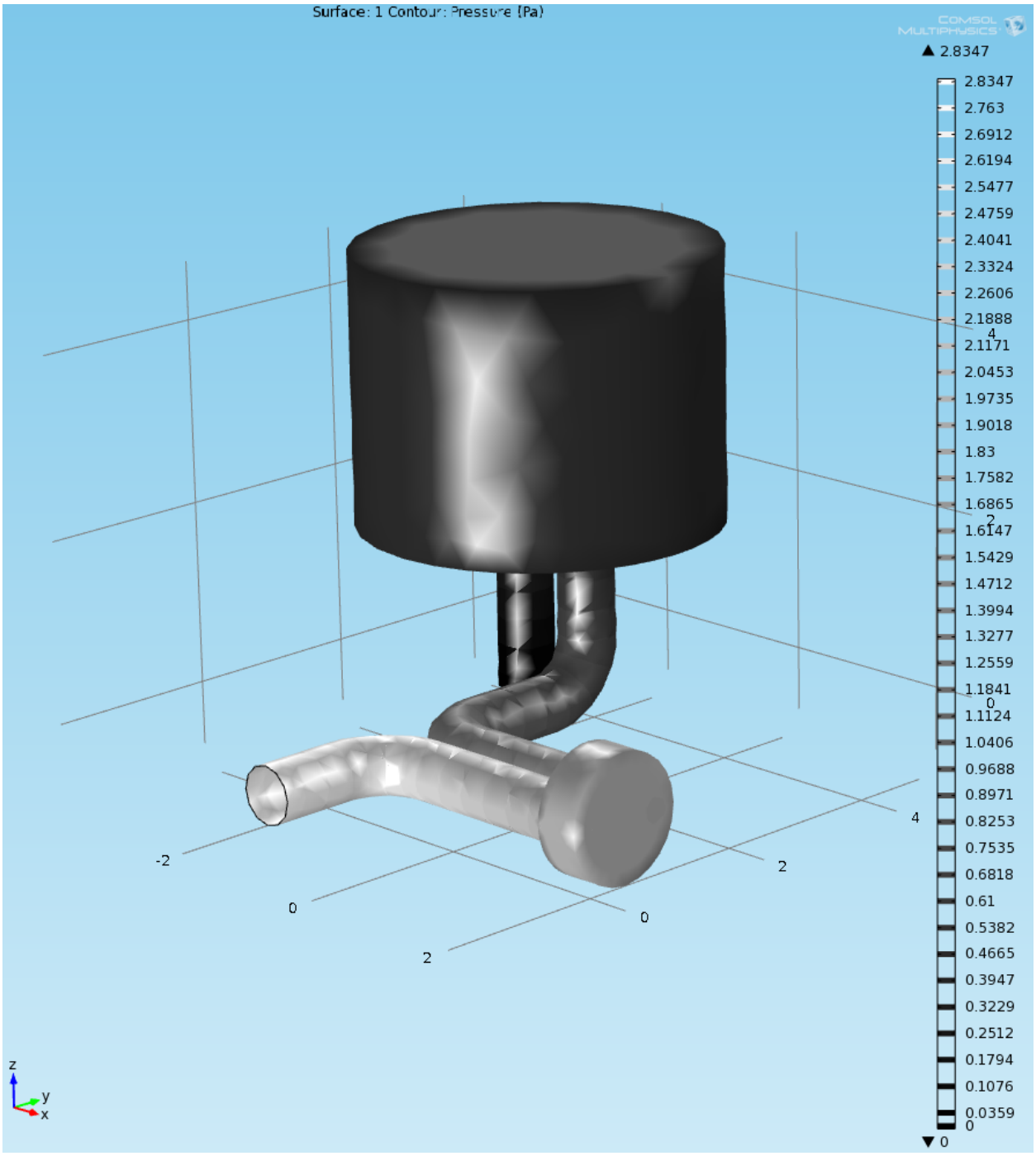

Figure C.3: Pressure in continuously flushing inlet caused by flow of a fluid with viscosity 30 cP (69 wt% glycerol and HPAM polymer solution).

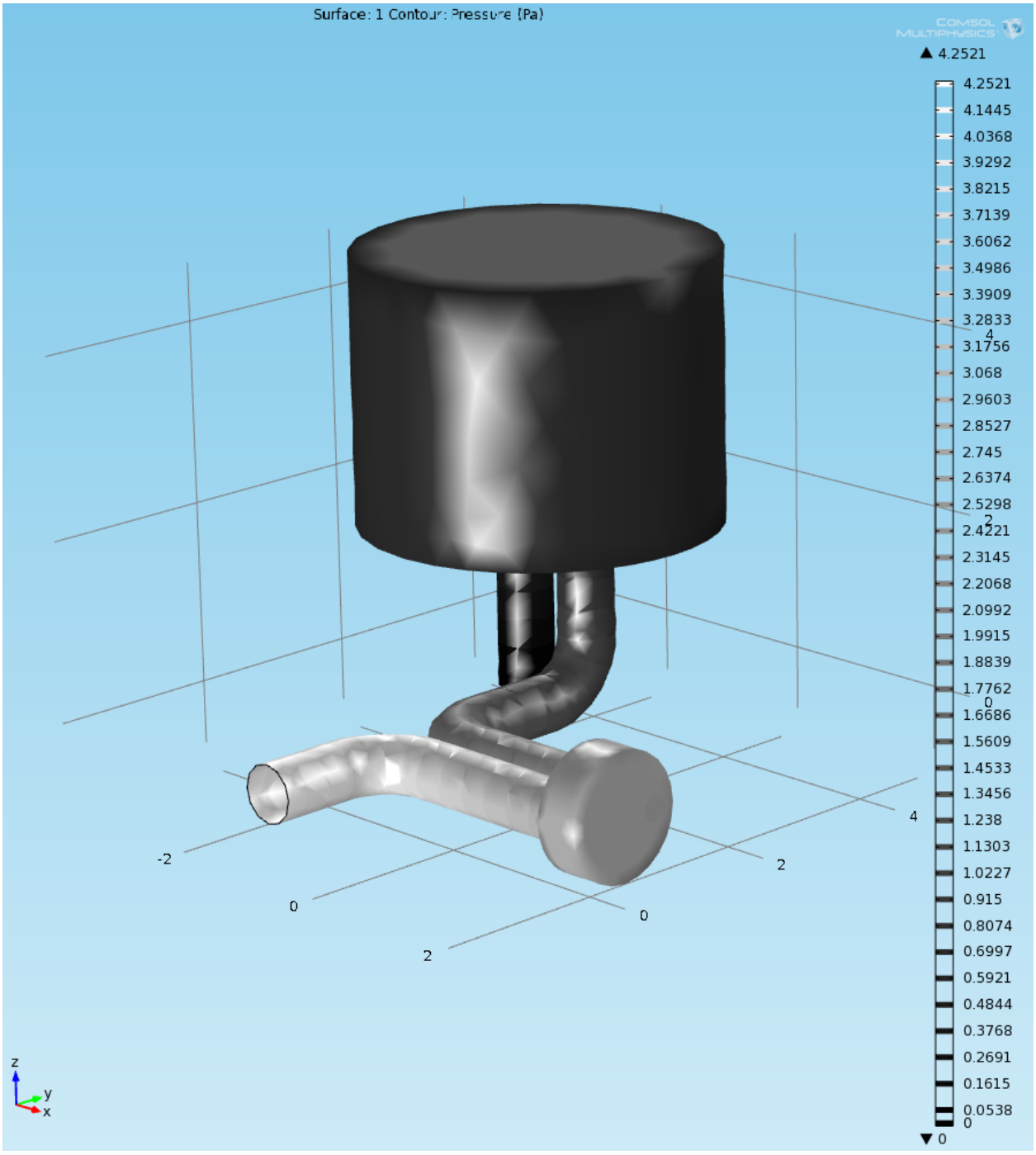

Figure C.4: Pressure in continuously flushing inlet caused by flow of a fluid with viscosity 45 cP (72 wt% glycerol solution).

D HMDS treatment procedure

Outlined procedure
• Boil in Nitric acid (68%) for 30 min • Dilute and neutralize solution • Dilute solution with distilled water and dry • N2 - Vacuumed purge cycles • HMDS Vapor prime • Remove excess HMDS

Method	Purpose	Procedure	HSE and PPE	Litterature
Boiling the sample in Nitric acid	Oxidized and clean. Improve surface properties for silan retions	• Put sample into a Dean Stark bottom boiling chamber. Max 2¨ diameter and total length of 15 cm. And 250 ml of Sand • Slowly add Nitric acid (68%), until it completely covers the samples, approx. 450 ml • Turn the heating on, use full effect until boiling starts approx. 25 min • Boil for 30 min, at ¾ of full effect • Turn heating of • Cool down, min. 1 hour	• Concentrated nitric acid is a very strong acid and a powerful oxidizing agent, which must be handled with great care. • Faceshield, lab coat or overalls • Suitable glows, Barrier • Respirator (**E**-filter/ABEK) • All handling and storage should be done under fume • Incompatibility with other fluids (e.g. organic solvents)	1
Dilute and neutralize	Reduce the ph to 7	• Pour excess acid into a beaker, and then over to a bottle. • Pour the samples and the rest of the acid into a bath filled with 2 l of distilled water. • Neutralize the diluted acid solution containing the samples by slowly adding concentrated sodium hydroxide, until the ph is between 4-9. • Measure the pH using the pH-meter and stir the solution while performing the neutralization.		2
Wash and dry	Remove sodium nitrate salt. Evaporate water	• Dilute the neutralize solution containing the samples. • Cores: Put them into a beaker filled with distilled water, change the water several times for the tree next days. • Sand: Put it into a beaker filled with water for two hours. Pure the sand over a sieve (mash finer than the sand), flush with excess amount of desilted water. • Dry the samples in a heating cabinet		
N2 - Vacuumed purge cycles	Dehydrate and remove oxygen	• Fill a 10ml measuring cylinder with HMDS, place the cylinder inside the HMDS chamber. • Mount the system according to Fig 1. • Turn on the heat (90 C) • Evacuate the whole system and perform 3 Purge cycles with N2-vacuume • Evacuate the core chamber and perform 5 Purge cycles with N2-vacuume	• Pressurized gas into glass chamber, correct use of pressure regulator • Warm water bath	3
HMDS Vapor prime	Change the samples surface to hydrophobic	• Open the valve from HMDS chamber to core chamber, reduce the pressure a low pressure (0.5T). • Close valve to pump • Let the samples rest in HMDS vapor for 2? hours at 90 degrees	• Prevent skin contact, use nitril glowes, 0,4mm (Solvex) .faceshield and Overall • Work under fume and use ABEK full face mask	3, 4
Remove excess HMDS	Remove hazardous excess HMDs	• Evacuate the system by performing 3 Purge cycles with N2-vacuume to ensures complete removal of excess HMDS • Perform vacuum pump cleaning procedure. (see vacuum pump manual) Will update	• Fluids in the in the water trap might contain HMDS.	3

Figure D.1: HMDS procedure, page 1. (Document by PhD candidate Tore Føyen).

1 http://onlinelibrary.wiley.com/doi/10.1002/wrcr.20367/full

2 https://assist.asta.edu.au/sites/assist.asta.edu.au/files/SOP_Diluting%20concentrated%20nitric%20acid.pdf

3 http://www.yieldengineering.com/Portals/0/HMDS%20Application%20Note.pdf

4 https://research.utdallas.edu/cleanroom/manuals/hmds-process

https://www.microchemicals.com/products/adhesion_promotion/hmds.html

https://www.pcimag.com/ext/resources/PCI/Home/Files/PDFs/Virtual_Supplier_Brochures/Gelest_Additives.pdf

https://books.google.no/books?id=WCcTTSMVhYEC&pg=PA15&lpg=PA15&dq=Hexamethyldisilazane+bulk+vapor&source=bl&ots=2__pXNBKNb&sig=Z8FCYxN6sBi4KbmgbgkTRb4IZgg&hl=no&sa=X&ved=0ahUKEwjI7KfnufjYAhXLkCwKHd5bBnYQ6AEIKDAA#v=onepage&q=Hexamethyldisilazane%20bulk%20vapor&f=false

http://www.yieldengineering.com/Portals/0/HMDS%20Application%20Note.pdf

Åndedrettsvern Når risikovurdering viser at åndedrettsvern med filterapparat er hensiktsmessig, bruk helmaske med kombinasjonsfilter eller type ABEK-filter (EN 14387) som støtte til eksterne ventilasjonssystemer. Dersom åndedrettsvern er den eneste beskyttelsen, bruk luftforsynt åndedrettsvern med helmaske. Bruk åndedrettsvern og komponenter som er testet og godkjent etter standarder som NIOSH (US) eller CEN (EU).

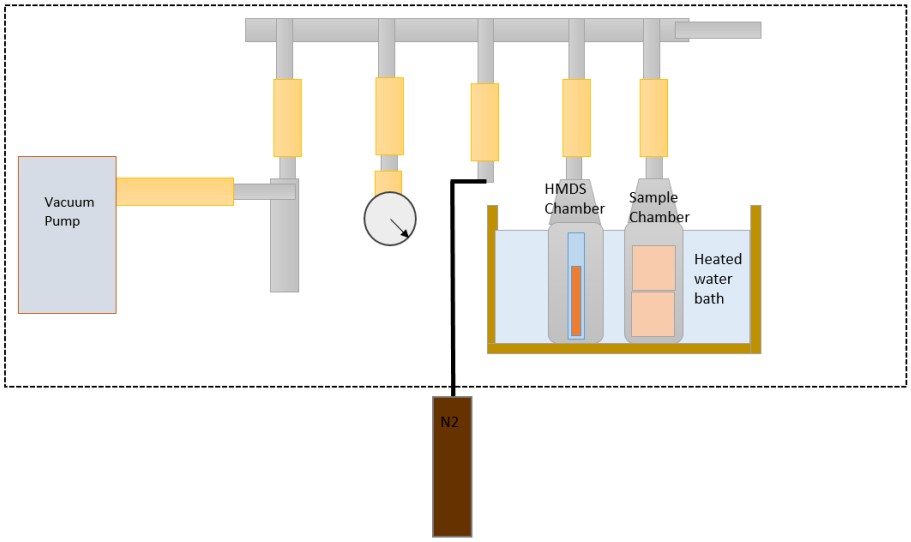

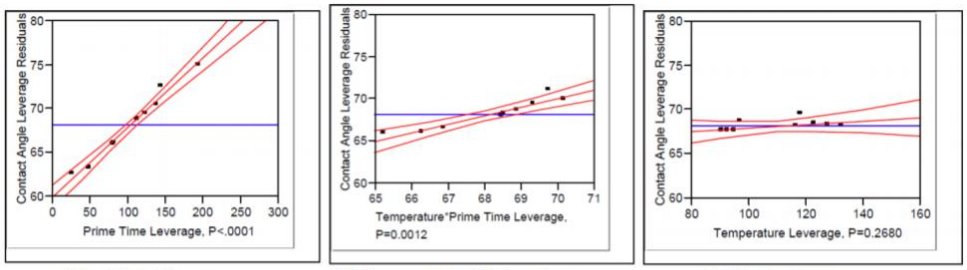

(a) Prime Time (b) Temperature* Prime time (c) Temperature

**Figure 6: Vapor Prime Time effects are graphically depicted in figures a, b, and c respectively.

Figure D.2: HMDS procedure, page 2. (Document by PhD candidate Tore Føyen).

Table 2. Contact Angle Measurements on Simultaneously HMDS-Silanized Silica and Glass Surfaces After Various Pretreatment Methods

	Contact Angles		Air-Water			Oil-Water[a]		
Thermal History	Surface Pretreatment	Surface	Mean	Std Dev	*n*	Mean	Std Dev	*n*
RT	Nitric acid, RT, 1 week[b,c,d]	Silica	101	1.6	9	154	2.7	9
		Glass	102	1.3	9	148	1.0	3
400°C	Nitric acid, RT, 1 week	Silica	100	0.8	9	152	3.0	9
		Glass	95	1.5	9	102	5.0	9
400°C	Nitric acid, boiling, 30 min	Silica	95	2.1	9	140	7.5	9
		Glass	98	2.0	9	141	2.2	9

[a]Hexadecane is the oil.
[b]RT is room temperature. The first entry in the first column indicates the prior thermal history of the glass.
[c]Those labeled 400°C were baked at 400°C for 25 min and then cooled prior solution cleaning.
[d]Concentrated nitric acid in each of these experiments.

Table 1. Contact Angle Measurements on Silanized Silica and Glass Surfaces Using Silanes Intended to Yield Oil-Wet Surfaces[a]

Contact Angles		Air-Water			Oil-Water[b]			
Surface Modification	Surface	Mean	Std Dev	*n*	Mean	Std Dev	*n*	Cleaning Method
Hexamethyldisilazane	Silica	97	2.2	9	140	4.9	9	UV-ozone[a]
	Glass	97	1.1	9	91	3.0	9	Aqua regia
	Glass	96	2.3	9	114	2.7	9	SC1
	Glass	100	1.8	9	150	3.8	9	Boiling nitric acid[c] (30 min)
Dodecyltriethoxysilane	Silica	102	1.9	9	148	4.7	9	UV-ozone[a]
	Glass	102	1.5	9	110	2.6	9	UV-ozone

[a]Hexadecane is the oil.
[b]Results on silica from our previously published work [*Grate et al.*, 2012].
[c]Concentrated nitric acid.

Figure D.3: HMDS procedure, page 3. (Document by PhD candidate Tore Føyen).